

Fundamental Physics Searches with IACTs

Contribution submitted for inclusion in ‘Advances in Very High Energy Astrophysics’, Mukherjee & Zanin, World Scientific (2022) <https://www.worldscientific.com/worldscibooks/10.1142/11141>

Michele Doro¹, Miguel Angel Sánchez-Conde², Moritz Hütten³

¹ University of Padova, Department of Physics and Astronomy, I-35131 Padova (Italy) michele.doro@unipd.it

² Instituto de Física Teórica, IFT UAM-CSIC, Departamento de Física Teórica, Universidad Autónoma de Madrid, ES-28049 Madrid (Spain) miguel.sanchezconde@uam.es

³ Institute for Cosmic Ray Research, the University of Tokyo (Japan) huetten@icrr.u-tokyo.ac.jp

Introduction

Gamma rays make up the highest energy end of the electromagnetic spectrum and are generated when interactions involve highly energetic leptons or hadrons. Those accelerated particles reaching us from outer space are collectively called cosmic rays, and are subject of intense studies for almost a century now. Gamma ray radiation is created in diverse non-thermal environments in the Universe. Today, cosmic-ray studies are performed with several tens of different instruments of different classes, including Imaging Atmospheric Cherenkov Telescopes (IACTs). The astrophysical reach of gamma-ray astronomy is huge, as largely proven in the past decade of scientific production and comprehensively resumed in this book. Besides for non-thermal astrophysical environments, gamma rays are an optimal probe to search for New Physics. Some of these exotic and exciting scenarios are the subject of this contribution.

All current IACTs have invested a great deal of time and resources in searching for these signatures over the past two decades, investing a large fraction of their observation time, so precious for the other astrophysical target observations described in the book. In this chapter, we focus on a selection of topics in fundamental physics such as the indirect search for weakly interacting massive particles (WIMPs; Sec. 8.1) and the search for axion-like particles (ALPs; Sec. 8.2). We follow with less debated, yet interesting studies on the search for primordial black holes (PBHs; Sec. 8.3), tau-neutrinos (Sec. 8.4), and magnetic monopoles (Sec. 8.5). Final remarks will close the chapter. Other topics in Fundamental Physics such as Lorentz Invariance tests are reported elsewhere in this book (see Chap. XX).

We structured the contribution trying to provide a self-contained (yet minimal) theoretical framework, as well as a complete report of all IACTs published contribution to the topics under consideration. Our aim is to provide a reference review as well as take a photograph of the effort of the current generation of IACTs and the challenges taken, in preparation of the next-generation instrument to come, the Cherenkov Telescope Array.

8.1 Massive Particle Dark Matter

For several decades now, the term ‘dark matter’ is not only known from all physicists worldwide, but also probably by all high-school students and many citizens, and has entered to pop culture¹. This is due to the innumerable studies written about the evidence for Dark Matter (DM), the so far inconclusive effort to identify its nature (but knowing today a lot about what DM *is not*), and the theoretical mapping of potential candidates. There are also countless reviews of this knowledge. It is therefore a challenging task to summarize even a fraction of what we learned so far about the DM. For the purpose of this book, we will review the search for massive DM candidates, so-called weakly interacting massive particles (WIMPs), performed with IACTs. Within this scope, we will limit ourselves to the basic information that will be needed for such review. In particular, we will limit ourselves to *particle* DM as opposed to theories of modified gravity (as, e.g., by [Milgrom, 1983](#)) that would have no evident signatures for IACTs. Beyond that, we refer the interested reader to the literature: we recommend [Bertone and Hooper \(2016\)](#) for a profound, detailed account on the history of DM in which also some myths are dismantled, such as that affirming that the term itself was coined by F. Zwicky in 1933. Other comprehensive reports are [Bertone et al. \(2005a\)](#),

¹ “*I don’t want to be human. I want to see gamma rays, I want to hear X-rays, and I want to smell dark matter. . .*” Cylon Model Number One in the Fiction TV Serie “Battlestar Galactica”.

Feng and Kumar (2008), and many more. Fine lecture notes taken from schools are e.g. Hooper (2017), Lisanti (2017), Profumo (2013). Dedicated textbooks are, e.g., Hooper (2006), Profumo (2017), Sanders (2014).

Background of gamma-ray searches for WIMP DM

To date, we still experience DM only through its gravitational manifestation. We do not know its microscopic character, its composition and coupling to ordinary matter, nor if it displays at all interaction with the non-dark sector. However, we know that DM does *not* interact electromagnetically, and any scattering cross-section must be very weak. Therefore, having excluded neutrinos to make up the DM, the nature of this particle – or several particles – must go beyond the ensemble of particles of the Standard Model (SM). Such strange particles would have permeated the whole Universe from its beginning, and shaped the Universe’s evolution and structure formation due to their dominance. In fact, we have today a remarkably accurate knowledge about these structures and the distribution of DM throughout the Cosmos. We measure that DM is clustered in *halos* at very diverse cosmic scales, hosting in turn astrophysical systems from the scale of dwarf galaxies to that of galaxy clusters. We know that, despite being elusive, weakly interacting and very much stable, there is room for many theoretical models predicting interactions that could be observable with different classes of instruments, from X-ray to gamma-ray telescopes.

Tracking the particle DM evolution. One of the most compelling evidence of DM is its imprint on the spatial anisotropy spectrum of the Cosmic Microwave Background (CMB). This diffuse radiation encodes the acoustic oscillations of the Universe matter and radiation fields at the epoch of matter recombination, when the Universe was about 380,000 years old. The power of a specific scale of anisotropy sensibly depends on the composition of matter species. For example, a particle such as DM exhibits a different anisotropy spectrum than a particle such as a quark that additionally couples to photons. Today’s reference for the measurement of the CMB anisotropy is obtained with the *Planck* satellite detector. By decoding the matter composition at the recombination epoch and extrapolating to current times, this measurement yields values of (Aghanim et al., 2020):

$$\Omega_{\text{DM}} h^2 = \frac{\rho_{\text{DM}}}{\rho_{\text{crit}}} h^2 = 0.1198 \pm 0.0012 \quad \text{and} \quad \Omega_{\text{SM}} h^2 = 0.02233 \pm 0.00015, \quad (8.1)$$

where $\rho_{\text{crit}} = 3H_0^2/8\pi G = 10^{-6} \text{ GeV cm}^{-3}$, $h = 10^{-2}H_0 \text{ km s}^{-1}\text{Mpc}^{-1} = 0.6737 \pm 0.0054$ the reduced Hubble parameter at redshift zero, and G is the Gravitational Constant. That is, roughly 26% of today’s Universe’s energy density is in the form of DM and DM makes up 84% of the total mass of the Universe.

Being over-abundant with respect to ordinary matter and having left thermal equilibrium before baryons, DM would then drive and shape galaxy formation: after their decoupling, baryons would fall into already existing and growing DM overdensities. These overdensities would gather and merge, slowly giving rise to the large-scale filamentary structure that is supported by current observations. Being the observed matter distribution very clumpy, this puts strong requirements on any DM candidate made of elementary particles: generically, particle DM candidates are classified into *hot*, *warm* and *cold* DM (HDM, WDM, CDM), according to whether they were highly relativistic (hot) or non-relativistic (cold) at the time they decoupled in the early Universe by ther-

mal freeze-out or any other production mechanism.² Due to their high velocity, hot DM particles inherit a large free-streaming length which would have brought to extremely diluted DM clustering, which is in contradiction with observations. This was clarified only thanks to N-body cosmological simulations (S. and Y., 1966, White et al., 1983), which for example ruled out cosmogenic neutrinos as DM candidates. In turn, CDM provides at large a better agreement with observations.

It is important to track the evolution of DM in the early Universe in order to assess the observability now. The evolution of a comoving particle field density n_χ in a Universe with Hubble parameter H is governed by the law (Dodelson, 2003):

$$\frac{dn_\chi}{dt} + 3Hn_\chi = -\langle\sigma v\rangle (n_\chi^2 - n_{\chi,\text{eq}}^2), \quad (8.2)$$

where $\langle\sigma v\rangle$ is the self-annihilation cross-section between two particles in the field averaged over their relative velocity, and the density at equilibrium has reached $n_{\chi,\text{eq}}$ when particles are in thermal and chemical equilibrium with the environment. The Hubble parameter, expressing the expansion rate of the Universe, evolves with the effective fields composition as well as the equilibrium temperature T . As a consequence, the number density of a given particle species evolves with the effective Universe composition and temperature as well. Specifically, when the temperature decreases to values below a certain particle mass, $T \lesssim m_\chi$, the comoving density of that particle starts decreasing exponentially as:³

$$n_{\chi,\text{eq}} = g_\chi \left(\frac{m_\chi T}{2\pi}\right)^{3/2} e^{-m_\chi/T}. \quad (8.3)$$

This trend stops when the particle self-annihilation becomes inefficient, that is, when the Hubble expansion rate gets larger than the particle annihilation rate. This event is called *freeze-out* of the particle density which subsequently stays constant in a comoving volume. For particle masses at the GeV scale, the freeze-out happens at a temperature T_F roughly 20 to 30 times smaller than the particle mass,

$$T_F \sim \frac{m_\chi}{25},$$

which means that these particles are at that moment already non-relativistic, i.e., cold. Considering such frozen-out particle species χ as DM candidate, a curious fact emerges. If one evolved the DM density from freeze-out to today, considering plausible values for the total number of degrees of freedom g^* according to the known particles in the Universe, one obtains for $m_\chi \sim \text{GeV}$:

$$\rho_\chi h^2 \simeq 0.12 \rho_{\text{crit}} \left(\frac{80}{g^*}\right)^{1/2} \left(\frac{m_\chi}{25 T_F}\right) \left(\frac{2.2 \times 10^{-26} \text{cm}^3 \text{s}^{-1}}{\langle\sigma v\rangle}\right), \quad (8.4)$$

which tells the interesting fact that if that particle χ made up all the DM content of the Universe found according to Equation 8.1,

$$\Omega_{\text{DM}} = \Omega_\chi = \frac{\rho_\chi}{\rho_{\text{crit}}} = 0.12,$$

then, a velocity-averaged annihilation cross-section at freeze-out of

$$\langle\sigma v\rangle \approx 2.2 \times 10^{-26} \text{cm}^3 \text{s}^{-1} \quad (8.5)$$

²HDM must consist of very light, $\lesssim \text{eV}$ particles, while CDM can be at any mass scale, depending on the production mechanism (Primack and Gross, 2000).

³In Equation 8.3, g_χ denotes the degrees of freedom of the particle species χ . In the following, we presume Majorana fermions (Spin 1/2 and $\bar{\chi} = \chi$), such that $g_\chi = 2$.

is required. Such value is remarkably close to the leading order scattering cross-section at the weak scale, $\langle\sigma v\rangle\sim\hbar^2/c\times\alpha_W^2/m_W^2$. This means that in a DM scenario where DM is made up of a yet unknown particle species of mass at the weak scale, a weak-scale freeze-out annihilation cross-section would be naturally required. This fact is commonly dubbed as *WIMP miracle*.

This picture is only one possible realization. There are theories of valid particle DM alternatives that were not in thermal equilibrium in the Universe, or interacted in more complicated ways with the ambient fields exist. Yet, in addition to being one of the preferred and most studied DM particle model, the WIMP scenario provides a very generic framework, and several of the search methods developed for this scenario can be easily reformulated for other cases. As such, we limit ourselves to this case hereafter.

Dark Matter Particle Candidates. The appeal of such generic WIMP as DM candidate was even increased with the advent of the theory of Super-Symmetry (SUSY). Originally proposed to solve open questions unrelated to DM like the electroweak hierarchy problem or the unification of interactions in particle physics, it was soon recognized that supersymmetric particles could also account for WIMP DM (e.g., [Pagels and Primack, 1982](#)).⁴ SUSY depicts a symmetry of SM particles to a new sector populated with particles of similar quantum numbers but spin changed by $\pm 1/2$, thus swapping fermions with bosons, and by this expanding the number of elementary particles. However, why supersymmetric particles have never been observed? Clearly a quantum rule must protect the couplings between the SM and SUSY sectors: the R-parity, which, combining particle spin, baryon and lepton number, provides SM particle with parity number $R = 1$ and SUSY particles with $R = -1$. The conservation of this symmetry not only shields the SM from the SUSY sector, but also automatically makes the lightest SUSY particle stable. Here is the most studied WIMP candidate, the lightest supersymmetric particle (LSP). There is not one single LSP candidate. Yet the one that emerged the most as the best candidate for WIMP DM is the lightest neutralino, mass eigenstate of the superpartners of the photon, the W,Z particle and the two Higgs fields. In principle, if the R-parity was slightly broken, a LSP could have a finite lifetime, as long as it is much larger than the age of Universe or in agreement with lower limits for specific models (e.g. [Buchmuller et al., 2007](#), for gravitino DM). This also holds to any other mechanism to provide stability to a heavy particle. Therefore, it is worth to also watch out for DM decays, as long instruments are able to probe them for such sufficiently large lifetimes. As we will see later, we indeed can probe lifetimes larger than these lower bounds.

Gravitational anomalies and the DM distribution in astrophysical targets. The term DM was probably first used by H. Poincaré in 1906 albeit with the more classical meaning of ‘non emitting light’ (*matière obscure* in [Poincare, 1906](#)).⁵ In fact, at the turn of last century, astronomers started to investigate the distribution of visible objects in the sky and their motion, trying to understand from first principles why matter was clustered in specific form. Early studies by Lord Kelvin, using thermodynamics arguments, and Poincaré, using the virial equilibrium hypothesis, applied to the Milky Way (MW), started to show that a significant fraction of mass was not attributable to stars but needed to be explained by different *dark bodies* such as meteors, or gas clouds. Evidence of missing mass started also to pile up at a much larger scale, that of galaxy clusters. First [Hubble and Humason \(1931\)](#) and then [Zwicky \(1933\)](#) in the first decades of the last

⁴See [Bertone and Hooper \(2016\)](#) for a full historic account.

⁵See [Bertone and Hooper \(2016\)](#).

century found a large scatter in the velocities of galaxies within galaxy clusters, up to 2,000 km/s, difficult to explain with only the visible matter in such clusters. Indeed, Zwicky used the virial theorem on a sample of a thousand galaxies in the Coma cluster and arrived at the conclusion that 500 times more mass was present in the cluster than the one inferred from the visible counterpart⁶. This is the so-called *mass-to-light ratio*, that is, the ratio of the total estimated mass with respect to the mass expected from the luminous matter alone. Thus, this mass-to-light ratio is a measure of how much an astrophysical object is DM dominated. Similar gravitational evidence continued accumulating by the middle of the 20th century, but the “missing mass” problem started to become more intriguing as soon as standard explanations started to be ruled out: X-ray observation limited the amount of hot gas in galaxies to be below 2% (Meekins et al., 1971) and stellar nucleosynthesis could not generate enough helium to accommodate the observed abundance (Burbidge et al., 1957). The advent of precise spectrographs in the 1970s allowed to measure the velocity of gas and stars within galaxies, which in turn allowed determining the mass of individual galaxies. In particular, in spiral galaxies, stars and gas move approximately on circular orbits around the galaxy’s centre. Newtonian dynamics infers that an object placed at distance r from a barycenter should display a circular velocity

$$v_c(r) = \sqrt{\frac{GM(< r)}{r}}. \quad (8.6)$$

That is, objects well outside the size R of a mass distribution, where the total mass $M(< R)$ no longer grows, should have circular velocities following simply $v_c(r) \sim \sqrt{1/r}$. However, in the 1970s, Bosma, Rubin and colleagues (Bosma, 1978, Rubin et al., 1978, Rubin et al., 1980) used samples of ten to dozens of spiral galaxies and found unambiguous evidence of flat circular ($v_c(r) \sim k$) velocities of gas regions well outside the size R determined from the optical extension of the galaxies. These observations allowed to robustly infer for the first time that the distribution of the missing mass extends by several factors beyond the visible mass in individual galaxies, confirming previous findings by Einasto et al. (1974) and early findings for the M31 galaxy (Babcock, 1939). Spectrography is still the best technique nowadays to infer the DM content in galaxies, and is being widely used with instruments such as the Dark Energy Spectroscopic Instrument (DESI, DESI Collaboration et al., 2016).

Driven by insights from N-body cosmological simulations, the DM density profiles of cosmic DM overdensities can be commonly parametrized with the Zhao-Hernquist expression (Hernquist, 1990, Zhao, 1996):

$$\rho(r) = \frac{\rho_0}{\left(\frac{r}{r_s}\right)^\gamma \left[1 + \left(\frac{r}{r_s}\right)^\alpha\right]^{(\beta-\gamma)/\alpha}}, \quad (8.7)$$

where r is the distance from the DM halo centre, r_s and ρ_0 are the so-called scale radius and characteristic DM density, respectively, and α, β, γ are free parameters (Kuhlen et al., 2012). A specific case of this profile, widely used in the literature, is the Navarro-Frenk-White (NFW) parametrization (Navarro et al., 1996) with fixed $\alpha = 1$, $\beta = 3$ and $\gamma = 1$. A profile very similar to the NFW parametrization, but describing the innermost halo slopes in simulations slightly better with one additional parameter α (Navarro et al., 2004, Springel et al., 2008a, Wang et al., 2020) is the so-called Einasto-profile,

⁶This value was based on the estimate of the Hubble parameter H_0 at the time, that was overestimated by a factor of ~ 10 . With the present estimation the imbalance noted by Zwicky would reduce down to a factor 8.

$$\rho(r) = \rho_0 \exp \left\{ \frac{-2}{\alpha} \left[\left(\frac{r}{r_s} \right)^\alpha - 1 \right] \right\}. \quad (8.8)$$

A different analytic description was found for some dwarf spiral galaxies to better fit the inferred DM profile, namely, the so-called Burkert profile (Burkert, 1996),

$$\rho(r) = \frac{\rho_0}{\left(1 + \frac{r}{r_s}\right) \left(1 + \frac{r^2}{r_s^2}\right)}, \quad (8.9)$$

which shows a density plateau in the inner halo centre.

Gamma-ray signatures of DM. Besides trying to produce DM in collider events and to observe their annihilation or decay into more known particles, DM can be observed through nuclear or atomic recoils in noble gas or semiconductors. This method is usually called “direct detection” technique, and there is ample literature about it, e.g., Schumann (2019). A third avenue is to explore DM signatures “indirectly” by observing very-high-energy (VHE) gamma rays generated in relic annihilations or decays of the DM throughout the Cosmos.

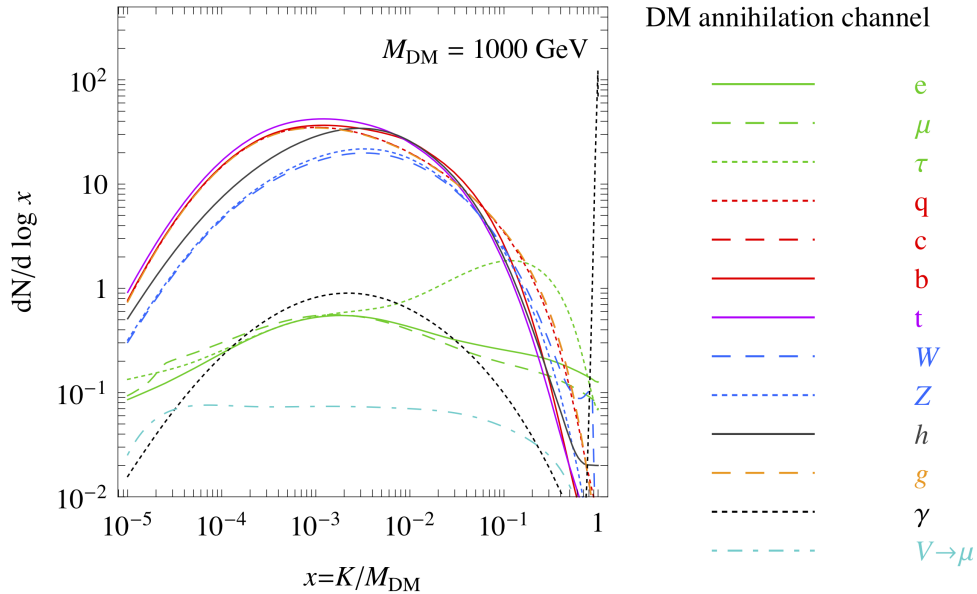


Figure 8.1: Primary DM gamma-ray spectra for various annihilation models. For DM decays, the same spectra are expected, yet with the energy scale shifted to half these values, as the energy is equally distributed in two decay particles. Extracted from Fig. 3 of Cirelli et al. (2011) with the permission of the authors.

High-energy photons are found primarily as a result of neutral pion decay, where the pions are created after fragmentation of quarks expected to be produced in DM annihilations or decays. Such origin of gamma radiation results in a continuous spectrum (Fig. 8.1). As such, the latter may be indistinguishable from other astrophysical processes in which pion decays are found. However, if

the DM is cold, i.e. non-relativistic, an abrupt spectral cutoff is expected at the DM mass for annihilating DM, or at its half for decaying DM. In more sophisticated scenarios, enhanced or even line-like emission may occur at the termination energy set by the particle mass (Bergstrom and Kaplan, 1994, Bringmann et al., 2008). Because of the peculiarity of searches for line-like signals with IACTs, these will be discussed separately in the following. In any case, all these cut-off features make the resulting spectra from DM annihilation or decay very distinct from those of other astrophysical phenomena. Another consequence arises from the energy scale of the annihilation products set by the mass of the cold DM particle: should the latter be of the order of the GeV to TeV, gamma rays would be generated at these same energies, and ground-based VHE gamma-ray detectors like IACTs would be perfectly suited for such indirect searches for DM. Indeed, at WIMP masses above several TeV, IACTs currently are the most sensitive instruments to search for such particles. Finally, there are several other avenues for indirect DM searches, by looking for other of DM annihilation or decay products, namely charged cosmic rays or neutrinos. While these searches are not in the scope of this review, on page 25 we will mention the possibility to use IACTs to study the cosmic-ray electron and positron flux to search for DM signatures.

Although DM possesses a nearly unique or very characteristic gamma-ray spectrum, the amount of annihilation or decay expected events – and therefore the detectability at Earth – ultimately depends on the integrated density, squared in the annihilating case, of DM along the line of sight. Because of that, overdense DM regions are clearly preferred, such as those at the centre of galaxies or clusters of galaxies. The computation of the double differential gamma-ray DM flux at Earth can therefore be written as:⁷

$$\begin{aligned}
 \text{Annihilation : } \quad & \frac{d\Phi}{dE d\Omega} = \frac{1}{4\pi} \frac{\langle\sigma v\rangle}{2m_{\text{DM}}^2} \frac{dN_\gamma}{dE} \frac{dJ_{\text{ann}}}{d\Omega}, \quad \text{with} \\
 & \frac{dJ_{\text{ann}}}{d\Omega} = \int_{\text{l.o.s.}} dl \rho^2(l, \Omega). \\
 \text{Decay : } \quad & \frac{d\Phi}{dE d\Omega} = \frac{1}{4\pi} \frac{1}{\tau_{\text{DM}} m_{\text{DM}}} \frac{dN_\gamma}{dE} \frac{dJ_{\text{dec}}}{d\Omega}, \quad \text{with} \\
 & \frac{dJ_{\text{dec}}}{d\Omega} = \int_{\text{l.o.s.}} dl \rho(l, \Omega).
 \end{aligned} \tag{8.10}$$

Here, m_{DM} is the DM mass, τ_{DM} the DM lifetime, $\langle\sigma v\rangle$ is the velocity-averaged annihilation cross-section; dN_γ/dE is the average number of photons per unity energy per reaction, J_{dec} is called the *astrophysical factor* (Bergstrom et al., 1998) for decaying DM, and J_{ann} is the astrophysical factor for the annihilating case. Note that, in order to derive the expected DM-induced flux from a given target, one needs to integrate along the line of sight (*l.o.s.*) and the aperture $\Delta\Omega$. Note also that Eq. 8.10 is factorized so that one factor entails information about the microscopic DM properties (mass, cross-section or lifetime, average photon emission) while the astrophysical factor encloses separately all the information on the DM spatial distribution.⁸ In most cases, for collisionless DM, the latter is almost independent on the specific microscopic nature of DM and thus the astrophysical factor is very general.⁹ Yet, other cases are also possible, such as self-interacting DM,

⁷The annihilation formula is valid for self-conjugate DM particles ($\bar{\chi} = \chi$), otherwise there is an additional factor 1/2.

⁸Strictly speaking, the factorization only holds for integration over a small redshift span, $\Delta z/z \ll 1$.

⁹However, the mass of the smallest predicted CDM halos is ultimately set by the properties of the DM particle

in which the exact DM density profile will depend on the DM particle’s characteristics (Kahlhoefer et al., 2019). In all cases, the expected gamma-ray spectra should look the same across different astrophysical targets. Thus, observing two independent targets with identical spectra would constitute a strong case in favour of the DM interpretation.

The density integral in Eq. 8.10 is very sensitive to the density scaling in the halo centre, in particular for integrating over the square-density in case of annihilation. Therefore, if interested in maximizing the DM-induced gamma-ray signals, the telescope should be pointed to those astrophysical environments exhibiting the highest DM concentrations at their centres. Also, since fluxes decrease as the inverse of the distance squared, the closer the targets, the better.¹⁰ Fortunately, a plethora of objects are such viable candidates for DM searches with IACTs: the closest and probably brightest in terms of DM-induced flux is the centre of the MW. Further out, dwarf spheroidal galaxies (dSphs) are optimal targets as well, especially those nearby and with large mass-to-light ratios. Much further out, galaxy clusters host a huge DM content, which could provide a significant emission at Earth as well. Less favored or more debated objects may also be interesting, such as Galactic globular clusters: their origin is still a matter of debate and there is the possibility that they could retain significant DM density spikes at their very centres (Brown et al., 2018). IACT DM searches in all these objects will be presented in the following.

Review of WIMP DM searches with IACTs

The search for WIMP DM with IACTs started along with the birth of this class of instruments, and strongly evolved in expectations, methods and dedications over the years. In the following, we gather all these observations as a summary of what it has been done so far and in order to guide our experience in the future.

Classical targets were first considered: the central region of the MW, the MW Dwarf Spheroidal Galaxies (dSphs) and galaxy clusters. The interest expanded to less established targets such as Intermediate Mass Black Holes (IMBHs) and dark satellites. In general, searches have been conducted looking for DM-induced continuum emission and line-like emission, and both for decaying and annihilating DM. Not only gamma-ray signatures, but also antiparticle signatures which may originate from DM annihilation or decay have been searched for, demonstrating the capability of IACTs as antiparticle detectors from the ground. It is interesting to see how early efforts invested relatively low observation times of the order of few hours, while later observation campaigns show more than a hundred hours devoted to single targets. Considering the total available observation time in a year of a single IACT experiment is about 1,000 h, it is obvious that a large time investment has been made, with more than 1,500 h of observation time devoted exclusively to dSphs as of today.

In Table 8.1 we have collected, to the best of our knowledge, all the DM search campaigns carried out by IACTs. The table, an update of the one in Doro (2014), now including results up to 2021, gathers the numerous targets scrutinized as of today. The content is organized by target class and year of observation, and also the duration of observation is reported. In the following, we decide to discuss in detail all these observations according to target class.

itself; this fact may have important implications in computations of the DM-induced gamma-ray flux involving halo substructure, as those that will be commented later on in this section.

¹⁰The inverse square-distance scaling is contained, but hidden in Equation 8.10 by the factor $1/l^2$ cancelling out the l^2 in the volume element.

Table 8.1: Summary of the campaigns carried out by IACTs to indirectly search for DM with gamma rays. We report observations from the Whipple, H.E.S.S., MAGIC, and VERITAS experiments, sorted by astrophysical target class. First column is the name of the target. Second and third columns refer to the year and duration (in hours) of observations, respectively. The fifth column informs about the type of limit, either annihilation or decay. Unconfirmed dSph candidates are marked with an asterisk. H.E.S.S. data including the H.E.S.S. Phase II telescope are marked with a †, MAGIC data from monoscopic observations with MAGIC-I are marked with a ‡. Times in parentheses denote data which are also a subset of other analyses. We also include yet unpublished data presented at conferences.

| Target | Year | Time [h] | IACT | Limit | Ref. |
|--|-------------|-------------|-----------|---------|---|
| The Milky Way central region & halo | | | | | |
| MW Centre | 2004 | (48.7) | H.E.S.S. | Ann. | Aharonian et al. (2006) |
| MW Inner Halo | 2004 – 2008 | (112) | H.E.S.S. | Ann. | Abramowski et al. (2011) |
| | 2010 | 9.1 | | Ann. | Abramowski et al. (2015) |
| | 2004 – 2014 | 254 | | Ann. | Abdallah et al. (2016) |
| | 2014 – 2020 | 546 | H.E.S.S.† | Ann. | Montanari et al. (2021) |
| MW Outer Halo | 2018 | 10 | MAGIC | Decay | Ninci et al. (2019) |
| Dwarf Satellite Galaxies | | | | | |
| Draco | 2003 | 7.4 | Whipple | Ann. | Wood et al. (2008) |
| | 2007 | 7.8 | MAGIC‡ | Ann. | Albert et al. (2008b) |
| | 2007 | (18.4) | VERITAS | Ann. | Acciari et al. (2010) |
| | 2007 – 2013 | (49.8) | | Ann. | Archambault et al. (2017) |
| | 2007 – 2018 | 114 | | – | Kelley-Hoskins (2018) |
| | 2018 | 52.6 | MAGIC | Ann. | Maggio et al. (2021) |
| Ursa Minor | 2003 | 7.9 | Whipple | Ann. | Wood et al. (2008) |
| | 2007 | (18.9) | VERITAS | Ann. | Acciari et al. (2010) |
| | 2007 – 2013 | (60.4) | | Ann. | Archambault et al. (2017) |
| | 2007 – 2018 | 161 | | – | Kelley-Hoskins (2018) |
| Sagittarius | 2006 | (11.0) | H.E.S.S. | Ann. | Aharonian et al. (2008) |
| | 2006 – 2012 | 90 | | Ann. | Abramowski et al. (2014) |
| | 2006 – 2012 | (85.5) | | Ann. | Abdalla et al. (2018a) |
| Canis Major | 2006 | 9.6 | H.E.S.S. | Ann. | Aharonian et al. (2009a) |
| | Willman 1 | 2007 – 2008 | 13.7 | VERITAS | Ann. |
| | | | (13.6) | | Ann. |
| Sculptor | 2008 | 15.5 | MAGIC‡ | Ann. | Aliu et al. (2009) |
| | 2008 | (11.8) | H.E.S.S. | Ann. | Abramowski et al. (2011) |
| Carina | | | | Ann. | Abdalla et al. (2018a) |
| | 2008 – 2009 | 12.5 | | Ann. | Abramowski et al. (2014) |
| | 2008 – 2009 | (14.8) | H.E.S.S. | Ann. | Abramowski et al. (2011) |
| | 2008 – 2009 | (12.7) | | Ann. | Abramowski et al. (2014) |
| | 2008 – 2010 | 22.9 | | Ann. | Abdalla et al. (2018a) |

Table 8.1 – Continued on next page

Table 8.1 – continued from previous page

| Target | Year | Time [h] | IACT | Limit | Ref. |
|------------------------|-------------|----------------|-----------------------|-------|--|
| Segue 1 | 2008 – 2009 | 29.4 | MAGIC [‡] | Ann. | Aleksić et al. (2011) |
| | 2010 – 2011 | (47.8) | VERITAS | A.+D. | Aliu et al. (2012) |
| | 2010 – 2013 | (92.0) | | Ann. | Archambault et al. (2017) |
| | 2010 – 2013 | 157.9 | MAGIC | A.+D. | Aleksić et al. (2014) |
| | | | | Ann. | Ahnen et al. (2016b) |
| Boötes 1 | 2010 – 2018 | 184 | VERITAS | – | Kelley-Hoskins (2018) |
| | 2009 | 14.3 (14.0) | VERITAS | Ann. | Acciari et al. (2010) Archambault et al. (2017) |
| Coma Berenices | 2010 – 2013 | (8.6) | H.E.S.S. | Ann. | Abramowski et al. (2014) |
| | 2010 – 2013 | 10.9 | | Ann. | Abdalla et al. (2018a) |
| | < 2018 | 37 | VERITAS | – | Kelley-Hoskins (2018) |
| | 2018 | 50.2 | MAGIC | Ann. | Maggio et al. (2021) |
| Fornax | 2010 | 6.0 | H.E.S.S. | Ann. | Abramowski et al. (2014) Abdalla et al. (2018a) |
| Ursa Major II | 2014 – 2016 | 94.8 | MAGIC | Ann. | Ahnen et al. (2018a) |
| Triangulum II* | 2014 – 2016 | 62.4 | MAGIC | Ann. | Acciari et al. (2020) |
| | < 2018 | 181 | VERITAS | – | Kelley-Hoskins (2018) |
| Segue II | < 2018 | 19 | VERITAS | – | Kelley-Hoskins (2018) |
| Canes Ven I | < 2018 | 14 | VERITAS | – | Kelley-Hoskins (2018) |
| Canes Ven II | < 2018 | 14 | VERITAS | – | Kelley-Hoskins (2018) |
| Hercules | < 2018 | 13 | VERITAS | – | Kelley-Hoskins (2018) |
| Sextans | < 2018 | 13 | VERITAS | – | Kelley-Hoskins (2018) |
| Draco II | < 2018 | 10 | VERITAS | – | Kelley-Hoskins (2018) |
| Leo I | < 2018 | 7 | VERITAS | – | Kelley-Hoskins (2018) |
| Leo II | < 2018 | 16 | VERITAS | – | Kelley-Hoskins (2018) |
| Leo IV | < 2018 | 3 | VERITAS | – | Kelley-Hoskins (2018) |
| Leo V | < 2018 | 3 | VERITAS | – | Kelley-Hoskins (2018) |
| Reticulum II | 2017 – 2018 | 18.3 | H.E.S.S. [†] | Ann. | Abdalla et al. (2020) |
| Tucana II | 2017 – 2018 | 16.4 | H.E.S.S. [†] | Ann. | Abdalla et al. (2020) |
| Tucana III* | 2017 – 2018 | 23.6 | H.E.S.S. [†] | Ann. | Abdalla et al. (2020) |
| Tucana IV* | 2017 – 2018 | 12.4 | H.E.S.S. [†] | Ann. | Abdalla et al. (2020) |
| Grus II* | 2018 | 11.3 | H.E.S.S. [†] | Ann. | Abdalla et al. (2020) |
| Dark satellites | | | | | |
| 1FGL J2347.3+0710 | 2010 | 8.3 | MAGIC | – | Nieto et al. (2011a) |
| 1FGL J0338.8+1313 | 2010-2011 | 10.7 | MAGIC | – | Nieto et al. (2011a) |
| 2FGL J0545.6+6018 | 2013-2015 | 8.5 | VERITAS | Ann. | Nieto (2015) |
| 2FGL J1115.0-0701 | 2013-2015 | 13.8 | VERITAS | Ann. | Nieto (2015) |
| H3FHL J0929.2-4110 | 2018-2019 | 7.8 | H.E.S.S. [†] | Ann. | Abdallah et al. (2021a) |
| 3FHL J1915.2-1323 | 2018 – 2019 | 3.0 | H.E.S.S. [†] | Ann. | Abdallah et al. (2021a) |
| 3FHL J2030.2-5037 | 2018 – 2019 | 8.8 | H.E.S.S. [†] | Ann. | Abdallah et al. (2021a) |
| 3FHL J2104.5+2117 | 2018 – 2019 | 5.5 | H.E.S.S. [†] | Ann. | Abdallah et al. (2021a) |

Table 8.1 – Continued on next page

Table 8.1 – continued from previous page

| Target | Year | Time [h] | IACT | Limit | Ref. |
|--------------------------------------|-------------|----------|-----------------------|-------|---|
| Intermediate Mass Black Holes | | | | | |
| Galactic Plane Survey | 2004 – 2007 | 400 | H.E.S.S. | Ann. | Aharonian et al. (2008a) |
| | 2005 – 2006 | 25 | MAGIC [‡] | Ann. | Doro et al. (2007) |
| Globular Clusters | | | | | |
| M15 | 2002 | 0.2 | Whipple | Ann. | Wood et al. (2008) |
| | 2006 – 2007 | 15.2 | H.E.S.S. | Ann. | Abramowski et al. (2011) |
| NGC 6388 | 2008 – 2009 | 27.2 | H.E.S.S. | Ann. | Abramowski et al. (2011) |
| Other galaxies | | | | | |
| M33 | 2002 – 2004 | 7.9 | Whipple | Ann. | Wood et al. (2008) |
| M32 | 2004 | 6.9 | Whipple | Ann. | Wood et al. (2008) |
| WLM | 2018 | 18.2 | H.E.S.S. [†] | Ann. | Abdallah et al. (2021b) |
| Galaxy Clusters | | | | | |
| Abell 2029 | 2003 – 2004 | 6.1 | Whipple | – | Perkins et al. (2006) |
| Perseus (Abell 426) | 2004 – 2005 | 13.5 | Whipple | – | Perkins et al. (2006) |
| | 2008 | 24.4 | MAGIC [‡] | Ann. | Aleksić et al. (2010) |
| | 2009 – 2017 | 202.2 | MAGIC | Decay | Acciari et al. (2018) |
| Fornax (Abell S0373) | 2005 | 14.5 | H.E.S.S. | Ann. | Abramowski et al. (2012) |
| Coma (Abell 1656) | 2008 | 18.6 | VERITAS | Ann. | Arlen et al. (2012) |
| Line searches | | | | | |
| MW Inner Halo | 2004 – 2008 | (112) | H.E.S.S. | Ann. | Abramowski et al. (2013c) |
| | 2014 | 15.2 | H.E.S.S. [†] | Ann. | Abdalla et al. (2016) |
| | 2004 – 2014 | (254) | H.E.S.S. | Ann. | Abdalla et al. (2018b) |
| | 2013 – 2019 | 204 | MAGIC | Ann. | Inada et al. (2021) |
| Segue 1 dSph | 2010 – 2013 | (157.9) | MAGIC | A.+D. | Aleksić et al. (2014) |
| Five dSph galaxies | 2006 – 2012 | (137.1) | H.E.S.S. | Ann. | Abdalla et al. (2018a) |
| Five dSph galaxies | 2007 – 2013 | (229.8) | VERITAS | Ann. | Archambault et al. (2017) |
| WLM | 2018 | (18.2) | H.E.S.S. [†] | Ann. | Abdallah et al. (2021b) |
| Charged particles | | | | | |
| All-electron | 2004 – 2007 | 239 | H.E.S.S. | – | Aharonian et al. (2008b, 2009b) |
| | 2009 – 2012 | 296 | VERITAS | – | Archer et al. (2018) |
| | 2009 – 2010 | 14 | MAGIC | – | Borla Tridon et al. (2011) |
| Moon shadow | 2010 – 2011 | 20 | MAGIC | – | Colin et al. (2011) |
| | 2014 | 1.2 | VERITAS | – | Bird et al. (2016) |

Observations of the MW Centre and halo. The Galactic Centre (GC) is a prime target for DM searches with IACTs. It is best observed from the Southern Hemisphere, where the High Energy Stereoscopic System (H.E.S.S.) telescopes are located. This guarantees the lowest energy threshold and a longer observability. In 2006, H.E.S.S. published the observation of a signal from

the Galactic Centre (GC) above 160 GeV and its interpretation in terms of DM after an observation campaign of about 50 h (Aharonian et al., 2006). In that work, DM density profiles as obtained from N-body cosmological simulations of MW-size halos were adopted, namely the NFW (Equation 8.7 with $\alpha, \beta, \gamma = 1, 3, 1$) and Einasto (Equation 8.8). Large differences between the two DM profile parametrizations occur only at the very centre of the halo, where the NFW profile is more strongly peaked, while already at distances from the GC larger than ~ 10 pc the density descriptions become very similar when adopting the same profile normalization at the Solar position. This was the reason for H.E.S.S. to focus on an analysis region at a projected Galactocentric distance of 45 – 150 pc that corresponds to an angular distance of $0.3 - 1.0^\circ$ from the GC. Furthermore, the contamination from known and expected gamma-ray astrophysical sources at this distance from the GC is largely reduced with respect to the very central region. Limits on the annihilation cross-section were first presented in Abramowski et al. (2011) using 112 h of data and remained for long the most constraining upper limits on DM annihilations from IACTs. More recently, Abdallah et al. (2016) gathered 10 years of H.E.S.S. datataking, involving a total of 254 h good quality data, which resulted in the DM exclusion limits shown in Fig. 8.2 for the $b\bar{b}$ and $\tau^+\tau^-$ pure annihilation cases. The limits were obtained after an elaborated selection of both the signal and background regions in the proximity of the GC, that removes the Galactic plane and known TeV emitters. It can be seen that, while the limits for $b\bar{b}$ approach the thermal relic cross-section value at few TeV, the ones for $\tau^+\tau^-$ actually already skim the canonical parameter space. These limits represent the strongest ones obtained by IACTs at present, recently even extended by the announcement of the publication of a data set comprising almost 550 h of data (Montanari et al., 2021). Also the Major Atmospheric Gamma-ray Imaging Cherenkov (MAGIC) telescopes (Albert et al., 2006) and the Very Energetic Imaging Telescope Array System (VERITAS) (Beilicke, 2012) observed the GC along the years, yet with more modest performance compared to H.E.S.S. due to their location in the Northern Hemisphere as opposed to H.E.S.S.. Because of that, neither MAGIC nor VERITAS were able to draw conclusions on DM physics.

It must be noted that all mentioned DM limits are only valid as long as a cuspy profile of the distribution of DM toward the MW centre is assumed, as it is the case for both NFW and Einasto profiles. However, it is still equally plausible that the actual DM profile toward the GC is more cored and closer to the so-called Burkert profile, Equation 8.9. This would strongly reduce the DM sensitivity, not only because of a much smaller J -factor, but also because most DM analyses of IACT data rely on the existence of a DM density contrast between a signal and background region. Such cored profiles can appear e.g. when baryonic feedback occurs in connection with strong stellar activity that sweeps outward the matter and dilutes the DM concentration in the innermost regions of the Galaxy (Di Cintio et al., 2013, Lazar et al., 2020, Read et al., 2019, Tollet et al., 2016). Also, self-interacting DM is expected to form pronounced halo cores (e.g., Rocha et al., 2013, Tulin and Yu, 2018). Due to the crowded line of sight towards the GC and the complex dynamics in the Galactic bulge, an empirical, direct determination of the inner GC DM density profile from e.g. kinematics data of different tracers in the area is very difficult. Therefore, the inner profile is yet poorly constrained (Benito et al., 2019, 2021). For these reasons, despite being far more constraining than others, GC limits need to be treated with special caution. In 2015, the H.E.S.S. collaboration published a study constraining DM annihilation from a DM core around the GC, based on 9 h of dedicated observations with a background subtraction region $\gtrsim 5^\circ$ away from the GC (Abramowski et al., 2015). A similar methodology addressing DM decay in the Galactic halo has been pursued by the MAGIC collaboration (Ninci et al., 2019). In the conclusion of this

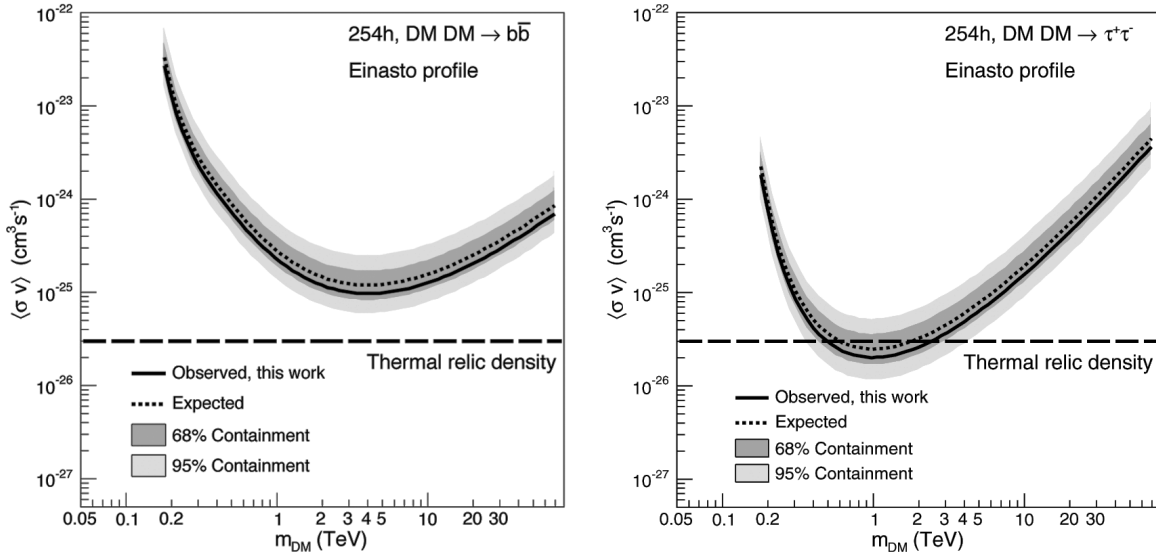


Figure 8.2: Constraints on the velocity-weighted annihilation cross section derived from 10 years of GC observations by H.E.S.S. for the $b\bar{b}$ (left panel) and into $\tau^+\tau^-$ (right panel). The observed upper limit is plotted as a solid black line. Expected limits are derived from blank-field observations at high Galactic latitudes. The mean expected limit (black dashed line) is plotted together with the 65% (dark gray) and 95% (light gray) confidence bands. The natural scale for the annihilation cross-section is given as long-dashed black line. Figures from [Abdallah et al. \(2016\)](#), courtesy of the H.E.S.S. collaboration.

section, we will discuss the significant improvement that the Cherenkov Telescope Array (CTA) will bring even for this pessimistic scenario of a cored DM profile in the GC. Note that the caveat of potential DM cores is also present in the case of dSphs. Yet it is considered much less severe compared to the GC case. First, because the inner dSph DM profiles are better constrained, and second, because the dSph galaxies are expected to show, at least for standard CDM, cuspier inner profiles due to their comparatively low baryonic content.

Observation of dSphs. DSphs are small galaxies, with masses of the order $10^7 - 10^9 M_\odot$, gravitationally bound to their host galaxy ([Strigari et al., 2008](#)). In the MW, they are located within the MW virial radius at typical heliocentric distances of 20 – 250 kpc.¹¹ They are considered to be in internal dynamical equilibrium and exhibit mass-to-light ratios of the order of 100 – 1000, meaning that they are highly DM dominated systems. In addition, the great interest in these objects for indirect DM searches stems from the fact that dSphs display very reduced stellar activity in the past few Gyr. This turns out in an unlikely emission of high-energy photons of an astrophysics origin, that is, photons coming from the depletion of interstellar gas and sources of high-energy cosmic rays. Thus, any putative gamma-ray signal in these objects would be, most likely, of exotic origin. As a result, dSphs are considered one of the cleanest targets for indirect DM searches. Furthermore, the low stellar activity may have allowed an efficient DM contraction, with reduced

¹¹See [Strigari \(2018\)](#) for an excellent overview on these targets.

matter redistribution to e.g. supernova explosions and shocks propagation (Lazar et al., 2020, Read et al., 2019). Because of this, such compact DM overdensities result in promising conditions for annihilating DM searches according to Equation 8.10, yet less for decays (Bonnivard et al., 2015b, Geringer-Sameth et al., 2015). Estimates of the total number of MW dwarf satellites in a Λ CDM universe predict the existence of hundreds of these objects within the MW virial radius (Hargis et al., 2014, Tollerud et al., 2008). Discrepancies between observations and expectations from N-body cosmological simulations were reported in the past (the so-called “missing satellite problem” discussed in e.g. Hargis et al., 2014, Klypin et al., 1999, Moore et al., 1999, Strigari et al., 2007). However, not only our census of dSphs is known to be incomplete, but more importantly, the discrepancy may be related to the fact that a large fraction of dSphs, especially at the smallest scales, are expected to contain little or no baryonic material in the form of stars and gas. Therefore they would remain basically as dark DM overdensities (Bullock and Boylan-Kolchin, 2017, Sawala et al., 2015). An additional potential issue with these targets is the fact that Λ CDM predicts a larger number of massive dSphs than what it is actually observed. In other words, these massive galaxies should necessarily contain visible counterparts which are nevertheless not seen. This is the so-called “too big to fail” problem (Boylan-Kolchin et al., 2011, Read et al., 2006). Possible arguments to mitigate this issue include a more accurate description of subhalo disruption and mass loss, and of the role and evolution of the baryonic contents in these objects (Brooks and Zolotov, 2014, Garrison-Kimmel et al., 2018, Helmi et al., 2012, Tomozeiu et al., 2016).

dSphs are commonly classified in “classical” and “ultra-faint” galaxies, depending on whether they were discovered before or after the Sloan Digital Sky Survey (SDSS; York et al., 2000), which roughly translates into a brightness cut. Yet, this distinction shadows more subtle differences: ultra-faint dSphs possess more compact sizes, less visible stars, and are typically more DM dominated systems than the classical ones, with mass-to-light ratios sometimes exceeding $1000 M_{\odot}/L_{\odot}$ (Bonnivard et al., 2015b). In addition, observation (Hayashi et al., 2020) and numerical simulations (e.g., Lazar et al., 2020, Read et al., 2019) suggest that the inner cusp of the DM profile increases with decreasing baryonic activity, as expected from classical dwarf systems down to ultra-faint ones. In addition to the nine classical dSphs known, nearly 50 ultra-faint dSph *candidates* have been discovered in photometric surveys since then, mostly with SDSS itself and, most recently, with Dark Energy Survey (DES) data (Drlica-Wagner et al., 2015, 2018). From this number, about 40 have already been confirmed to be dSphs by means of follow-up spectroscopic measurements. For each dSph, the J -factor is computed via the Jeans hydrostatic equilibrium equation from the measured positions and velocities of member stars. To solve the equation one needs to input a model for the star phase-space and another one for the DM density profile, whose normalization is left as a free parameter.¹² This technique relies on several assumptions on the geometry of the DM subhalo hosting the dSph: triaxiality, anisotropy, and co-rotation all constitute relevant ansatzes. Another factor is the misreconstruction of interloper stars, especially that of binary systems, whose intrinsic high velocities strongly affect the computation of velocity distribution and, ultimately, of the dSph J -factor. However, the main limiting factor is the very small number of stars, down to few tens, observed in the dimmer ultra-faint dSphs compared to the thousands of stars observed in the larger ones. The interplay between these ansatzes and limitations are discussed by, e.g., Ando et al. (2020), Bonnavard et al. (2015a, 2016), Chiappo et al. (2017), Ichikawa et al. (2017, 2018), Klop et al. (2017).

Since 2004, these targets have been extensively studied by IACTs in the context of DM searches

¹²All the details of these calculations are reviewed, e.g., by Strigari (2012).

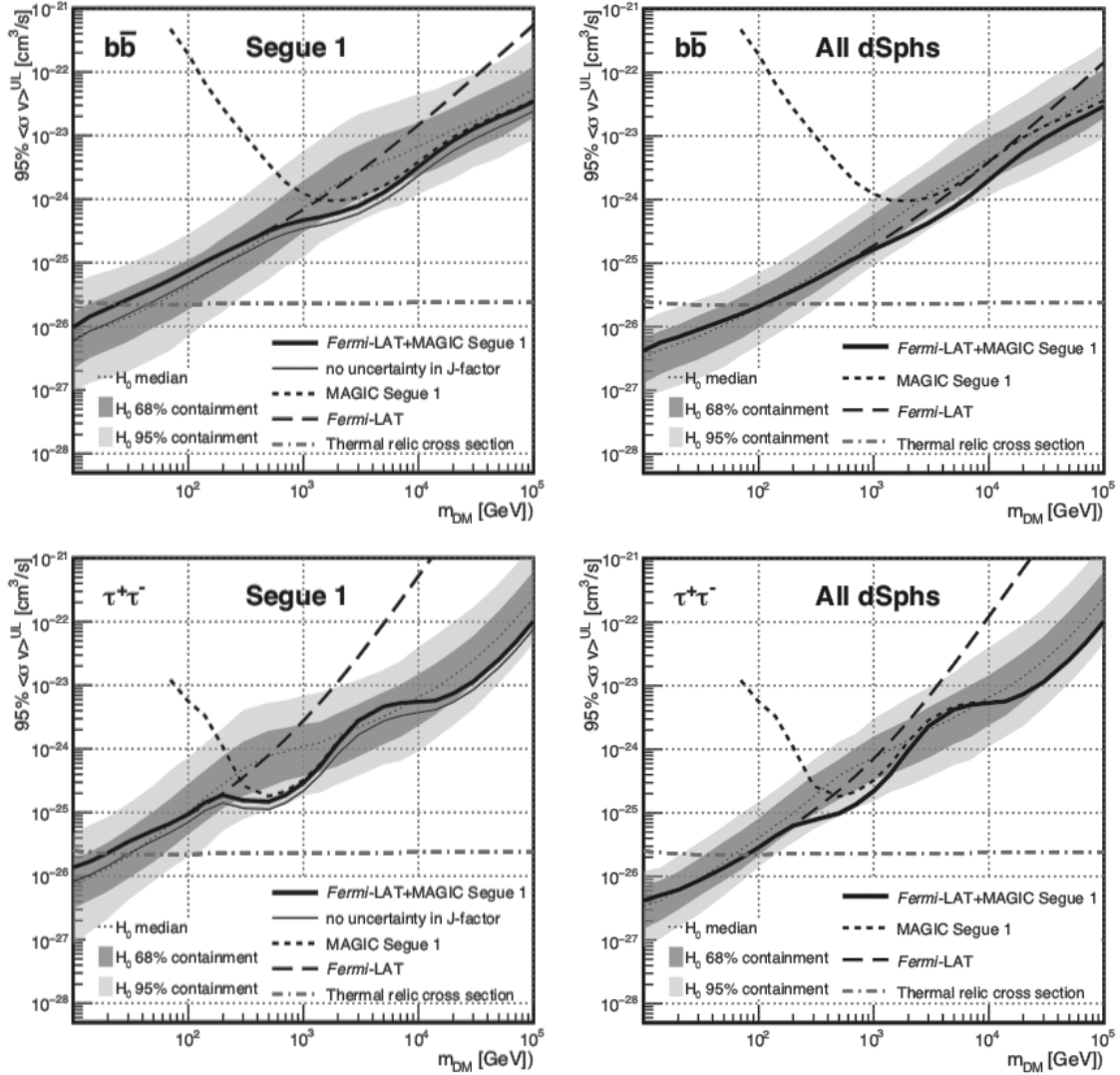


Figure 8.3: 95% C.L. upper limits on the thermally-averaged cross-section for DM particles annihilating into $b\bar{b}$ (top row) and $\tau^+\tau^-$ (bottom-row). Thick solid lines show the limits obtained by combining Segue 1 observations from *Fermi*-LAT and MAGIC (left column), and the observations of 15 dSphs with the *Fermi*-LAT and Segue 1 with MAGIC (right column). Dashed lines show the observed individual MAGIC (short dashes) and *Fermi*-LAT (long dashes) limits. The thin-dotted line, dark and light gray bands show, respectively, the median and the symmetrical, two-sided 68% and 95% containment bands for the distribution of limits under the null hypothesis. The red-dashed-dotted line shows the thermal relic cross-section from [Steigman et al. \(2012\)](#). Image courtesy of the MAGIC Collaboration and reproduced from [Ahn et al. \(2016b\)](#).

as shown in Table 8.1. Many targets have been sighted with exposures ranging from few hours to more than 150 h. Along almost 20 years we have observed the classical dSphs Canis Major, Carina, Draco, Fornax, Leo I-II, Sextans, Sculptor, and Ursa Minor; the tidally-disrupted Sagittarius; and the ultra-faint systems Boötes, Canes Venatici I-II, Coma Berenices, Draco 2, Grus-II, Leo IV-V,

Hercules, Reticulum II, Segue 1-2, Triangulum II, Tucana II-III-IV, Ursa Major 2 and Willman 1.¹³ We already noted that in early times only few hours were devoted to single targets. Part of the reason is that, back then, the prospects of detection were in general more optimistic than today (Bergstrom and Hooper, 2006). Also, the large uncertainties related to the estimation of the DM content in dSph galaxies asked for a diversification strategy, such that a larger pool of different dSphs was targeted. As a matter of fact, the exclusion DM limits have significantly improved since the first publications for the classical dSphs to the latest ones on both classical and ultra-faint dwarf systems. This was possible thanks to extended observation times and improved analysis techniques, as reviewed in detail by Rico (2020). Aleksic et al. (2012) were the first to present a dedicated maximum likelihood approach for DM analyses with IACTs, which allows to account for both the spectral and morphological shape of putative DM emission, this way significantly enhancing the sensitivity to DM. This work was also the first one to combine data from different sources and instruments. The same approach was consequently applied to analyses of the deep observations performed with the MAGIC stereo system (Acciari et al., 2020, Ahnen et al., 2016b, Ahnen et al., 2018a, Aleksić et al., 2014). As used in Acciari et al. (2020), Ahnen et al. (2018a), the likelihood binned in energy is built as follows:

$$\begin{aligned}
\mathcal{L}(\langle\sigma v\rangle; \nu_i | \mathcal{D}_i) &= \mathcal{L}(\langle\sigma v\rangle; s_{ij}, J, \tau_i | N_{ij}^{\text{ON}}, N_{ij}^{\text{OFF}}) \\
&= \prod_{j=1}^{\text{bins}} \left[\frac{(s_{ij}(\langle\sigma v\rangle + b_{ij}))^{N_{ij}^{\text{ON}}}}{N_{ij}^{\text{ON}}!} e^{-((s_{ij}(\langle\sigma v\rangle + b_{ij})))} \times \frac{(\tau_i b_{ij})^{N_{ij}^{\text{OFF}}}}{N_{ij}^{\text{OFF}}!} e^{-(\tau_i b_{ij})} \right] \\
&\times \prod_{j=1}^{\text{bins}} [\mathcal{G}(\tau_i | \tau_{\text{obs},i}, \sigma_{\tau_{\text{obs},i}})] \times \mathcal{G}(J | J_{\text{obs}}, \sigma_J)
\end{aligned} \tag{8.11}$$

where the likelihood is the product of likelihoods over the number of N_{bins} energy intervals that have $\langle\sigma v\rangle$ as parameter of interest, the astrophysical J -factor, the normalization between signal and control regions τ_i and the estimated number of signal and background events s_{ij}, b_{ij} as nuisance parameters. The number of measured events in the signal and background extraction regions are N_{ij}^{ON} and N_{ij}^{OFF} , respectively; The terms $\mathcal{G}(J)$ and $\mathcal{G}(\tau_i)$ are the Gaussian likelihoods for the J -factor and the ratio of the signal- to background-region exposure. The estimated signal s_{ij} depends on the parameter of interest $\langle\sigma v\rangle$ as:

$$s_{ij}(\langle\sigma v\rangle) = T_j^{\text{obs}} \int_{\text{bin},j} dE'_{\text{bin},j} \int dE \frac{d\phi(\langle\sigma v\rangle)}{dE} A_{\text{eff}}(E) G(E'|E), \tag{8.12}$$

where T_j^{obs} is the observation time, $\phi(\langle\sigma v\rangle)$ is the intrinsic flux, $A_{\text{eff}}(E)$ the effective area and $G(E'|E)$ the migration matrix between true and reconstructed energy.

Marginalizing the instrument response functions and the J -factor uncertainties in a full likelihood approach not only allows to stack results of the same instrument, but also, as said, to combine limits from different instruments. In Ahnen et al. (2016b), the unbinned approach from Aleksic et al. (2012) was used to combine for the first time IACT data from MAGIC on Segue 1 with multi-dSph data from *Fermi*-LAT. These limits are shown in Fig. 8.3, and still provide the most constraining results for indirect DM searches at dSphs with IACTs.¹⁴ A similar unbinned likelihood analysis method based on *event weighting* has been developed by the VERITAS collaboration

¹³Note that not all of these ultrafaint systems are already confirmed dSphs.

¹⁴Note, however, that these limits could be deteriorated by some yet unaccounted uncertainty on the Segue I DM content and its corresponding J -factor (Bonnivard et al., 2016).

using individual event information to improve the sensitivity from a joint analysis of five individual dSph targets into a single limit (Archambault et al., 2017). Also, the H.E.S.S. collaboration had adopted a simplified version of Equation 8.11 to combine data from five dSphs, to search both for continuum (Abramowski et al., 2014) and line (Abdalla et al., 2018a) emission. Currently, a collaborative effort is ongoing among the H.E.S.S., MAGIC, VERITAS, *Fermi*-LAT, and High Altitude Water Cherenkov Experiment (HAWC) collaborations to provide combined DM limits using a vast amount of data collected from dSphs so far (Armand et al., 2021). This study shall include more than 500 h of IACT data plus 10 years *Fermi*-LAT integrated time on 20 dSphs and 1038 days of HAWC exposure on 12 dSphs.

In summary, limits from dSphs now reach values of cross-section of the order of $10^{-24} \text{ cm}^3 \text{ s}^{-1}$ and are perceived by the community as the most robust obtained with IACTs. In the outlook of this section, we will shortly discuss the expectation for CTA on dSphs.

Observation of dark satellites. In the standard cosmological framework, small dense DM structures form first in the early Universe and later merge to larger halos. A natural consequence of this scenario of hierarchical bottom-up structure formation is that it predicts abundant substructures, or “subhalos”, inside larger halos like our own Galaxy. The most massive of these subhalos in our own Galaxy host the known dwarf satellite galaxies of the Milky Way, while smaller subhalos with masses below $\sim 10^7 M_\odot$ may harbour no stars or gas at all and thus may remain completely dark. These less massive DM subhalos, with no astrophysical counterparts at other wavelengths, can represent excellent targets for indirect DM searches as well (Strigari, 2013): they may be located close and thus ease the detection of gamma radiation from DM annihilation or decay, while background processes are absent by definition. Indeed, N-body simulations of Milky-Way-sized halos predict the existence of thousands of them (Diemand et al., 2008, Springel et al., 2008b, Stadel et al., 2009) and some are expected to yield large DM annihilation fluxes at Earth given their typical distances and masses (e.g., Ackermann et al., 2012a, Coronado-Blázquez et al., 2019a, Hütten et al., 2016, Schoonenberg et al., 2016, Zechlin et al., 2012).

Since we do not know a priori the exact location of these “dark subhalos”, current IACTs are not particularly suited to discover them given their narrow field of view of a few degrees wide. This is in contrast with the *Fermi*-LAT, which continually surveys the entire gamma-ray sky and thus naturally arises as the ideal instrument to search for dark subhalo candidates in the GeV energy range. Recently, the HAWC observatory, with a broad field of view as well, came into operation and enabled such searches also in the TeV regime. In most cases, the dark satellites’ search strategy is based on looking for them among the pool of unidentified gamma-ray sources (unIDs) in current point-source catalogs. The key point is to identify those unIDs that exhibit spectral or spatial properties compatible with that expected from DM annihilation. Indeed, it is intriguing that about one third of the sources in all available gamma-ray catalogs are still unidentified and some of them may be dark satellites just awaiting for a proper classification. In the absence of an unequivocal DM signal, this strategy allows to set competitive DM constraints by comparing the number of DM subhalo candidates among the list of unIDs to that expected from a combination of N-body simulation results and flux instrumental sensitivity (Abeysekara et al., 2018, Ackermann et al., 2012a, Belikov et al., 2012, Berlin and Hooper, 2014, Bertoni et al., 2015, 2016, Buckley and Hooper, 2010, Calore et al., 2017, Calore et al., 2019, Coronado-Blázquez and Sánchez-Conde, 2020, Coronado-Blázquez et al., 2019a,b, Hooper and Witte, 2017, Mirabal et al., 2012, 2016, Schoonenberg et al., 2016, Zechlin and Horns, 2012, Zechlin et al., 2012). Traditionally, however, these DM

constraints have been subject to large uncertainties given the lack of a precise characterization of the DM subhalo population, such as their structural properties and radial distribution in the Galaxy. A statistical approach on the computation of the number of expected dark subhalos and their prospects of detection with CTA were reported by [Coronado-Blázquez et al. \(2021\)](#).

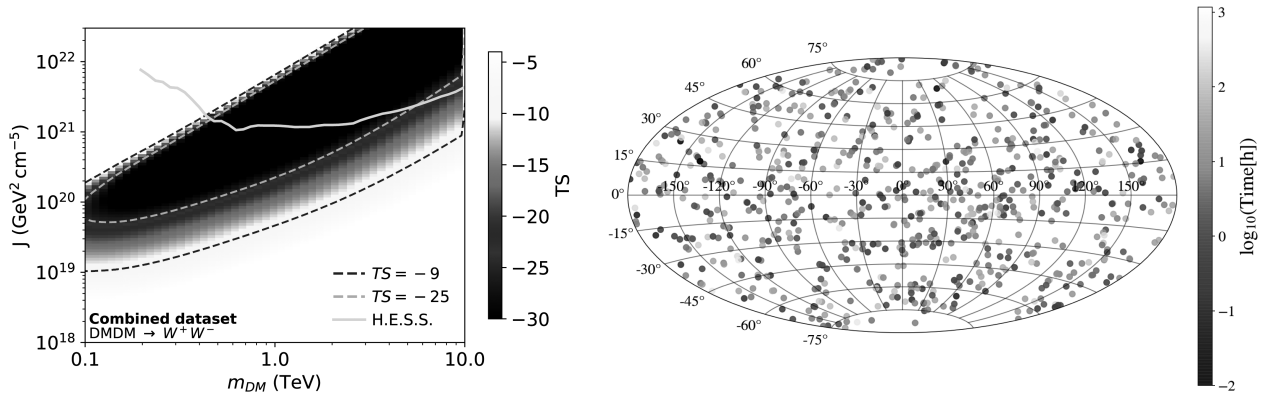


Figure 8.4: The two approaches to search for dark satellites with IACTs. First, by following up observations by suitable unidentified gamma-ray sources detected by *Fermi*-LAT, which is the most viable strategy with current IACTs: the left panel, taken from [Abdallah et al. \(2021a\)](#), shows the upper limit on the sum of the J -factors in a combined analysis of three unIDs observed by H.E.S.S. under the assumption of a thermal DM annihilation cross-section (solid light gray line). Under the assumption that the signals detected by *Fermi*-LAT in fact stem from DM subhalos and annihilation into W^+W^- bosons (likelihood contours in the background), the H.E.S.S. null results significantly restrict the possible J -factor range. Second, with the future CTA, also the serendipitous discovery in any observation’s field of view becomes a feasible search strategy: the right figure shows a random realization of sky coverage with the CTA within the first decade, extrapolated from MAGIC stereo observations. Figure from [Coronado-Blázquez et al. \(2021\)](#), see page 29 for further discussion.

While current IACTs are not the best-suited instruments to discover dark satellites, they have been used to scrutinize in further detail some of the best DM subhalo candidates among the pool of unIDs identified in the above mentioned works, given their superior sensitivity at TeV energies and angular resolution. In [Nieto et al. \(2011a,b\)](#), the MAGIC Collaboration reported on the observation of two objects in 2010 and 2011, namely 1FGL J2347.3+0710 and 1FGL J0338.8+1313, among the list of 630 unIDs present in the First *Fermi*-LAT catalog of point sources (1FGL; [Abdo et al., 2010](#)). No VHE gamma rays were detected after an exposure of around 10 h on each source. These two objects were selected as the most promising out of ten after having survived several selection criteria that were based on the expected DM signal properties. In particular, they selected only non-variable sources located at high ($|b| > 10^\circ$) Galactic latitudes, to avoid contamination from Galactic objects like pulsars, and whose spectra are well described by a power law in the *Fermi*-LAT energy band and are particularly *hard* (spectral index $\Gamma > -2$). They also performed a careful study to search for counterparts of all unIDs at other (X-ray, optical, radio) wavelengths. Later, the VERITAS Collaboration reported on the observation of two other unIDs in a DM context, namely 2FGL J0545.6+6018 and 2FGL J1115.0-0701, with again around 10 h exposure on each target ([Geringer-Sameth, 2013](#), [Nieto, 2015](#)). These objects were identified as the best candidates among the 576 unIDs in the Second *Fermi*-LAT catalog of point sources (2FGL;

Nolan et al., 2012). As summarized by Nieto (2015), VERITAS adopted the same selection criteria proposed by MAGIC in Nieto et al. (2011a,b), the only difference with respect to MAGIC being the VERITAS peculiarities in terms of observation site and instrumental sensitivity. Once again, the null detection of VHE gamma rays from the location of these two unIDs only led to set upper limits to the flux from these objects. In Abdallah et al. (2021a),¹⁵ the H.E.S.S. collaboration recently reported the follow-up observation of dark-satellite candidates among unIDs in the Third Catalog of Hard *Fermi*-LAT sources (3FHL; Ajello et al., 2017). Applying similar selection criteria as by the MAGIC and VERITAS works to 177 unIDs in the 3FHL, they obtained six subhalo candidates out of which four were observed for between three and nine hours (see Table 8.1). As among these four, the source 3FHL J2104.5.2117 was recently associated with high probability to an AGN in the 4FGL catalog (Abdollahi et al., 2020). No signal was detected from either of the four targets. As no robust assumption on the J -factor of the putative DM subhalos can be made for this source class, the H.E.S.S. collaboration adopted a reverse conclusion: on the assumption of a thermal DM annihilation cross-section in the order of Equation 8.5, upper limits on the dark-satellite J -factor were derived. This is illustrated in Figure 8.4 (left).

Yet, we note that although no detection was obtained in neither MAGIC, VERITAS, or H.E.S.S. observations of unIDs, the resulting flux or J -factor upper limits in all cases may be still useful to test the DM subhalo hypothesis and to shed further light on the nature of these sources. So far, no IACT dark satellite observations have been yet performed of any of the unIDs in the most recent *Fermi*-LAT 4FGL catalog (Abdollahi et al., 2020), containing more than one thousand unIDs. Also, Coronado-Blázquez et al. (2019a,b) have recently highlighted potential DM subhalo candidates among the 2FHL (Ackermann et al., 2016), 3FGL (Acero et al., 2015), and 3FHL catalogs which also have not yet been observed by IACTs.

Finally, thanks to a significantly larger field of view and foreseen large-scale survey observations, also dark satellite discovery searches may be feasible with the next-generation IACT, the CTA. This is illustrated in Figure 8.4 (right) and further discussed on page 29 in the outlook of this section.

Observation of IMBHs. There are theories that predict the existence of black holes (BHs) of masses between $10^2 - 10^6 M_\odot$, sometimes referred to as IMBHs: they could form as remnants of collapse of Population III stars, resulting in $10^2 M_\odot$ -mass BHs (scenario A, Heger et al., 2003, Madau and Rees, 2001) or from direct collapse of primordial huge gas overdensities in early-forming halos, resulting in $10^6 M_\odot$ -mass BHs (scenario B, Koushiappas et al., 2004). Many of them could reside in the MW halo. The average number of IMBHs in the MW was estimated by numerical simulations to be of the order of a thousand (scenario A) to a hundred (scenario B) (Bertone et al., 2005b). As a result of the increased gravitational potential due to infalling baryons on a central accreting system, the DM could have readjusted and shrunk, giving rise to the formation of so-called “mini-spikes” (Bertone et al., 2009, 2005b). On the other hand, mini-spikes are rapidly disrupted as a result of dynamical processes like BH formation or merging events. The interesting fact is that, starting from a typical NFW distribution for the DM, the adiabatic growth of the spike leads to a final DM density profile even cuspier than NFW, with a central slope of index $-7/3$ as opposed to -1 for NFW (Bertone et al., 2009). For scenario B, which foresees more luminous objects than scenario A, the corresponding gamma-ray luminosity would be of the order of the gamma-ray luminosity of the entire MW halo, which made IMBHs very interesting targets for DM searches (Bertone et al.,

¹⁵Note that the recent publication by Abdallah et al. (2021a) is the only IACT study on this topic so far published in a peer-review journal.

2005b). Similarly to the dark satellites’ case discussed above, it is possible that some IMBHs are hidden in unidentified EGRET or *Fermi*-LAT point-like sources. Before the advent of *Fermi*-LAT, and after having performed a selection of the best EGRET unidentified sources, MAGIC observed the brightest of them in 2006 for 25 h, with no detection (Doro et al., 2007). The source was later on associated with a bright pulsar using *Fermi*-LAT data. Also, using 400 h of data collected from 2004 to 2007 in the region between -30 and $+60$ degrees in Galactic longitude, and between -3 and $+3$ degrees in Galactic latitude, H.E.S.S. could exclude the IMBH formation scenario B at a 90% confidence level for DM particles with annihilation cross-section values $\langle\sigma v\rangle$ above 10^{-28} $\text{cm}^3 \text{s}^{-1}$ and masses between 800 GeV and 10 TeV (Aharonian et al., 2008a).

Observation of globular clusters. Globular clusters are star compounds that share properties with dSphs. They are in general more compact and with narrower metallicity distributions than dSphs. There is a large debate on how these clusters formed, considering that it is possible to find globular clusters already 1 Gyr after the Big Bang. Despite they are generally thought to contain low amounts of DM, the debate on whether or not they reside in a DM halo is still open (Baumgardt, 2017, Bradford et al., 2011, Creasey et al., 2019, den Brok et al., 2014, Ibata et al., 2013, Lane et al., 2010, Mashchenko and Sills, 2005a,b). From the cosmological point of view, there is no conflict in telling that they were formed in DM overdensities, as the dSphs, however, there is no strong observational evidence for the presence of a DM halo as of today. One possibility is in fact that the luminous part of a globular cluster is just located in the inner region of a flat DM overdensity, which would not modulate significantly the stellar velocities for different radii (Ardi and Baumgardt, 2020). The interest in globular clusters from the DM search perspective is active, and recently revived after a claim on the observation of a 30 GeV DM line-signal in 47 Tuc (Brown et al., 2018), though soon discarded by Bartels and Edwards (2018).

For what regards the observation of globular clusters with IACTs, M15 was observed from 2002 to 2004 by Whipple (Wood et al., 2008) and later re-observed together with NGC 6388 by H.E.S.S. in 2006–2009 (Abramowski et al., 2011), shown in Fig. 8.5. MAGIC also invested more than 150 h on M15, with which only upper limits on the gamma-ray emission were obtained, and discussed in the context of astrophysics (Acciari et al., 2019). The interpretation in terms of DM is under preparation. The best exclusion curves for annihilating DM come from the observation of NGC 6388 by H.E.S.S., and are of the order of $10^{-24} - 10^{-25}$ $\text{cm}^3 \text{s}^{-1}$. However it must be noted that these results rely on strong assumptions about the amount of DM in this particular object.

Observation of galaxy clusters. Within the standard Λ CDM scenario, galaxy clusters, with masses around $10^{14} - 10^{15}$ M_{\odot} , are the largest gravitationally bound objects in the Universe and the most recent structures to form (Voit, 2005). They are relevant for what concerns indirect DM searches (e.g., Colafrancesco et al., 2011, Gao et al., 2012, Jeltema et al., 2009, Pinzke et al., 2011, Sanchez-Conde et al., 2011), because DM is the dominant mass component within this type of systems, accounting for up to 80% of the total virial mass.¹⁶ However, galaxy clusters are extragalactic objects, many of them located at cosmological distances, and therefore any radiative signal from DM annihilation or decay would be significantly diluted or attenuated by the extragalactic background light. Given their large halo masses, the presence of a large amount of substructures in clusters is expected to be particularly important for DM searches, as they intrinsically boost the total J -factor for annihilating DM by a factor of 30 – 50 (Hiroshima et al.,

¹⁶The remainder component is dominated by intra-cluster medium (ICM) gas.

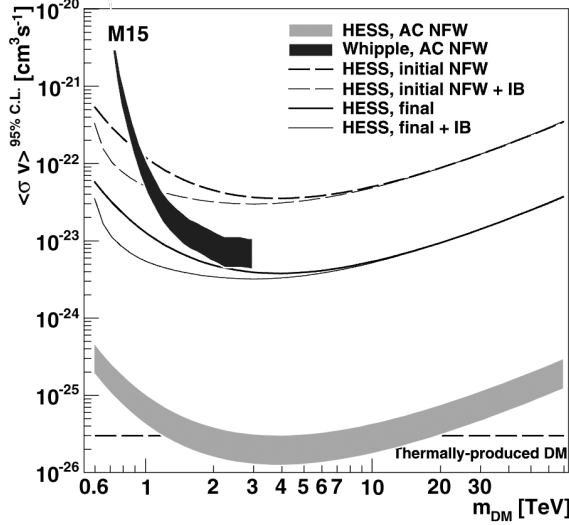


Figure 8.5: 95% C.L. upper limits on the DM annihilation cross-section by H.E.S.S. (Abramowski et al., 2011) and Whipple (Wood et al., 2008) observations of the globular cluster M15. Limits were calculated for Whipple (blue band) and H.E.S.S. (brown band) assuming an NFW density profile, adiabatically contracted (AC) due to the presence of an IMBH. Additionally taking into account for kinetic heating by stars results into the “final” profile assumed by H.E.S.S. (solid lines). The dashed lines denote an initial DM halo model assuming $M_{\text{vir}} = 10^7 M_{\odot}$. The final-state gamma-ray spectrum is modeled in this work according to Bergstrom et al. (1998). IB refers to accounting for internal bremsstrahlung effects. Figure from Abramowski et al. (2011).

2018, Moliné et al., 2017, Sánchez-Conde and Prada, 2014, Sanchez-Conde et al., 2011, Zavala and Afshordi, 2016). Because of that, galaxy clusters are targets competitive to dSphs for indirect DM searches in term of expected J -factors (Sanchez-Conde et al., 2011). Although this *subhalo boost* is not present in a decaying DM scenario, for which the “clumpiness” of DM is not relevant, galaxy clusters are even more competitive compared to dSphs in the case of decaying DM: this is to be understood by the huge total mass budget of a cluster integrated within a small opening angle. Note also that, as in other targets, in galaxy clusters any potential DM-induced gamma-ray emission is not only expected as prompt emission, but also as secondary emission mostly generated by synchrotron and inverse Compton processes from high energy electrons and positrons produced in DM interactions (Colafrancesco et al., 2006).

Clusters of galaxies also host strong astrophysical gamma-ray emitters in many cases (Blasi and Colafrancesco, 1999). Thus, any careful search for DM signatures in galaxy clusters must disentangle these from more “conventional” astrophysical contributions. For instance, AGNs sitting in individual cluster galaxies or a sizeable interaction of cosmic rays (CRs) with the ICM may potentially yield gamma-ray fluxes larger than the one expected from DM interactions. Fortunately, a different spatial morphology of the gamma-ray signal is expected in each case: while the signal from DM is more extended, especially in the case of decay, the signal from CR interactions and radiative energy losses is more compact, and individual galaxies are point-like. This can be used as a powerful tool for discriminating between the different components, as discussed by Doro et al. (2013).

To date, the deepest scrutiny of a galaxy cluster in gamma rays is the one performed with

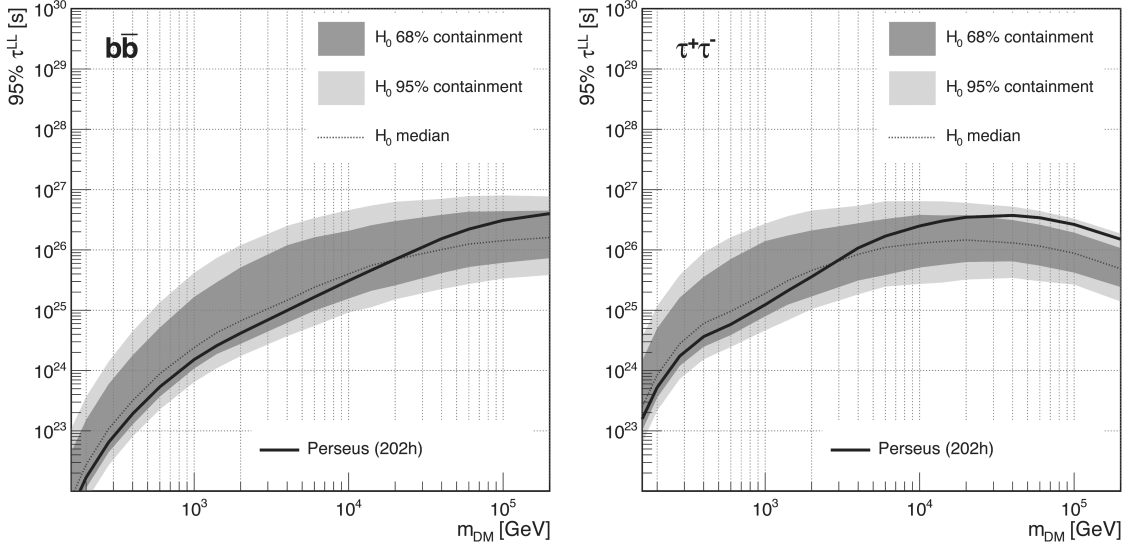


Figure 8.6: 95% C.L. lower limits on the DM decay lifetime τ^{LL} (solid black lines) as obtained from the 202 h observation of the Perseus cluster of galaxies with the MAGIC telescopes for the $b\bar{b}$ (left panel) and $\tau^+\tau^-$ (right) decay channels. The expected limits (dashed lines) and the two sided 68% and 95% containment bands are also shown. These are the most constraining decay limits obtained so far above few hundreds GeV. Figure from [Acciari et al. \(2018\)](#).

the MAGIC telescopes for the Perseus cluster ([Acciari et al., 2018](#)). MAGIC observed this object for more than 400 h over several years. This deep observation of the Perseus cluster allowed to set the strongest constraints to date on decay DM using a subset of 202 h of data ([Acciari et al., 2018](#)). Such constraints are reported in Fig. 8.6 for two pure decay channels that roughly bracket the minimum and maximum number of photons expected from decay, i.e., by decays into purely $b\bar{b}$ quarks or $\tau^+\tau^-$ leptons. These MAGIC limits are of the order of 10^{26} s, that is, more constraining than any other limit set to decaying DM in the DM mass range above few hundreds of GeV. At lower energies, stronger constraints are found using *Fermi*-LAT data of the diffuse emission ([Ackermann et al., 2012d](#)).

For DM annihilation, the strongest DM constraints from clusters as of today were set by H.E.S.S. by the observation of the Fornax cluster ([Abramowski et al., 2012](#)), which is one of the clusters with the highest expected DM annihilation signal. Apart from Perseus and Fornax, also the Coma cluster was observed for 18.6h by the VERITAS telescopes ([Arlen et al., 2012](#)), however, yielding less stringent constraints on DM annihilation.

Constraints on line-like spectral signatures. Self-annihilation or decay of DM particles may create unique line-like gamma-ray spectral features not expected at TeV energies from any other astrophysical process ([Bertone et al., 2005b](#)). In particular, narrow spectral lines can be expected from events such as $\chi\chi \rightarrow \gamma\gamma$ and $\chi\chi \rightarrow X\gamma$, where $X = Z^0, H, \dots$ are found at loop or enhanced level ([Arina et al., 2010](#), [Beneke et al., 2018](#), [Bergstrom and Kaplan, 1994](#), [Bergstrom and Ullio, 1997](#), [Jungman and Kamionkowski, 1995](#), [Rinchiuso et al., 2018](#)). Furthermore, in case the annihilation is mediated by a heavy particle, also peculiar features such as ‘box’-like features in the gamma-ray spectral energy distribution may occur ([Ibarra et al., 2012](#)). Also, emission from virtual

internal states can happen for specific particle models via bremsstrahlung, providing a pronounced component peaked towards the spectral cutoff at the highest energies (Bringmann and Calore, 2014, Bringmann et al., 2008, 2009).

Such a signal would be readily distinguishable from astrophysical high-energy gamma-ray sources that are expected to only produce continuous spectra, and may constitute a robust "smoking-gun" identification of DM. For WIMP masses above several hundreds of GeV and above the energy reach of space-based detectors, Earth-bound gamma-ray detectors are moreover the only instruments to search for such features. Also, for IACTs, line-like features are even easier to be searched for than continuous spectra: the large residual cosmic-ray background is a generic challenge for IACTs, yet line-like gamma-ray spectra are very distinct from the background spectral energy distribution and, thus, a powerful discrimination between background and signal is possible in terms of their spectral properties. Nevertheless, specific analysis algorithms must be developed in order to look for such signatures in IACT data. In particular, IACTs are not only, like any other instrument, affected by a limited energy resolution, in this case of the order of 10%, but may also show specific systematic uncertainties at the energy scale as a result of using the atmosphere as calorimeter.

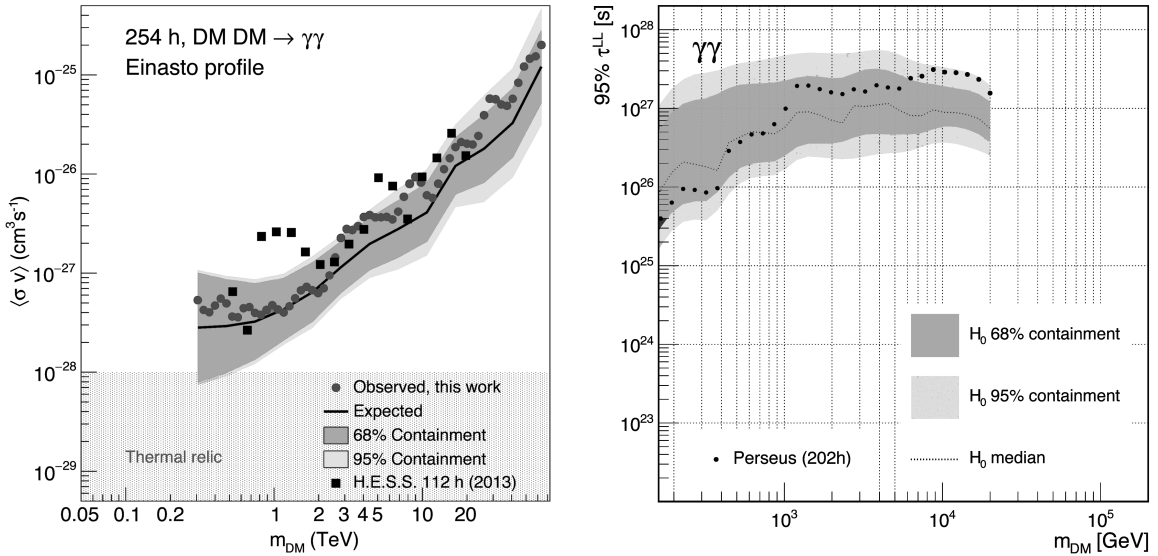


Figure 8.7: Constraints on the velocity-averaged annihilation cross-section $\langle\sigma v\rangle$ for the prompt annihilation into two photons derived from H.E.S.S. observations of the inner GC region (left), and of the lifetime from prompt DM decay into two photons derived from MAGIC observations of the Perseus galaxy cluster (right). Figures from Abdalla et al. (2018b), Acciari et al. (2018), respectively.

Using data collected with H.E.S.S., upper limits on line-like emission have been obtained in the energy range between 100 GeV and 70 TeV from the central part of the MW halo (Abdalla et al., 2016, 2018b). For a DM particle mass of 1 TeV, limits on the velocity-averaged DM annihilation cross-section $\langle\sigma v\rangle$ reach the level of $10^{-27} \text{ cm}^3 \text{ s}^{-1}$ when adopting an Einasto DM density profile for the Galaxy. Using combined dSph observations, limits were derived between 300 GeV and 20 TeV by H.E.S.S. (Abdalla et al., 2018a) and between 100 GeV and 10 TeV by VERITAS (Archambault et al., 2017). Additional limits were obtained by MAGIC after a 158 h observation of the Segue 1 dSph (Aleksić et al., 2014); also an analysis of the GC region was recently presented by MAGIC

(Inada et al., 2021). Line emission can be likewise emitted in DM decay processes, and this was scrutinized by Acciari et al. (2018) in the analysis of 202 h of data towards the Perseus galaxy cluster. The current best limits on line-like emission from DM annihilation (left) and decay (right) at TeV energies are shown in Fig. 8.7. Note that these limits correspond to a pure annihilation or decay process into two photons. For this process only constituting a small fraction among other annihilation or decay channels, as expected for a loop-suppressed process, the total constrained annihilation cross-section may be much larger (and correspondingly, the lifetime be shorter) than suggested by the shown data. In Fig. 8.7 (left), this is considered by the grey-shaded region of an expected signal for thermal WIMPs downshifted to $\langle\sigma v\rangle \lesssim 10^{-28} \text{ cm}^3 \text{ s}^{-1}$ already implying annihilations into two photons happening with a branching ratio smaller than 10^{-2} .

Searches with charged particles. In the annihilation or decay process of DM particles, hadrons and leptons are abundantly produced (see, e.g., Donato et al., 2004). Below these, antiparticles would constitute a species that could be easier discriminated against the astrophysical cosmic-ray background, as, e.g., the antiparticles produced after the spallation of CRs in the interstellar medium. This possibility gained a great interest a decade ago after the accumulation of evidence of a positron excess from satellite-borne particle detector experiments such as PAMELA (Adriani et al., 2009), *Fermi*-LAT (Ackermann et al., 2012b) and subsequently AMS (Aguilar et al., 2013). As no antiproton excess was found simultaneously, an explanation for this positron excess that generated particular interest in the community was to invoke the existence of *leptophilic* DM, i.e., DM particles that prefer leptonic annihilations or decays over hadronic channels. Also, the balloon-borne ATIC reported an excess in the electron+positron spectrum around 500 GeV (Chang et al., 2008). However, the sensitivity of these balloon or space-borne measurements was limited to energies below a few TeV. In turn, IACTs are sensitive to Cherenkov light generated in atmospheric showers initiated by sufficiently energetic photons or charged particles. In this sense, they are also suitable detectors for cosmic electrons, positrons and antiprotons beyond TeV energies.

Leptonic showers from cosmic electrons or positrons are currently indistinguishable from gamma-ray induced showers. Yet, in contrast to gamma-ray induced showers, which are always aligned to a very localized cosmic gamma-ray source, cosmic leptons reach the Earth from perfectly isotropical directions. As such, in a data sample without a gamma-ray source in the field of view, electrons or positrons can be discriminated from the residual hadronic cosmic-ray background in IACT data by comparing the whole data sample with corresponding Monte Carlo (MC) simulations of hadron events, via the definition of discriminator parameters specifically designed for that purpose. Consequently, the systematic uncertainties need to be carefully controlled, because even a small mismatch between MC and real data would result in a bias in the estimated electron flux. This search was pioneered by H.E.S.S. back in 2008, which used 239 hrs of data, extending the measured electron+positron spectrum deeper into the TeV range (Aharonian et al., 2008b). They found evidence for a steepening in the all-electron spectrum above 600 GeV, while they excluded the spectral peak previously claimed by ATIC (Aharonian et al., 2009b). An analogous measurement by VERITAS confirmed a spectral break in the energy spectrum at around 700 GeV (Archer et al., 2018), as did a preliminary measurement presented by MAGIC (Borla Tridon et al., 2011). The DAMPE satellite detector published an all electron+positron spectrum up to 4.6 TeV, confirming a spectral break in the all-electron spectrum at around 900 GeV (Ambrosi et al., 2017), as so did the CALET experiment measuring the spectrum to 4.8 TeV on the International Space Station (Adriani et al., 2018).

Unfortunately, the IACT detection technique does not directly allow to discriminate electrons from positrons, to investigate the excess of positrons at TeV energies. However, the Earth’s magnetic field is separating electrons from positrons, and this separation could be observable where the isotropic flux is shadowed by the Earth (as exploited by the *Fermi*-LAT measurement; Ackermann et al., 2012b) or the Moon. In fact, the feasibility of disentangling electrons and positrons by observing a cosmic-ray *Moon shadow* with IACTs has already been investigated and some data been collected with the MAGIC and VERITAS telescopes despite the big observational challenges (Bird, 2016, Colin et al., 2011).

Conclusions and outlook

The length of Tab. 8.1 substantiates the huge effort in the pursuit of DM made by IACTs over the past decade. Not only target classes have been diversified, but also novel analyses and algorithms have been developed specifically for such searches. In Fig. 8.8 we report some of the most important limits produced by IACTs so far. It is important to comprehensively discuss this effort.

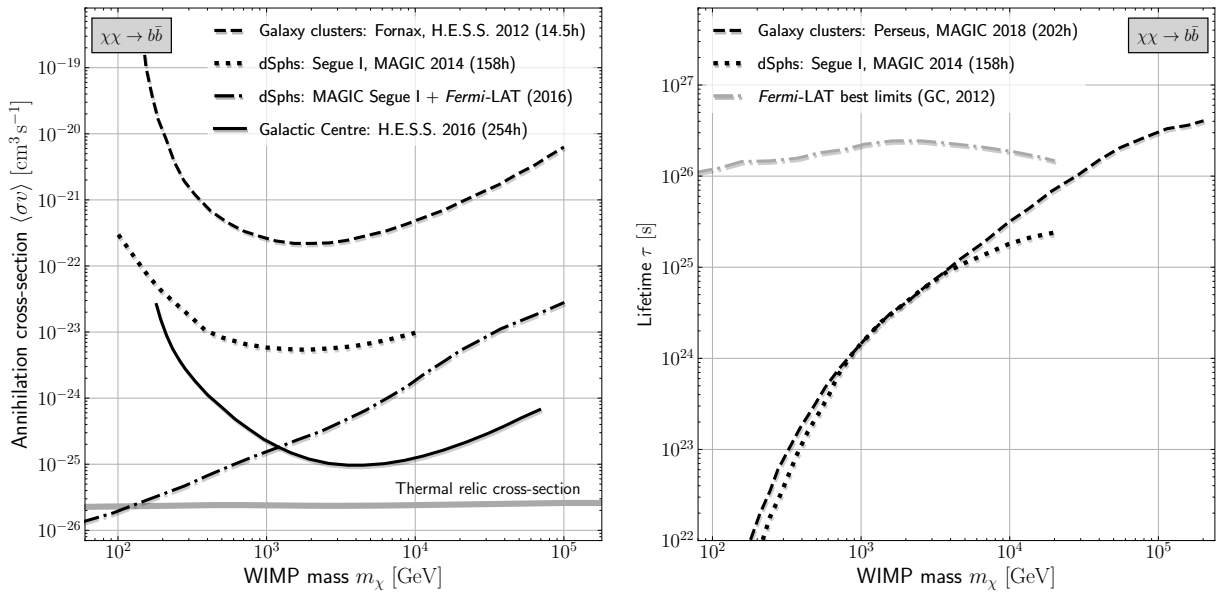


Figure 8.8: Selection of some of the most representative WIMP limits by IACTs for the $b\bar{b}$ annihilation channel (left) and the $b\bar{b}$ decay channel (right).

On the left panel of Fig. 8.8 we report some of the most relevant limits obtained on annihilating DM for the $b\bar{b}$ channel. We show the H.E.S.S. observation of the GC halo adopting an NFW profile as a solid line (Abdallah et al., 2016), the MAGIC stereo observations of the Segue 1 dSph in dotted (Aleksić et al., 2014), the *Fermi*-LAT combined limits from the observation of 15 dSphs with 6 years of data together with MAGIC Segue I with a dot-dashed line (Ahnen et al., 2016b), and the 14.5 h limits obtained with H.E.S.S. observation of the Fornax galaxy cluster in dashed line (Abramowski et al., 2012). This figure is emblematic. We see that only searches in an object with a large DM concentration and close distance such as the GC (J -factor of the order of $10^{21} \text{ GeV}^2 \text{ cm}^{-5}$) have a chance to skim the thermal relic value at masses about 1 – 10 TeV. The

second best limits, although possibly less subject to model uncertainties, are those obtained with Segue 1, a very DM-dominated dSph (J -factor of the order of $10^{19} \text{ GeV}^2 \text{ cm}^{-5}$). Galaxy clusters provide weaker constraints, albeit it must be noted that the corresponding limits were obtained with a much more reduced exposure than the others shown in the same figure. On the other hand, at lower masses, *Fermi*-LAT dominates the sensitivity.

This is not necessarily the end of the game. For instance, there are several mechanisms that can provide a cross-section larger than the thermal one, such as Sommerfeld effects (Nagayama et al., 2021), which are activated resonantly for some DM masses due to the particles' extremely non-relativistic velocities today. These resonant phenomena predict that there are some values of mass for which the cross-section may be much larger than what predicted by the thermal limit scale, still consistent with today's observed DM density. However, such resonances can appear at virtually any mass. Therefore, indirect detection of DM could be 'around the corner' for such models. Furthermore, it is important to remember that, should more than one DM particle exist, the thermal value would need to be re-discussed. In any case, the IACTs DM annihilation limits obtained so far are the strongest for DM masses in the TeV scale.

On the right panel of Fig. 8.8 we report some of the most relevant limits obtained on decaying DM with IACTs. We report the results from 202 h observation of the Perseus galaxy cluster (dashed line) and those obtained with 158 h exposure on the Segue 1 dSph galaxy (dotted line) with MAGIC (Aleksić et al., 2010, 2011). We also show, for comparison, the *Fermi*-LAT decay limits from the GC (Ackermann et al., 2017). One can see that for energies larger than 10 TeV, lower limits at the order of 10^{26} s are obtained with IACTs, and they are competitive with those obtained at lower energies with *Fermi*-LAT. Here, there is no reference value to be reached, in contrast to the annihilation case, and in line of principle, any value above the exclusion curve is equally probable. We are not in the position to assess the likelihood of a model.

Outlook IACTs have certainly produced unique information about DM candidates at the TeV mass scale, with a sensitivity unmatched by any other technique or experiment. Yet, these results should be put into context with the other gamma-ray detectors in the field, operating or planned. Throughout this Chapter, we already presented results from *Fermi*-LAT, a pair-production detector hosted aboard a satellite, sensitive to gamma rays from hundreds MeV to hundreds GeV. Data from *Fermi*-LAT dominate the DM limits shown in Fig. 8.8 at the lowest DM masses. Towards the high energy end of the IACT sensitivity range, we find a different kind of detector class, that of the shower-front detectors that sample the very particles in the extended atmospheric showers. Instruments of this class have been the decommissioned ARGO-YBJ and MILAGRO experiments, now followed by the HAWC and Large High Altitude Air Shower Observatory (LHAASO) (He et al., 2019) detectors. All these were or are hosted in the Northern Hemisphere. A project for a Southern Hemisphere shower front detector goes under the name of Southern Wide-field Gamma-ray Observatory (SWGRO) (Barres de Almeida, 2021). The sensitivity of these instruments for DM particles is competitive with current IACTs, as shown in Fig. 8.9 for LHAASO (dashed line). At lower energies, direct detection experiments hardly reach the sensitivity needed to test DM candidates with masses of few hundred GeV, and particle accelerators similarly cannot access the energy scale of multi-TeV particles. Therefore, IACTs are crucial to probe the parameter space of heavy WIMP candidates between a few TeV and the unitary upper bound for WIMP masses expected at around few hundreds of TeV (Griest and Kamionkowski, 1990).

A huge leap will be made with the Cherenkov Telescope Array (CTA) (Acharya et al., 2013),

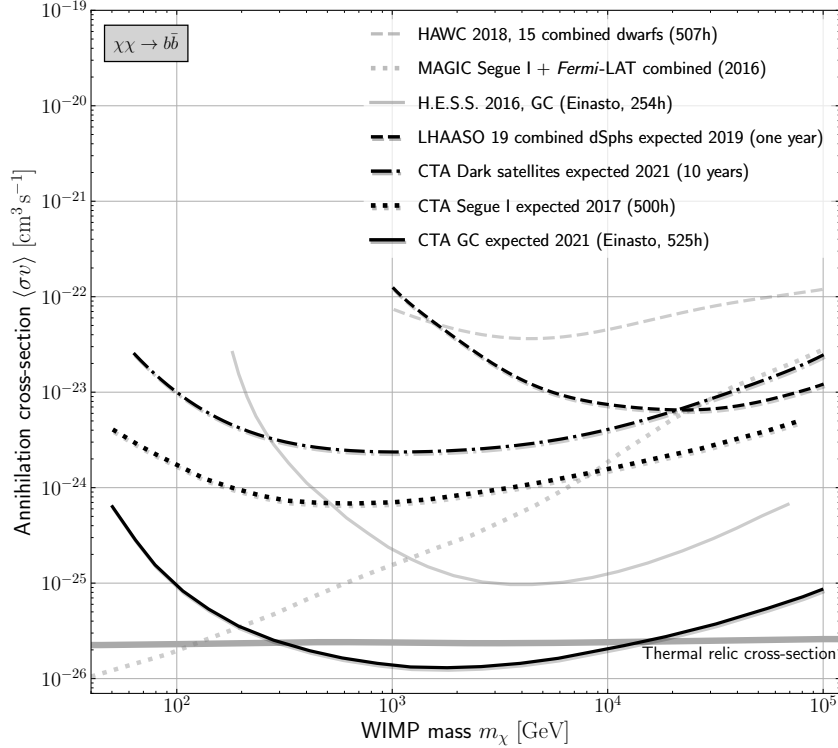


Figure 8.9: Selection of some of the most representative sensitivity prospects for WIMP searches with future gamma-ray detectors, namely, CTA (Acharya et al., 2017, Acharyya et al., 2021, Coronado-Blázquez et al., 2021) and LHAASO (He et al., 2019). In shaded colors, a selection of current limits by IACTs (as shown in Figure 8.8) and HAWC (Albert et al., 2018) are overlaid.

which will supersede in the coming decade the IACTs we have discussed in this chapter, H.E.S.S., MAGIC, and VERITAS. CTA will not only have an improved sensitivity, but also both a better energy and angular resolution compared to current IACTs. A better sensitivity will obviously boost the performance obtained for the same observation time. In practice, this will significantly increase our chances for detection and, in the absence of it, will translate into more constraining DM limits. The improved energy and angular resolutions will allow to provide more robust constraints: the peculiarity of DM spectra can be assessed only if the energy resolution is good enough not to wash out their unique properties. An improved angular resolution will allow for a better investigation of the DM signal region, especially in those cases for which abundant and complicated astrophysical emission is expected to be found, such as the GC or galaxy clusters, or in cases where the spatial extension itself can be a DM smoking gun, as expected in dark satellites (Coronado-Blázquez et al., 2019b). The envisioned CTA strategy for DM searches is discussed in Acharya et al. (2017): a deep survey of the GC region, a dedicated pointing on the best available dSph at the time, and deep surveys of both the Perseus galaxy cluster and the Large Magellanic Cloud are all parts of the so-called CTA Key Science Programs for the first decade.

For the GC region, a deep scan over 525 hours will be performed in the first three years of operation primarily with CTA South, covering a circular area of ten degrees in diameter around the GC. Additionally, an extended survey with over 300 more hours on a large area North or South

of the GC region is envisaged (Acharya et al., 2017). Acharyya et al. (2021) studied in detail how this wealth of data can be used to probe WIMP candidates with annihilation cross-sections below the thermal relic value. In Figure 8.9, it is displayed how this expectation compares to current limits on DM annihilation in the TeV range, with a sensitivity exceeding the best current limit by H.E.S.S. by one order of magnitude (solid line). Importantly, Acharyya et al. (2021) shows that this sensitivity is even guaranteed when accounting for the uncertainty of the instrumental background and astrophysical emissions being present in the data. Furthermore, they found that, even for a cored inner Galactic DM density profile, a sensitivity closely reaching the thermal value can be achieved thanks to the large covered area and a template-fitting analysis approach. As a result, CTA may robustly allow the discovery of TeV DM at the canonically expected thermal cross-section. In parallel to the observation of the GC region, 300 hours of the most promising dSph target are guaranteed in the first three years of operation of CTA. In addition to the interest that such deep observation possesses by itself to search for DM in this type of objects, there is one more reason that makes it particularly useful. Indeed, in case of a putative detection of a DM signal in the GC region, this additional time on a dSph may allow to further scrutinize such discovery in a DM context by means of other type of target, and to test or exclude possible alternative explanations. In Figure 8.9, DM prospects are shown assuming the Segue I dSph with its currently best estimated J -factor and for a total of 500 h exposure time (dotted line). Independently of the success of these initial DM searches with CTA, 700 more hours will be dedicated in the first decade of CTA operations to hunt for DM either at the GC or at the position of the best dSph target (Acharya et al., 2017).

Not only the GC and dSphs are viable targets for CTA. Brun et al. (2011), Coronado-Blázquez et al. (2021), Hütten et al. (2016) also discussed CTA’s capabilities to search for dark satellites. In contrast to current IACTs, CTA may also have a high chance to realistically *discover* these objects. This is not only due to the improved sensitivity, but also to its larger field of view and planned dedicated large-area Galactic-plane and extragalactic surveys (Dubus et al., 2013). While Brun et al. (2011), Hütten et al. (2016) only investigated the individual surveys for such discovery potential, Coronado-Blázquez et al. (2021) recently scrutinized the chances for a serendipitous discovery of a dark satellite in all CTA data taken within the first decade of CTA operations. As shown in Figure 8.9 (dot-dashed line), this strategy could yield a sensitivity competitive to those obtained by a dedicated deep CTA observation of the most promising dSph galaxy to date.

Can we expect novelties beyond the advent of CTA? Certainly new dSphs have been discovered these years thanks to the Dark Energy Survey (Abbott et al., 2018), and opportunities to identify promising targets for indirect DM searches will be greatly increased with the Very Rubin Observatory in the near future (Drlica-Wagner et al., 2019). Possibly, in a decade from now, all or the majority of MW dSph satellites will be detected (Hargis et al., 2014). Improved spectroscopic capabilities, like DESI (DESI Collaboration et al., 2016) or the Prime Focus Spectrograph recently put in operation at the Subaru telescope (Tamura et al., 2018) will also allow for more precise member star velocity estimations and, thus, for a more accurate DM modeling. Data from the GAIA satellite will also enable a better removal of interloper stars (Helmi et al., 2018). All together, this information should lead to a boost in accuracy of the determination of dSph J -factors. It is also still possible to find a dSph exhibiting a higher J -factor than any other dSph currently known. It was shown in Doro (2017) that current IACTs may reach the thermal cross-section value if they were able to observe for 500 h a dSph with a J -factor five times the one of Segue 1. Another possibility is that this J -factor was reached by a dark satellite serendipitously detected, both massive

and close enough to the Earth.¹⁷ Also, multi-wavelength approaches complementing IACT DM searches from the radio band to MeV gamma rays are more and more identified as very useful. Data from other wavelengths either may set strong constraints on heavy DM candidates on their own (Regis et al., 2021), or allow to improve the VHE gamma-ray analysis by providing additional information (as e.g. for *Fermi*-LAT in Di Mauro and Winkler, 2021).

All in all, the next decade will gather great expectations for the discovery of TeV WIMP DM or in challenging the paradigm of massive particle DM. Even if particle DM may be first discovered in colliders or direct detection experiments, an accurate DM *identification* and *characterization* will only be possible by combining signatures from different detectors and methods (Cahill-Rowley et al., 2015). A signature in telescopes is furthermore necessary to establish the definitive link between a potential DM signal at the lab and the long sought DM in the Universe. To this aim, IACTs to study the properties and budgets of massive particle DM in astrophysical reservoirs play a crucial role, already today and all the more in the future.

Verification

Q8.1: Why the expected gamma-ray spectrum of DM annihilation is *exactly* cut-off at the rest mass of the DM particle (at half the rest mass for decay)?

Q8.2: Why does one not search for WIMP relic annihilations or decays of local DM particles in a detector?

Q8.3: According to the canonic scenario of thermal DM freeze-out in the early Universe, would there be less or more DM left over today if the annihilation cross-section was larger than $\langle\sigma v\rangle \sim 10^{-26} \text{ cm}^3 \text{ s}^{-1}$?

Q8.4: After first results of IACT DM searches were published with few hours of data, why improved limits from the same instruments were published not before hundreds of more hours had been accumulated?

8.2 Axion-like Particles

As of today, the so-called Peccei-Quinn (PQ) mechanism – proposed in the late ’70s of the past century (Peccei and Quinn, 1977) – represents the most convincing solution to the strong Charge-Parity (CP) problem in Quantum Chromodynamics (QCD), i.e., the absence of CP violation in strong interactions. It was soon realized that a by-product of the proposed PQ mechanism is the existence of a pseudo-Nambu-Goldstone boson called *axion* (Weinberg, 1978, Wilczek, 1978).¹⁸ Very interestingly, these QCD axions may account for a fraction or the whole (cold) DM content in the Universe and, indeed, constitute one of the most valid alternatives to WIMPs at present. Contrary to WIMPs though, the axion would be very light, as its mass has already been experimentally constrained to be $\ll \text{eV}$. In fact, axions represent the most famous exponent of the whole class of so-called weakly interacting slim particles (WISPs) (see e.g. Arias et al. (2012) for a recent review).

¹⁷In this case, however, it may be difficult to assess the underlying DM particle physics model until we have some knowledge on its exact distance and mass by other means.

¹⁸The name *axion* is typically attributed to Frank Wilczek, who supposedly took it from a laundry detergent alluding to the fact that the new particle would “remove a stain”.

One interesting property of these axions, particularly relevant for the purposes of this book, is a predicted interaction with photons in the presence of external magnetic or electric fields described by the following Lagrangian (Dicus et al., 1978, Sikivie, 1983):

$$\mathcal{L}_{a\gamma} = -\frac{1}{4} g_{a\gamma} F_{\mu\nu} \tilde{F}^{\mu\nu} a = g_{a\gamma} \mathbf{E} \cdot \mathbf{B} a, \quad (8.13)$$

where a is the axion field, $g_{a\gamma}$ is the coupling strength, F is the electromagnetic field-strength tensor, \tilde{F} its dual, \mathbf{E} the electric field, and \mathbf{B} the magnetic field. For the QCD axion, the mass is proportional to the coupling strength. Yet, there are other, more general states arising from extensions of the SM, for which this relation does not hold, frequently known as *axion-like* particles (ALPs) because they still share many similarities with the QCD axion (Chikashige et al., 1978, Conlon, 2006, Langacker et al., 1986, Wilczek, 1982, Witten, 1984). In string theory, for example, it is possible to properly formulate the entire PQ mechanism, which leads to predict the existence of many of these “generalized” axions or ALPs, the QCD axion being just a particular case (Arvanitaki et al., 2010, Cicoli et al., 2012, Conlon, 2006, Witten, 1984).

The interaction with photons described by Eq. (8.13) represents the main vehicle used to experimentally search for axions and ALPs up to present (Anastassopoulos et al., 2017, Andriamonje et al., 2007, Duffy et al., 2006, Irastorza and Redondo, 2018, Wagner et al., 2010, Zioutas et al., 2005). This interaction results in conversions or *oscillations* of photons into ALPs and vice-versa; see Fig. 8.10. This same property of axions and ALPs can be used to look for them by means of astrophysical observations as well, whose main observable is precisely photons. Indeed, should ALPs and photons couple to each other, significant distortions in the spectra of astrophysical sources may be induced that could be measured, e.g., in the gamma-ray energy range with current or future IACTs.¹⁹ Thus, photon-ALP conversions may potentially have very important implications for gamma-ray astrophysics and, very excitingly, ALPs offer the possibility to search for new physics with gamma rays. Even in the absence of ALP-induced spectral features in gamma-ray data, a null result might be used to provide valuable insight, i.e, competitive experimental constraints, on the precise ALP nature.

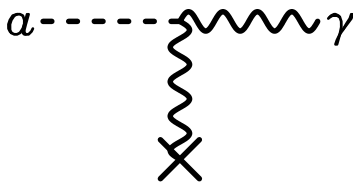


Figure 8.10: Feynman diagram showing the interaction of photons and ALPs in the presence of an external electric or magnetic field. This interaction obeys the Lagrangian in Eq. (8.13).

ALP-induced imprints in the spectra of gamma-ray sources are expected to happen around and above a particular critical energy for conversion that, in convenient units for gamma-ray experiments, can be expressed as (Hooper and Serpico, 2007)

$$E_{\text{crit}} \equiv \frac{m_a^2}{2 g_{a\gamma} B} \sim 2.5 \text{ GeV} \frac{m_{\mu\text{eV}}^2}{g_{11} B_G}, \quad (8.14)$$

¹⁹Note that we only refer to ALPs here: the search for QCD axions is in principle not possible in gamma rays given the too small couplings expected at the axion masses that can be probed by gamma-ray telescopes (see, however, Farina et al. (2017) for “boosted” photon/axion couplings). This will be further discussed later in the section.

where the sub-indices refer to dimensionless quantities: $m_{\mu\text{eV}} \equiv m_a/\mu\text{eV}$, $g_{11} \equiv g_{a\gamma}/10^{-11}$ GeV and $B_G \equiv B/\text{Gauss}$; m is an effective ALP mass $m^2 \equiv |m_a^2 - \omega_{\text{pl}}^2|$, with m_a the ALP mass and $\omega_{\text{pl}} = 0.37 \times 10^{-4} \mu\text{eV} \sqrt{n_e/\text{cm}^{-3}}$ the plasma frequency of the medium under consideration (n_e being its electron density). Recent results from the CAST experiment (Anastassopoulos et al., 2017) provide an upper limit of $g_{11} \leq 6.6$ for ALP masses $m_a \leq 0.02$ eV. At present, this bound represents the most general and stringent limit in this ALP mass range.

Just around this E_{crit} an oscillatory spectral pattern is expected whose exact properties will depend on both the morphology and orientation of the magnetic field along the direction of propagation of the ALP. The mixing between photons and ALPs becomes maximal above E_{crit} and independent of the energy, the probability for conversion being just proportional to $(g_{a\gamma} \times B)^2$. This is the so-called *strong mixing regime*. A modification of the observed photon flux is then expected within this energy interval, because photons convert into ALPs and vice-versa. The mixing remains maximum up to an energy $E_{\text{max}} \sim 2.2 \times 10^6$ GeV $g_{11} B_{\mu\text{G}}$, where birefringence effects heavily start to suppress the conversions. We note that other effects might significantly alter this general picture. For instance, at TeV energies, Kartavtsev et al. (2017) recently noticed that photon-photon refraction is expected to diminish the expected photon-ALP maximal mixing, this attenuation being more and more efficient as the energy increases.

The probability for photon-ALP conversion is proportional to the modulus of the magnetic field *times* the physical size, s , where this field is confined. More precisely, it is (Hooper and Serpico, 2007, Sánchez-Conde et al., 2009):

$$P_{a\gamma} = \frac{1}{1 + (E_{\text{crit}}/E_\gamma)^2} \sin^2 \left[\frac{B s g_{a\gamma}}{2} \sqrt{1 + \left(\frac{E_{\text{crit}}}{E_\gamma} \right)^2} \right]. \quad (8.15)$$

This means that an efficient conversion can happen not only in relatively small regions of the Universe exhibiting very strong magnetic fields (e.g., AGNs, neutron stars) but also along large physical volumes filled with weak magnetic fields (e.g., the intergalactic medium between galaxies, the intra-cluster medium in galaxy clusters or the interstellar medium in a galaxy like our own). Very interestingly, this particular “property” is very closely connected to the so-called *Hillas criterion* which is required to accelerate high-energy cosmic rays in astrophysical objects (see Fig. 8.11), in such a way that this criterion can be actually used as a good proxy for the identification of the best astrophysical targets for ALP searches.

The precise effect of photon-ALP conversions on gamma-ray spectra can be very diverse, as diverse are the possible astrophysical scenarios that potentially allow for efficient conversions; thus, a detailed, dedicated analysis must be done for each particular physical case. At first sight, it might seem that photon-ALP conversions would always lead to an attenuation of the gamma-ray flux at Earth, as a fraction of the emitted photons would convert into ALPs and therefore would never reach the Earth. Yet, reconversions of ALPs into gamma-ray photons along the line of sight are possible, which would alter the level of attenuated flux. An additional ingredient needed for an accurate prediction is the precise role of the so-called extragalactic background light (EBL). This EBL – the result of the light emitted by galaxies over the entire cosmic history – permeates the whole Universe and induces an attenuation of the gamma-ray flux by pair production, i.e., $\gamma\gamma^{\text{EBL}} \rightarrow e^-e^+$. The attenuation is maximal for a background photon energy $\epsilon \sim (500 \text{ GeV/E})$ eV, which means that infrared/optical background photons are the ones responsible for the attenuation in the energy range specific to IACTs. The inclusion of the EBL in the computations of photon-ALP conversion

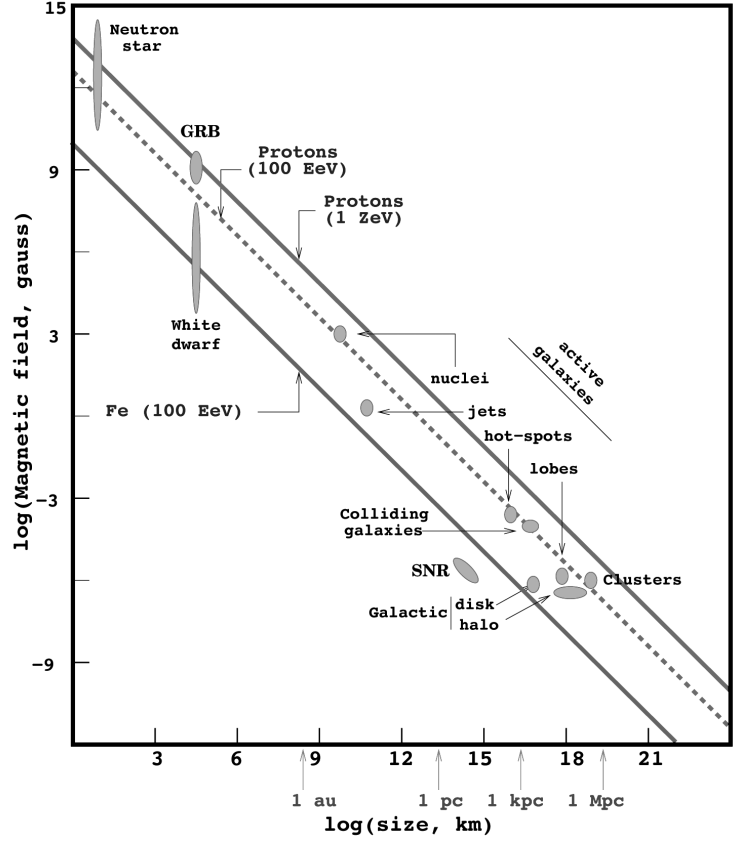


Figure 8.11: The Hillas criterium establishes a relation between physical sizes and magnetic fields in astrophysical objects/environments so that an efficient acceleration of ultra-high energy cosmic rays is possible. This correspondence can also be used as a very good proxy to understand where in the Universe an efficient conversion between photons and axions/ALPs can be expected. Figure taken from [Hooper and Serpico \(2007\)](#).

leads to very interesting predictions. Indeed, for distant VHE sources, ALP conversions in the intergalactic medium can lead to either an attenuation or an enhancement of the observed flux at Earth, depending on the exact configuration of the magnetic fields, energies considered, and source distance. An enhancement is possible because ALPs may travel unimpeded through the EBL and, only at later times before reaching the observer, some of them would convert back into gamma rays, for instance in the magnetic field of our galaxy. Intriguingly, this might potentially allow us to observe gamma-ray emitters located at distances larger than those expected from conventional EBL models. Additionally, it is interesting to note that photon-ALP conversion might also happen at the sources themselves, in this way providing an alternative scenario to avoid absorption of γ -rays in the dense ultraviolet radiation field of AGNs, see e.g. [Tavecchio et al. \(2012\)](#).

Note that none of the above given arguments explain the reason to perform the astrophysical ALP search particularly in the gamma-ray energy band and not at any other photon wavelengths. Indeed, the latter is certainly possible and has already been done in some works (see e.g. [Berg et al. \(2017\)](#), [Wouters and Brun \(2013\)](#) for X-ray astrophysical searches). When typical values of the astrophysical magnetic fields strengths are considered and the CAST upper bound is taken into

account, photon-ALP conversions are expected to show up in the \sim GeV-TeV range provided that the ALP mass is ultra light, i.e. $neV \leq m_a \leq \mu eV$; see Eq. (8.14).

Current status of ALP searches with IACTs. From an historical perspective, the event that triggered a rapidly increasing interest for ALPs within the gamma-ray astrophysics community was, very likely, the claim by the PVLAS collaboration back in 2006 of the observation of optical rotation generated in vacuum by a magnetic field – possibly associated to a neutral, light boson (Zavattini et al., 2006). Certainly, should such a light boson exist, it might have important astrophysical and cosmological consequences that could be tested (Archidiacono et al., 2015, de Angelis et al., 2008, Frieman et al., 1995, Mirizzi et al., 2008, Sikivie, 2008, Visinelli and Gondolo, 2010, Wantz and Shellard, 2010). The PVLAS claim was excluded soon after an upgraded setup (Zavattini et al., 2008); however the whole effort aimed at looking for ALP-induced features in the spectra of gamma-ray sources had already been boosted. The idea of using astrophysical observations to set constraints on ALP parameters was certainly not new and it had been already exploited well before 2006, e.g. Brockway et al. (1996), Csáki et al. (2002, 2003), Grifols et al. (1996), Mirizzi et al. (2005); yet the mentioned PVLAS claim first and, later, some astrophysical (gamma-ray) hints of photon-ALP conversions, as described below, generated a momentum in the community that stands until present time.

As said previously, efficient photon-ALP conversions may happen in those astrophysical environments that exhibit the right combination of magnetic field strength and size of the magnetized region. Indeed, prospects studies have been published that predict the size and shape of the expected ALP-induced spectral features due to conversions in or around the gamma-ray emitters themselves (Hochmuth and Sigl, 2007, Hooper and Serpico, 2007), within galaxy clusters (Horns et al., 2012), the intergalactic medium along cosmological distances (de Angelis et al., 2007, Mirizzi and Montanino, 2009, Mirizzi et al., 2008), our own galaxy (Simet et al., 2008), or a combination of these scenarios (Sánchez-Conde et al., 2009). With these predictions at hand, different approaches to look for ALPs with IACTs are possible; however all of them will be most likely based on the search and analysis of a systematic residual after applying the best-fit, conventional model to the available gamma-ray data. Only if we found significant departures with respect to this best-fit model, and after having discarded other possible conventional sources of error for such residuals, one might seriously consider it as a signal of exotic physics. On the contrary, the absence of any significant deviations with respect to the conventional baseline model can be used to set constraints on ALP parameters in such a way that all those combinations of ALP parameters that should have yielded a measurable effect in the data can now be excluded.

Along the years, two competing but complementary data analysis strategies were slowly arising as a consequence of both the predicted features and the matureness of the field: one aimed at statistically detecting the predicted spectral oscillations or *irregularities* around the critical energy for photon-ALP conversion; the other focused on the strong mixing regime, where the ALP-induced effect on the gamma-ray spectra is expected to be maximal. In most cases, the involved gamma-ray analyses were used to set limits on the ALP parameter space in the absence of any clear ALP-induced spectral trace in the data.²⁰ The obtained limits are nicely complementary to those achieved in the lab by other means, both in terms of the masses and of the couplings being tested. This is illustrated in Figure 8.12, which shows the current summary of limits obtained in the region of the ALP parameter space relevant to IACTs. In particular, the H.E.S.S. Collaboration

²⁰See, however, the claims made and briefly described below in this same section.

searched for ALP-induced irregularities in the spectrum of PKS 2155-304, an AGN located at $z = 0.116$ (Abramowski et al., 2013a). The authors of this work considered photon-ALP conversions happening both in the intergalactic medium between us and the source, and those in the intra-cluster magnetic field where the AGN resides. Since the magnetic field strength in each of these astrophysical scenarios is different by orders of magnitude (nG versus μG , respectively), according to Eq. (8.14) the data analysis will lead to two different sets of limits in the ALP parameter space. This can be seen in Fig. 8.12. The most competitive upper limits are obtained for the case of the intra-cluster medium, and are as good as $g_{11} < 2.1$ for $15 < m_{\text{neV}} < 60$ (at 95% C.L.).

Perhaps surprisingly, the H.E.S.S. collaboration so far is the only IACT experiment who has published ALP limits from their proprietary data, namely, on PKS 2155-304 (Abramowski et al., 2013a). In addition, using public H.E.S.S. data, Liang et al. (2019) have set limits on the ALP parameter space from a compilation of ten bright Galactic sources. Similarly, Guo et al. (2021) have combined public data from H.E.S.S. and *Fermi*-LAT on PKS 2155-304 and another extragalactic object (PG 1553+113) for a study of ALP implications.²¹ Galanti et al. (2020), Tavecchio et al. (2012) have studied an ample sample of blazar spectra at VHE energies seen by *Fermi*-LAT, H.E.S.S., MAGIC, and VERITAS, as did similarly Xia et al. (2019) with combined public data from *Fermi*-LAT and H.E.S.S., MAGIC, and VERITAS from supernova remnants to search for irregularities in the gamma-ray spectra. Although not strictly in the VHE band, other limits exist that were obtained with gamma-ray data as well, namely those using *Fermi*-LAT observations at lower, but partially overlapping energies than those covered by IACTs. In particular, a search for spectral oscillations in the spectrum of NGC1275, an AGN located at the center of the Perseus galaxy cluster, was used to set the most competitive ALP constraints derived from gamma rays as of today (Ajello, 2016). These limits exclude couplings $g_{11} > 0.5$ at ALP masses $0.5 \lesssim m_a \lesssim 5$ neV (95% C.L.) under the default (conservative) scenario considered by the authors to describe the configuration of the involved magnetic fields: the one in the galaxy cluster hosting the AGN and the one in our galaxy. Additional works using *Fermi*-LAT data to set constraints on the ALP parameter space are the ones by Xia et al. (2018) and Zhang et al. (2018). In the former, the authors used three supernova remnants as targets and reported a suspicious oscillatory behaviour of their spectra at small ($\sim 4.2\sigma$) significance. The uncertainties in the measurement do not allow extract robust conclusions and, instead, the authors speculated that this result could also be caused by different parts of the remnant contributing to the observed emission. In Zhang et al. (2018), the authors focused on PKS 2155-304 and set competitive limits with respect to those in Ajello (2016). Yet, their results are largely affected by important uncertainties in the modelling of the involved magnetic fields and, thus, the derived results should be taken with some caution.

In addition to setting meaningful limits on the ALP parameter space, some hints of the presence of ALPs were claimed along the years using gamma-ray data. Already back in 2007, ALPs with masses $\ll 10^{-10}$ eV were invoked to explain alleged anomalies in the flux of distant AGNs as measured by IACTs (de Angelis et al., 2007). At that time, the Universe seemed less opaque to gamma rays than predicted by the latest available EBL models; e.g. Aharonian et al. (2006), Albert et al. (2008a), Helgason and Kashlinsky (2012), Stecker and Scully (2009). This so-called “transparency hint” within the ALP and VHE communities, pointing to ultra-light ALPs as a possible (exotic) solution to the transparency problem, was reinforced a few years later by a statistical analysis of

²¹A similar work by Malyshev et al. (2018) focuses on the AGN labeled as NGC1275 in the Perseus galaxy cluster by a joint analysis of *Fermi*-LAT and public MAGIC data. The latter result suggests that those results in Ajello (2016) can be improved by roughly an order of magnitude under an optimistic, yet uncertain, configuration of the magnetic field. Yet, we note that this work has not been accepted as refereed article as of today.

Angelis et al., 2011); the intrinsic spectrum of a few AGNs showed a marginal deviation at the highest measured energies with respect to the expected power-law behavior (the so-called “pile-up problem”; Domínguez et al. (2011)); the existence of spectral hardening precisely at those energies where the EBL absorption is essential as well as its significant (12σ) unexpected dependence with redshift (Rubtsov and Troitsky, 2014); the existence of spectral breaks at a few GeV (Mena and Razzaque, 2013), the energy spectrum of some Galactic pulsars (Majumdar et al., 2018), etc. These apparent puzzles – although inconclusive and possible to explain within the boundaries of conventional VHE physics, e.g., particles accelerated at relativistic shocks (Stecker et al., 2007), internal photon-photon absorption (Aharonian et al., 2008), secondary gamma rays produced along the line of sight by cosmic-ray protons interaction with background photons (Aharonian et al., 2013, Essey and Kusenko, 2010, 2012, Essey et al., 2011) – gradually stacked up to offer the ultra-light ALP as a single, viable and very appealing explanation able to simultaneously resolve all of them. As a result, the momentum to perform the ALP quest in gamma rays persisted along the years and, indeed, continues intensively at present.

Future of ALP searches with IACTs. There is definitely room for further work on ALP searches in gamma rays, even with current IACTs. As described above, up to now only the H.E.S.S. Collaboration have published IACT data to search for ALPs and, in the absence of a signal, to set constraints on the ALP parameter space. Yet, both MAGIC and VERITAS are equally suited to perform similar studies in the Northern Hemisphere. Even more, archival data taken by these telescopes over the last years could be easily used as well to search for ALP-induced spectral features. A good example is the deep 400h observation of the Perseus galaxy cluster recently accomplished by the MAGIC telescopes. The initial goal of this observational campaign – the longest ever done by an IACT for a single object – was to look for the long-awaited first detection of cosmic-ray induced gamma-ray emission from clusters (Ahnen et al., 2016a) and, more recently, to set limits on DM decay (Acciari et al., 2018). Since these observations include NGC1275 and IC310 in the field of view, two AGNs sitting in the Perseus cluster and observed at a very high significance with MAGIC, the data possess all that it is necessary to search for spectral irregularities in a similar way than what was done by the *Fermi*-LAT collaboration in Ajello (2016). We remind that this LAT work, which also adopted Perseus as target, provided the best ALP limits derived from gamma ray observations so far. Another potential line of action to be further exploited by current IACTs can be provided by the measurement of new photons exhibiting very high opacities.²² A statistical analysis combining this hypothetical new data with what has been already observed, in a similar way to that done by Biteau and Williams (2015), Horns et al. (2012), Meyer et al. (2013), could provide further insight on the role of ALPs on photon propagation through cosmological distances.

Beyond current IACTs, CTA, with its ~ 10 times better sensitivity with respect to current IACTs, should make it possible to test the photon-ALP conversion scenario at an unprecedented sensitivity in the energy range between a few tens of GeV up to a few dozen TeV (Sanchez-Conde et al., 2013). Indeed, a 300h CTA observation of the Perseus galaxy cluster is foreseen during the first five years of CTA operations (CTA Consortium, 2019), which could be used to improve upon existing limits over a wider ALP mass range. A dedicated sensitivity estimate for gamma rays from NGC1275 inside the Perseus cluster shows that CTA could reach couplings as low as $g_{11} \gtrsim 0.1$ for masses around 10 neV (Abdalla et al., 2021). In this way, CTA may become the most sensitive

²²These may be possible to obtain from both new discoveries of sources located at cosmological distances and/or for already known sources observed at even higher energies.

instrument to ALPs at these masses, largely exceeding laboratory-based dedicated experiments such as CAST (Zioutas et al., 2005) or ALPS II (Bähre et al., 2013) and even competing with the future IAXO (Irastorza et al., 2013) at masses $5 \text{ neV} \lesssim m_a \lesssim 100 \text{ neV}$. These prospects were based on the search for ALP-induced spectral irregularities around the critical energy for conversion. In addition to the already discussed overlap and complementarity with *Fermi*-LAT, other next-generation instruments will complement CTA particularly in its low energy end as well, such as LHAASO (Bai et al., 2019, Long et al., 2021), or the future eASTROGAM (De Angelis et al., 2017) or AMEGO (Hartmann and AMEGO, 2018) missions. By design, these next-generation experiments are expected to possess superb spectral capabilities in the search for ALP-induced spectral features. Indeed, preliminary results focusing on photon-ALP conversions in the Perseus galaxy cluster (Caputo et al., 2018) show that these instruments could be sensitive to couplings $g_{11} > 0.3$ in the approximated ALP mass range $0.5 \lesssim m_a \lesssim 500 \text{ neV}$. Preliminary prospects work was also done that focused on using the spectral hardening of distant gamma-ray sources instead (Doro et al., 2013, Sanchez-Conde et al., 2013). This was further explored in detail for CTA by Meyer and Conrad (2014) by adopting a scenario consisting of four bright gamma-ray sources that are combined under the same consistent likelihood analysis. From this work, a significant detection of an ALP signal could be possible for ALP masses below 100 neV and couplings $g_{11} > 2$. At the highest energies covered by CTA, not only CTA but also HAWC (Abeysekara et al., 2017) and HiSCORE (Tluczykont et al., 2014), working in a complementary (even higher) energy range, will be much more sensitive to high energy photons from distant gamma-ray emitters compared to current IACTs. This increased sensitivity will allow to test at a higher confidence if the once claimed higher transparency of the Universe to gamma rays than expected from current EBL models is on solid grounds or not and, if so, whether ALPs could still represent a viable explanation. These and other instruments covering the VHE range up to tens to hundreds of TeV could also be used to search for spectral oscillations as well (Galanti and Roncadelli, 2018).

This whole picture of the near future of ALP searches with planned gamma-ray and other instruments is summarized in Fig. 8.13. In order to put this particular effort into the more general ALP search context, as done for Fig. 8.12, the figure also shows a broader energy range than the one that can be actually probed by gamma rays. Very interestingly, gamma rays may have the potential to look for ALPs in a region of the parameter space where they could constitute a portion or all of the DM content in the Universe, and which it is difficult to explore with any other current or planned detection technique or instruments. We refer to the interested reader the recently published review by Batković et al. (2021) for a further reading of the methods and technical challenges of ALP searches with IACTs.

Verification

- Q8.5: If all the DM in the Universe was made out of ALPs, would this scenario be in agreement with all gravitational evidence for DM (CMB, large-scale structure, mass distribution in galaxies and clusters)?
- Q8.6: Why is an enhancement of the gamma-ray flux at Earth possible for cosmological sources if photons oscillate into ALPs?
- Q8.7: Could there also be a way to probe the ALP DM particles present in the Universe?

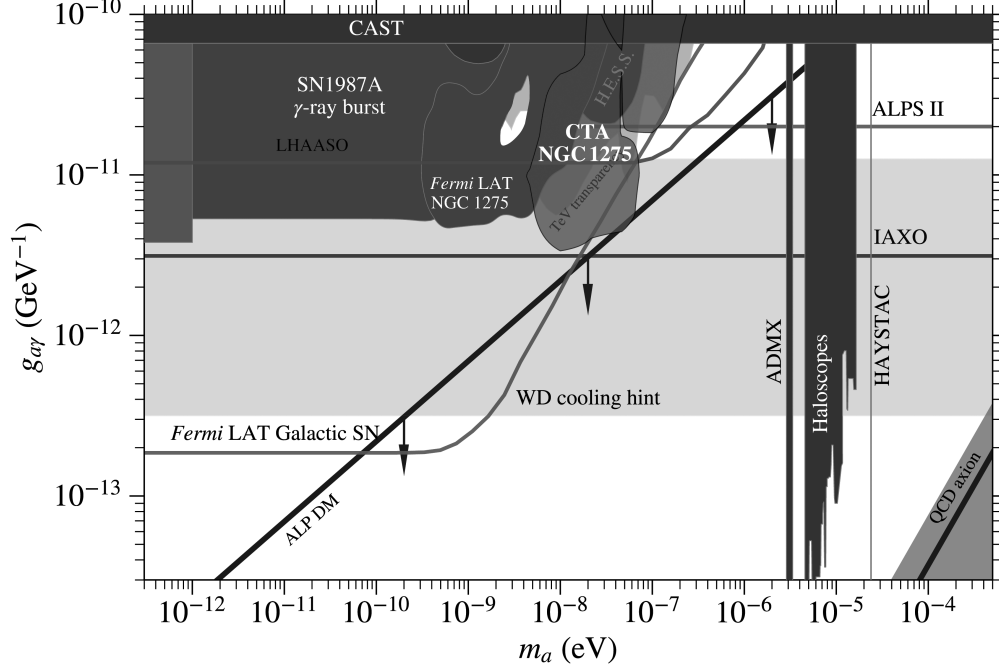


Figure 8.13: Future ALP search prospects for different experiments and astrophysical targets (depicted as horizontal lines and by the CTA excluding region). CTA should be able to provide very competitive limits around a few tens of neV, skimming the part of the parameter space where ALP could constitute the entirety of the DM in the Universe (region below the diagonal line). Figure taken from [Abdalla et al. \(2021\)](#).

8.3 Primordial Black Holes

The search for primordial black holes (PBHs) traces back to several decades ago. ([Hawking, 1971](#), [Zel'dovich and Novikov, 1967](#)). PBHs are different from astrophysical black holes (BHs). The latter form by gravitational collapse of dying heavy stars thus retrieving masses close to that of the progenitors. PBHs instead formed in the radiation dominated era, via different mechanisms that bounds their mass scale to the moment of generation. Because of their origin, they are not contributing to the count of baryonic matter. In half a century, numerous theoretical studies and experimental constraints have accumulated in search of evidence for PBHs, especially as DM candidate (see, e.g. [Carr et al., 2016](#), [Green and Kavanagh, 2021](#), [Sasaki et al., 2018](#), for recent reviews). There are several theoretically proposed formation mechanisms, which allow the mass to range from the Planck mass scale to that of the supermassive BHs ([Carr, 2005](#), [Carr et al., 2010](#)). An exact mapping of the PBH formation time and evolution combines constraints from cosmology, thermodynamics, general relativity and quantum mechanisms, at the extremes of their validity. The search for PBH gained significant momentum after the discovery of the GW150914 and merger event of two stellar mass BHs by the Ligo-Virgo collaboration (LVC; [Abbott et al., 2016a](#)). Since then, a large number of further confirmed GW events from merging BHs has been reported ([Bailes et al., 2021](#)). It was soon realized that BHs compatible with such merger events could constitute a large fraction or even the totality of DM (see Sec. 8.1) and be of primordial nature, thus opening new very intriguing possibilities ([Bird et al., 2016](#)). Clearly, a discovery of PBHs would constitute

a major breakthrough, shedding light onto the early Universe, quantum mechanics mechanisms, particle physics, and BH thermodynamics.

Most of the fate of a PBH relates to the time of formation, which foremost determines its mass. By relating the Universe density at time t with the critical density to generate a BH, one finds a relation between the PBH mass and the time of formation (Hawking, 1971):

$$M(t) \sim \frac{c^3 t}{G} \sim 10^{38} \frac{t}{1s} [g] = 0.5 \times 10^5 \frac{t}{1s} [M_\odot], \quad (8.16)$$

where t is the Universe age at the time of creation, M the PBH mass, c the speed of light, G the Cavendish constant. Different mechanisms allow the generation of PBHs. One general possibility is the collapse of regions with higher density than the surroundings. This could be the case during sudden pressure reduction, as possibly happened during the quark-hadron era, or during dust-like phases or slow reheating after inflation. Another possibility is are phase transitions, for example connected to bubble collisions, collapse of cosmic strings or domain walls. It is beyond the purpose of this text to properly summarize all theories and the reader is referred to specific review (such as Carr, 2005, Khlopov, 2010, and references therein).

The mass of the PBH has important consequences in the PBH evolution and affects several observable quantities. If the PBHs were formed at a precise moment, their mass distribution could be extremely narrow, however, this may well not be the case: if PBHs were generated through scale-invariant mechanisms, like generic quantum fluctuations of the space time, or during a wide time elapse, or have been subject to significant further mass accretion, they could have a wider mass distribution (Carr et al., 2010). The number density of PBHs is primarily constrained to be smaller than the DM at current times: $\Omega_{\text{PBH}} < \Omega_{\text{DM}} = 0.25$. However, their initial number could have been larger but constantly reducing over time due to the Hawking mechanism (Hawking, 1974). According to Hawking, BHs radiate over time, thus reducing their entropy and increasing their temperature, with faster pace as time goes by, eventually reaching a final stage of complete disruption called *evaporation*. The mass loss rate during the BH evolution in quantum decay scenarios is governed by:

$$\frac{dM_{\text{BH}}}{dt} = -\frac{\alpha(M_{\text{BH}})}{M_{\text{BH}}^2}, \quad (8.17)$$

where $\alpha(M)$ is a parameter that depends on the number of degrees of freedom (d.o.f.) available at any given time of the evaporation process. Clearly, the larger the temperature and the larger the number of d.o.f., the faster the pace of mass loss and the shortest the fate to evaporation. In particular, when the temperature exceeds the chromodynamics scale of 200 – 300 MeV, quarks and gluons start to be directly radiated, which subsequently fragment and generate hadrons, photons and leptons, which in turn produce a strong non-thermal emission. Above this value, considering the number of d.o.f. for quarks and gluons is larger than that for leptons and photons, the former dominate the observed gamma-ray spectrum (see for example Fig 1 of Halzen et al., 1991). While below the chromodynamics scale, the number of d.o.f. is more accurately known, one should mention that there are also models like that of Hagedorn (1968) that foresee a strong multiplication of the number of d.o.f. during the final stages of evaporation, which would imply an event faster final stage evolution before the evaporation, with complete disruption in nanoseconds to microseconds. It should be noted that the Hawking mechanism in its simpler description may not be accurate. Recently it was found for example that small mass BHs may become unstable due to quantum-gravitational effects earlier than predicted, with relevant consequences on observables like galaxy

clustering (Raccanelli et al., 2017). A PBH with mass M has a temperature (Halzen et al., 1991):

$$T_{\text{BH}}(M) = \frac{\hbar c^3}{8\pi G k_{\text{b}}} \frac{1}{M} \sim 100 \left(\frac{10^{15} \text{ g}}{M} \right) [\text{MeV}], \quad (8.18)$$

which increases over time as long as mass is lost, so that the life expectation for a BH, also called *evaporation time* is:

$$\tau_{\text{BH}}(M) = \frac{G^2 M^3}{\hbar c^4} \sim 10^{10} \left(\frac{M}{10^{15} \text{ g}} \right)^3 [\text{yr}] \quad (8.19)$$

where \hbar is the reduced Planck constant and k_{b} the Boltzmann constant. The temperature can be connected to the lifetime through the following formula (MacGibbon et al., 2015):

$$T_{\text{BH}}(\tau) \approx \left[4.8 \times 10^{11} \frac{1 \text{ s}}{\tau_{\text{BH}}(M)} \right]^{1/3} [\text{GeV}]. \quad (8.20)$$

The reason to use a reference mass of $M_{\dagger} = 10^{15} \text{ g}$ ($\sim 10^{-18} M_{\odot}$) is that Eq. 8.19 shows that all PBHs roughly lighter than this value would have already evaporated at present time. PBHs at about M_{\dagger} would instead be evaporating now, possibly associated with cataclysmic events such as long-duration Gamma-ray Bursts (GRBs). Heavier PBHs would be only mildly emitting radiation and almost stable, constituting a sort of non-baryonic collisionless cold fluid, and thus a possible contributor to the DM (Barack et al., 2018, Feng, 2013). Evaporated, evaporating, and non-evaporating PBHs imply therefore rather different observables and means for investigation, and quite different chances for detection. A collection of constraints can be found online²³.

For already evaporated PBHs, the limits are obtained with cosmological probes such as the CMB or theoretical arguments. In the range $< 10^{17} M_{\odot}$, evaporated PBHs would have filled the Universe with particles and radiation that would have affected baryogenesis, for example through injection of substantial amount of antiparticles, or through interaction with photons of the cosmic microwave background. In the range $10^{-17} M_{\odot}$ instead, PBHs would have strongly radiated MeV photons in their final phase, as shown in Eq. 8.16. This radiation would have filled the Universe, a prediction that is not observed on top of a standard astrophysical MeV diffuse background, thus providing very robust constraints too (Laha et al., 2020). PBH with masses around M_{\dagger} would be instead evaporating at present time. We could observe such events for example as gamma- or X-ray bursts or even through emission lines such as those observed from the GC. IACTs are sensitive in the TeV range, and would be therefore valid probes for PBH evaporating now, as we will discuss in more depth in the following. Finally, for larger initial masses, PBHs would appear as massive non-baryonic objects. As such, they would naturally act like weakly interacting massive objects, a standard requisite for a DM particle theory. For such objects, we could expect electromagnetic or hadronic signatures besides the gravitational ones. The detection of gravitational waves from black holes with estimated mass of few tens of GeV (Abbott et al., 2016b,c,d) revived the interest of PBHs as DM candidates of similar mass (Barack et al., 2018, Bird et al., 2016).

Search for PBHs with IACTs. How well do IACTs fit into this wide world of PBH observables? IACTs have narrow field of view (FOV) which makes any attempt of detection of diffuse emission hard to attain. Probably the main avenue for IACTs to search for signatures of ongoing PBH disruptions. As discussed, in the final phase, evaporating PBHs would deliver an increasing

²³<https://github.com/bradkav/PBHbounds>

emission, culminating with a disruption and a burst of very high energy (GeV to TeV) radiation, lasting however short time, from fractions of seconds (Hagedorn, 1968) to several seconds (see Fig. 3 of MacGibbon et al., 2015). The expectation for the gamma-ray spectrum a superposition of two components: A primary component comes directly from Hawking radiation and is thus peaked at around the PBH mass. A secondary component comes from the decay of hadrons produced in the fragmentation of primary quarks and gluons and peaks at somewhat lower energies. Due to available number of d.o.f., a large fraction of Hawking radiation from evaporating PBH would be in the form of quark and gluon jets. The secondary components would provide a photon contribution larger than the primary one.

Despite presumable intense radiation during evaporation, such disrupting events would not be easy to catch with IACTs: their short duration would in fact reduce the number of external triggers such as those provided by the Fermi GMB or LAT instruments, in reason of the small sensitivity for seconds-elapsing PBH evaporation. Evaporating PBHs could alternatively appear serendipitously as extremely ephemeral but bright emission anywhere in the FOV of IACTs during regular observations. Such events would likely not be automatically recognized by the standard trigger and data reconstruction mechanisms. A specific search for evaporating PBH must be developed on IACT data.

Results. The idea of using Cherenkov light to detect PBHs was first developed by Porter and Weekes (1978, 1979) and further implemented with the realization of a specific trigger system called SGARFACE (Krennrich et al., 2000, LeBohec et al., 2005). The SGARFACE detector, mounted on the single-dish Whipple telescope, was a specific trigger, based on analogue pixel summation, sensitive to gamma-ray 'glows' developing in the atmosphere after short and intense bursts of gamma rays above 100 MeV. The Cherenkov light at the ground from sub-GeV showers would be extremely spread, due to the increased Coulomb scattering of the atmospheric shower particles, much more than for TeV showers, almost impeding a directional reconstruction. Individually, they would not be detectable, but in case of a strong burst, the sum of all these 'glows' was simulated and shown to be detectable with SGARFACE. The motivation for SGARFACE was two-fold. First, it was to constrain the short time scale bursts from PBHs in the sub-microsecond to 100 microsecond scale, as predicted by Hagedorn (1968). But second and foremost, it was to be used to look for other short time scale bursts in the sub-GeV to GeV regime, including counterparts to giant radio pulses from pulsars. The intensity peaks were searched in windows of 60, 180, 540, 1620, 4860 ns and $15\mu\text{s}$, with digitization bin of 20 ns. The predicted sensitivity of SGARFACE was ranging from 0.8 to $50\text{ ph cm}^{-2}\text{s}^{-1}$ for primaries above 200 MeV and pulse width of 60 ns and $15\mu\text{s}$ respectively and for a burst modelled as a power law with spectral index of -2.5 . Results obtained with this instrument were presented by Schroedter et al. (2009) using 2.2 million events taken over 6 years of operation. That study also presents in details the instrument, the reconstruction and the analysis. The sensitivity limits were computed for PBH of mass 10^{13} g , for different burst durations, and ranged between 1 and 10^3 bursts per cubic parsec per year for duration from ns to μs if assuming the Hagedorn mechanism. Larger duration bursts, of the order of seconds, were constrained also using the Whipple telescope standard trigger (Connaughton et al., 1998, Linton et al., 2006), providing additional results on PBH evaporation from IACTs. In particular the latest result with Whipple (Linton et al., 2006) made use of about 2200 h of good quality data taken between 1998 and 2003. The search was made over time windows of 1, 3 and 5 seconds. A peak in emission was determined when a certain number of consecutive events were recorded within a certain window

of time. It is clear that the larger the window, the larger the probability of contamination from background events. The background contamination was attenuated by scrambling all the time of events. Statistically generated burst surviving the search criteria on the scramble sample were thus removed. The probability of observing a burst event of intensity b in a time window Δt at an angular direction θ and an astrophysical distance r can be written as (Linton et al., 2006):

$$n_{\text{BH}}(b, \Delta t) = \rho_{\text{BH}} \tau \int_{\Delta\Omega} d\omega \int r^2 P(b, N_{\text{d}}(r, \theta, \Delta t)) dr, \quad (8.21)$$

where ρ_{BH}, τ are the BH numerical volume density and τ the lifetime, ω is the solid angle of the signal search, and $P(b, N_{\text{d}}(r, \theta, \Delta t))$ is the Poisson distribution of a BH emitting N_{d} gamma-rays and producing an event of intensity b where the number of emitted gamma rays is:

$$N_{\text{d}}(r, \theta, \Delta t) = \frac{A(\theta)}{4\pi r^2} \int_{\Delta t} dt \int \frac{d^2 N(E, t)}{dE dt} A_0(E) dE, \quad (8.22)$$

where $A(\theta)$ is the effective area. These formulas can be used to provide upper limits on the PBH density using the number of detected bursts, once the initial gamma-ray spectrum is specified. Of course, this depends on the exact knowledge of the quantum process at work during the evaporation phase, as well as with BH properties (e.g. spin) and its surroundings (for example if a chromosphere is formed). This search provided the first constraints to the PBH density at 1.08×10^6 PBH $\text{pc}^{-3} \text{yr}^{-1}$ (see Fig. 8.14):

$$\frac{dN_{\gamma}}{dE} = 9 \times 10^{35} \times \begin{cases} \left(\frac{T_{\tau}}{1 \text{ GeV}}\right)^{-3/2} \left(\frac{E}{1 \text{ GeV}}\right)^{-3/2} \text{ GeV}^{-1} & \text{for } E < k_{\text{b}} T_{\tau} \\ \left(\frac{E}{1 \text{ GeV}}\right)^{-3} \text{ GeV}^{-1} & \text{for } E > k_{\text{b}} T_{\tau} \end{cases} \quad (8.23)$$

where $T_{\tau} = 7.8 k_{\text{b}}^{-1} (\tau/1 \text{ s})^{-1/3}$ [TeV] is the PBH temperature with a lifetime of τ .

In the thesis of Cassanyes (2015), the potential of MAGIC to search for PBHs was investigated for the first time. Cassanyes assumed $1 \div 10,000$ h of good quality data, and photons from 158 GeV to 10 TeV. He found that the largest sensitivity comes for integration times of about several minutes, a value larger than the few seconds found by VERITAS and H.E.S.S. This is probably explained by a different emission model than Eq. 8.23. Within this window, upper limits of the order of $\sim 10^4$ $\text{pc}^{-3} \text{yr}^{-1}$ can be achieved. However, MAGIC has not published any results on actual data with such technique.

Recently, there is increased activity in the field to analyze accumulated existing IACT data for PBH signatures: Tavernier et al. (2019, 2021) are analyzing so far almost 5000 hours of H.E.S.S. data in search of PBH events, reaching upper limits on the evaporation rate to < 527 $\text{pc}^{-3} \text{yr}^{-1}$ (see Fig. 8.14. Also the VERITAS collaboration is pursuing such reanalysis of their data (Pfrang, 2021), with also looking for short-term optical fluctuations by PBH microlensing events (Pfrang et al., 2021).

Outlook. Are the current limits interesting? These limits are several orders of magnitude away from the limits obtained with e.g. the extragalactic background (EGB), in the range of PBH evaporating at present times. However, the theoretical mapping of PBH formation and evolution still allows for a wide range of possibilities to significantly make these limits stronger. There are at least two direct ways to improve the limits. First, the mass loss of the BH is governed by the number of d.o.f. As such, if one relaxes the assumption that only Standard Model d.o.f. are to

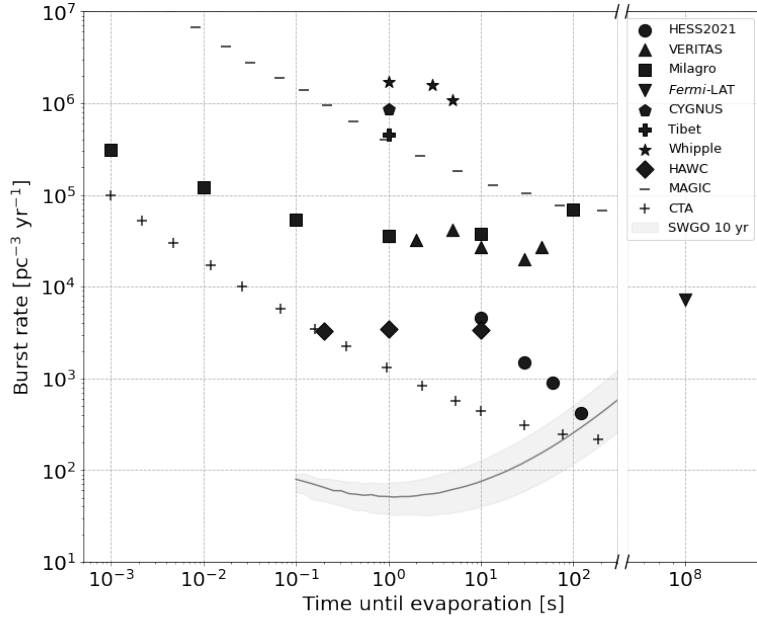


Figure 8.14: A collection of limits on the PBH volume density as a function of the time to evaporation for PBH of mass of the order of $10^{15}g$. The image is an update of Fig. 4 of López-Coto et al. (2021) after inclusion recent H.E.S.S. data from Tavernier et al. (2021) and the predictions for MAGIC and CTA by Cassanyes (2015).

be used, boosted emission can occur as a result of multiplication of d.o.f. during the final stage of evaporation (Hagedorn, 1968). Secondly, those limits assume an homogeneous PBH distribution in the Universe. However, clustering in galaxies is plausible (Raccanelli et al., 2017), which would significantly change these limits. Finally, one should not forget that possibly PBHs have a narrow mass range and therefore a limit in one mass region does not necessarily affect limits in other part of the mass spectrum.

There are instruments sensitive to PBHs in the TeV range,²⁴ specially the wide FOV air shower detectors such as MILAGRO and HAWC. MILAGRO (Abdo et al., 2015) provided results with 4.58 years of data. Such large observation time compared to IACTs is justified by the fact that MILAGRO observed particles within the showers, and thus have a daily duty cycle. The optimal search time for MILAGRO was between 1 and 100 seconds. At smaller intervals, the sensitivity gets low, at larger intervals, the background contamination becomes dominant. Limits were obtained of the order of $\sim 10^5 \text{ pc}^{-3} \text{ yr}^{-1}$. In the same work by Abdo et al. (2015), an extrapolation for the performance of HAWC was attempted, resulting again with limits in the ballpark of $\sim 10^4 \text{ pc}^{-3} \text{ yr}^{-1}$. More recently, López-Coto et al. (2021) investigated the prospects for this search with the planned instrument SWGO, showing how this instrument detector can improve of more than one order of magnitude the limits from HAWC as shown in Fig. 8.14. An endeavor to compute the

²⁴Note that there are also efforts to search for PBHs at lower, MeV gamma-ray energies (LeyVa et al., 2021, Ray et al., 2021).

prospects for CTA was made by [Cassanyes \(2015\)](#). Cassanyes used the same method to estimate the performance of MAGIC with CTA’s figure of merit. He found that the sensitive PBH volume of CTA would be a factor of about 790 larger than in MAGIC: a factor of 25 due to the larger FOV, and a factor of $10^{3/2}$ because the 10-times better sensitivity allows for a $\sqrt{10}$ farther distance. With this performance, CTA could set constraints of the order of $\sim 10^2 \text{ pc}^{-3} \text{ yr}^{-1}$. The advantage is that no specific time is required to IACTs: PBHs could appear serendipitously as bright and short bursts, lasting from sub-second to seconds, anywhere in the field of view. Detecting these events require to build a specific off-line reconstruction pipeline. As discussed by [Doro \(2017\)](#), considering that CTA will surely strongly compress and reduce the global information from its hundreds of cameras in order to save disk space, these pipelines should be developed and investigated as soon as possible in order to avoid losing important data for PBH searches.

Verification

Q8.8: Can the imprint of non-baryonic matter in the CMB anisotropies be caused by PBHs?

Q8.9: What gamma-ray instruments are best suited to search for PBHs evaporation?

Q8.10: What gamma-ray instruments are best suited to search for evaporated PBHs?

Q8.11: Why a tailored analysis is needed by IACTs in search for PBHs?

Q8.12: Why CTA may be less competitive than other gamma-ray instruments in the same energy band?

8.4 Tau-Neutrinos

The nature of the astrophysical emission of neutrinos is for many decades one of the hottest topics in astrophysics. The interest has been boosted in recent times by the measurement of an astrophysical diffuse flux of high-energy neutrinos by IceCube ([Aartsen et al., 2014b](#)) and the significant spatial and temporal coincidence observed between a 290 TeV neutrino event by IceCube and a flaring blazar by Fermi-LAT and MAGIC ([Aartsen et al., 2018](#)). Several unknowns are yet to be understood: What is the full spectrum and composition of the diffuse neutrino flux? What astrophysical targets are neutrino emitters and where does the neutrino emission takes place? Are neutrinos produced via leptonic or hadronic processes? Are neutrinos also the result of interaction of high energy cosmic rays with local ambient fields? These and others questions are effectively tackled by large-scale ground-based instruments such as the mentioned IceCube, Antares ([Adrian-Martinez et al., 2011](#)), the planned KM3NeT [Adrián-Martínez et al. \(2016\)](#) at TeV to PeV energies, and the Pierre Auger Observatory (PAO) ([Aab et al., 2015](#)), the All-sky Survey High Resolution Air-shower detector (ASHRA) ([Asaoka and Sasaki, 2013](#)), or the future Giant Radio Array for Neutrino Detection (GRAND) ([Alvarez-Muñiz et al., 2018](#)) and Probe of Extreme Multi-Messenger Astrophysics (POEMMA) observatory [Olinto et al. \(2020\)](#) at PeV energies and above. Also, although not primarily designed for neutrino detection, IACTs are instruments capable not only to detect electromagnetic counterparts to neutrino astrophysical targets, but also possibly to directly detect signatures of neutrino events crossing the Earth’s atmosphere or neutrinos emerging from the Earth’s crust in a technique called *Earth-skimming* detection technique [Fargion \(1999\)](#).

Extraterrestrial neutrinos are generated (see, e.g., [Baret and Van Elewyck, 2011](#), [Becker, 2008](#), for recent reviews) through general production mechanisms such as nuclear decay (proton-proton) or photopion (proton-photon) interactions eventually generating neutrinos through reactions such as:

$$\begin{aligned}
 p p &\rightarrow \pi^+ \pi^- \pi^0, \text{ followed by:} \\
 \pi^+ &\rightarrow \mu^+ \nu_\mu \rightarrow e^+ \nu_e \bar{\nu}_\mu \nu_\mu \quad \text{or} \\
 \pi^- &\rightarrow \mu^- \bar{\nu}_\mu \rightarrow e^- \bar{\nu}_e \bar{\nu}_\mu \nu_\mu
 \end{aligned} \tag{8.24}$$

and

$$\begin{aligned}
 p \gamma &\rightarrow \Delta^+, \text{ followed by:} \\
 \Delta^+ &\rightarrow p \pi^0 \quad (2/3) \quad \text{or} \\
 \Delta^+ &\rightarrow n \pi^+ \quad (1/3)
 \end{aligned} \tag{8.25}$$

Therefore, depending on the ambient matter and radiation fields, the above processes can give rise to neutrino emissions in a wide range of energies and fluxes ([Ackermann et al., 2019](#)). At MeV energies, a cosmic neutrino background is expected from solar MeV neutrinos generated within our Sun as well as from farther stars. Above 0.1 GeV the most abundant population is that of atmospheric neutrinos, generated by the interaction of cosmic rays with the Earth's atmosphere. Atmospheric neutrinos constitute the by-far larger background in large-scale neutrino detectors. In this energy range one can also find the rarer interesting extraterrestrial neutrinos produced e.g., in an Active Galactic Nucleus (AGN) or a GRB and possibly in all other non-thermal emission regions in which high energy cosmic rays are efficiently generated. Finally, above $5 \cdot 10^{19}$ eV, neutrinos are found after Δ resonances (Eq. 8.25) of ultra high energy cosmic rays with the cosmic microwave background ([Berezinsky and Zatsepin, 1969](#)) (cosmogenic neutrinos). Therefore, the phenomenology of neutrino production is wide, and often accompanied to high energy cosmic ray reservoirs.

During hadronic processes in Galactic and extragalactic environments, the expected neutrino generation rate ratio is $(\nu_e, \nu_\mu, \nu_\tau) = (1, 2, 0)$, due to the fact that positive, negative and neutral pions are produced equally during proton interactions. Therefore, ν_τ s are not expected to be produced significantly through these mechanisms at the source. However, during propagation, neutrino families mix because of the non vanishing mass eigenstates. Already for distances larger than few astronomical units, the mixing is total and a uniform neutrino family mix is expected at Earth: $(\nu_e, \nu_\mu, \nu_\tau) = (1, 1, 1)$ (for the computation of mixing, see [Becker \(2008\)](#)). It is important to recall that the family mixing depends on terms proportional to the difference of the squared masses of two neutrino flavors. Therefore, the detection of ν_τ s is very relevant not only to test astrophysical cosmic ray processes and unveil new emission mechanisms at the source, but also to test neutrino physics models.

By ice or water detectors with a huge instrumented volume (such as IceCube, Antares, or KM3Net), TeV-PeV neutrinos are observed through the Cherenkov light generated in particle showers produced by the neutrino interactions in the detector ([Aartsen et al., 2016b](#)). Above the PeV range, the ice or the water are increasingly opaque to the crossing of electron or muon neutrinos, and only ν_τ s can be detected from below. Above PeV energies, the technique to detect Earth-skimming cosmic ν_τ s comes into play: When neutrinos hit the Earth at its rim and cross a certain amount of the Earth's crust, they have a non negligible chance of converting to a lepton which subsequently may emerge into the air and induce an upwards-directed atmospheric shower. The advantage of this approach is very similar to seeking for signatures from cosmic primaries interacting with the atmosphere: One uses the Earth itself as suitable large interaction volume,

and only needs to place a detector in or close to the induced secondary particle showers. Also, while ν_τ s are the only candidates for the Earth-skimming technique, they probe indirectly the whole neutrino family of astrophysical origin due to the neutrino mixing. The Earth-skimming approach is pursued by the PAO (Fargion, 2002, Fargion et al., 2004), and detectors like ASHRA and GRAND are primarily designed for it. Finally, this technique can also be adopted by IACTs, detecting the Cherenkov light of the ultra-relativistic particles in the neutrino-induced atmospheric showers. The setup for detecting Earth-skimming ν_τ s with IACTs is illustrated in Fig. 8.15.

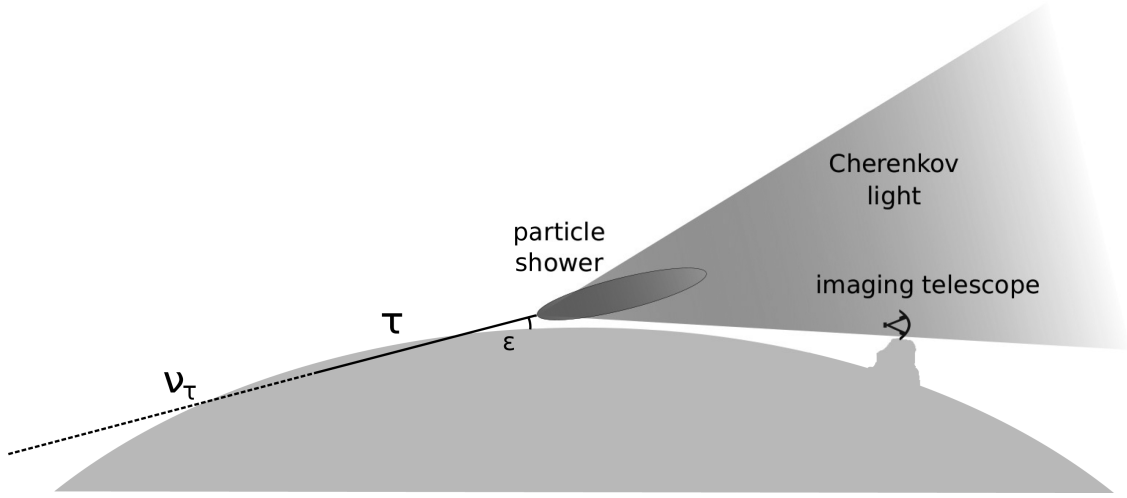


Figure 8.15: Artistic sketch of the Earth-skimming ν_τ -technique, with the basic scheme of detection for IACTs. The Cherenkov light cone is produced by charged shower particles emerging from the direction of the ν_τ . Courtesy of N. Otte, reproduced from Otte (2019).

Neutrino interactions with matter (N) happen with charged current (CC) and neutral current (NC) mechanisms:

$$\text{CC: } N + \nu_l \rightarrow \dots \rightarrow X + l \quad \text{where } l = e, \mu, \tau \quad (8.26)$$

$$\text{NC: } N + \nu_l \rightarrow X + \nu_l \quad \text{where } l = e, \mu, \tau \quad (8.27)$$

where X is a generic product that leads to a hadronic cascade. Of the leptons found in the reaction products, electrons are rapidly absorbed in matter and the chance of exiting the Earth's crust are low. When muons are created in these interactions, they also lose most of their energy inside the Earth, but with longer radiation length than electrons and occasionally pass through the crust and decay in the atmosphere. However, due to its rather large lifetime, a muon emerging from the Earth would rarely decay into a particle shower within the telescope field of view (F.O.V.) and only generate direct Cherenkov light, which mostly would go undetected. The situation drastically changes for tau neutrinos. A PeV tau particle created after a CC ν_τ interaction in the crust can travel through a rather large amount of matter with a significant chance to decay shortly after leaving the crust at the right distance from the telescopes and generate extensive air showers.²⁵

²⁵At the highest \sim EeV energies, the $\nu_\tau \rightarrow \tau \rightarrow \nu_\tau \rightarrow \tau \rightarrow \dots$, recreation chain increases the chance of a high-energy tau leaving the crust and, consequently, the telescopes' acceptance (Alvarez-Muñiz et al., 2018).

Table 8.2 (extracted from [Fargion, 2002](#)), summarizes the main tau decay modes: a large cross-section is found into hadronic-induced showers (65%), electromagnetic showers (18%) or muons (17%). The first two components are detectable if generated at the right distance range and within the telescopes F.O.V.

| Decay | Secondaries | Probability | Air-shower |
|---|--|-------------|----------------|
| $\tau \rightarrow \mu^- \bar{\nu}_\mu \nu_\tau$ | μ^- | 17.4% | – |
| $\tau \rightarrow e^- \bar{\nu}_e \nu_\tau$ | e^- | 17.8% | Pure e.m. |
| $\tau \rightarrow \pi^- \nu_\tau$ | π^- | 11.8% | Pure had |
| $\tau \rightarrow \pi^- \pi^- \pi^+ \nu_\tau$ | $2\pi^-, \pi^+$ | 10% | Pure had |
| $\tau \rightarrow \pi^- \pi^0 \nu_\tau$ | $\pi^-, \pi^0 \rightarrow 2\gamma$ | 25.8% | Mixed had/e.m. |
| $\tau \rightarrow \pi^- 2\pi^0 \nu_\tau$ | $\pi^-, 2\pi^0 \rightarrow 4\gamma$ | 10.79% | Mixed had/e.m. |
| $\tau \rightarrow \pi^- 3\pi^0 \nu_\tau$ | $\pi^-, 3\pi^0 \rightarrow 6\gamma$ | 1.23% | Mixed had/e.m. |
| $\tau \rightarrow \pi^- \pi^+ \pi^- \pi^0 \nu_\tau$ | $2\pi^-, \pi^+, \pi^0 \rightarrow 2\gamma$ | 5.18% | Mixed had/e.m. |

Table 8.2: Decay channels for the τ lepton. Probability and type of atmospheric showers are also shown ("e.m." for electromagnetic; "had" for hadronic). The table is reproduced from [Fargion \(2002\)](#).

Tau-neutrino searches with IACTs. For IACTs, the Earth-skimming ν_τ observation technique thus requires a suitable orography around the telescopes: The telescopes must be pointed at the ν_τ emission point, sufficiently distant, corresponding to the right amount of crossed matter within the Earth. This is for example doable if a mountain with right thickness is located in the telescopes' vicinity, or if the telescopes can be pointed downward toward a direction in which the amount of crossed matter is optimal. The MAGIC telescopes are located at the Roque de los Muchachos Observatory in the Canary Islands. The Roque mountain can be pointed by MAGIC. However, it is only few hundreds of meters away, and therefore a particle shower would be initiated through or behind the telescopes. On the other hand, from the MAGIC location, there is a window of observability toward the Atlantic Ocean in the Northern direction. If the telescopes are pointed at around 1.5 degrees below horizon, a window of $5 \times 80 \text{ deg}^2$ is accessible with an extraction point at the Ocean at 165 km, allowing sufficient space for the shower development. [Gaug et al. \(2007\)](#) were among the first to investigate this technique, and performed analytical computations to find the optimal observation strategy and the effective area. They also performed the first order-of-magnitude event rate estimation. However, at that time, a full simulation chain of neutrino interaction and shower development was not available. A complete Monte Carlo chain of simulation was provided by [Gora and Bernardini \(2016\)](#) by adapting the ANIS code ([Gazizov and Kowalski, 2005](#), [Gora et al., 2007](#)), as well as with publicly available orography maps. On this basis, [Gora et al. \(2017b\)](#) computed a precise sensitivity and angular acceptance for MAGIC.

Results. MAGIC published the results from the observation of 30 h of data in the direction of the Ocean ([Ahnen et al., 2018b](#)), summarizing the previous findings by [Gora et al. \(2017a,b\)](#). The observation was performed by pointing at an optimized direction toward the Ocean during several nights, in which high cirrus clouds were present. Such a condition normally does not allow for standard astronomical observation, however, it guarantees good visibility toward the Ocean. The most complex part of this technique is the discrimination of the signal parameter space from

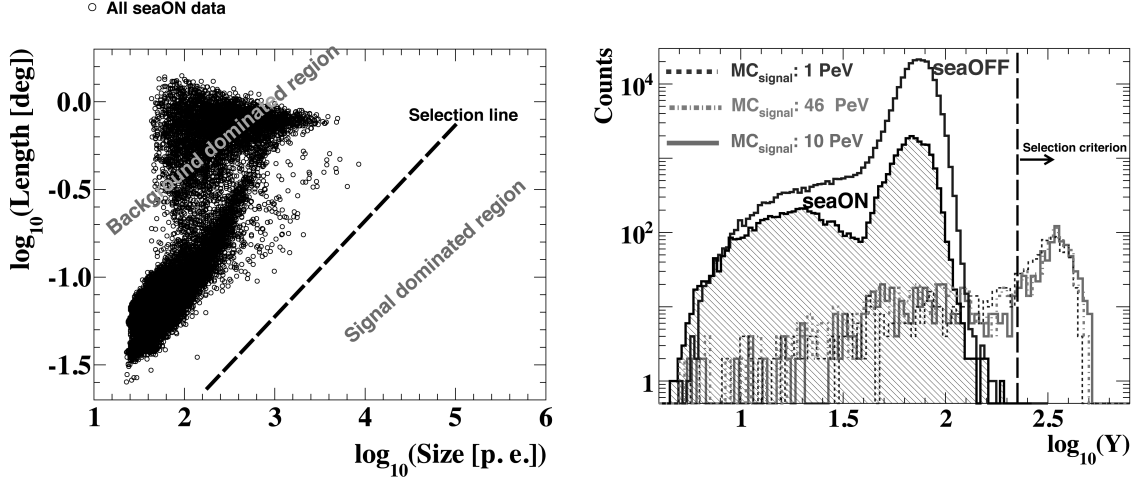


Figure 8.16: Left: The distribution of events in the space length-size of the image parameters. Background events and signal events are clearly separated by the cut selection Y . Right: Distribution of events after the selection cuts based on the same Y parameter (see text) in search for tau-neutrino signatures with MAGIC. ‘seaON’, ‘seaOFF’ and signal MC events represent the data taken pointing at the signal region (‘seaON’), at the background control region (‘seaOFF’) and the MC simulated tau neutrinos. In the region $\log_{10}(Y) > 2.35$, no neutrino candidates survive. The selection criterion keeps about 40% of MC signal events. Courtesy from MAGIC Coll. (Ahn et al., 2018b).

the background, as well as the corresponding Monte Carlo simulations. The central analysis steps and results are briefly summarized in the following: First of all, the background was estimated by pointing the telescope for 5.5 hours slightly above the Ocean, at 2.5 deg above horizon. This allows to gather a significant number of background events as expected in the later below-horizon observation. A combination of the Hillas size and length image parameter, dubbed Y ²⁶ was found to clearly separate signal and background, as shown in Fig.8.16. The figure also shows the Y parameter for ν_τ of energy 1, 10, 46 PeV. Muon bundles are the dominant background contribution whereas contributions from cosmic-ray electrons can be neglected: At horizontal directions the Cherenkov light from electromagnetic showers is strongly attenuated, even more than for proton primaries of similar energy, and below the detection threshold. To build the Monte Carlo simulations, besides the ANIS modified version (Gazizov and Kowalski, 2005, Gora et al., 2007), also CORSIKA (Heck et al., 1998, (v6.99)) and PYTHIA (Sjostrand et al., 2006, (v6.4)) were used. No event was found, after selection cuts, in 30 h of observation. The null detection was translated into an upper limit for ν_τ emission after a thorough estimation of the acceptance for these particles, which is not straightforward considering the geometry of the observation, the presence of mixed water and rocks in the ν_τ path, the inclusion of atmospheric transparency and the fact that multiple atmospheric showers can occur. The results are reported in Fig. 8.17 considering the diffuse neutrino flux as well as different neutrino emission models for AGNs. The latter were built based on models of real blazar flaring events. In particular, Blazar #4 and Blazar #5 of Fig. 8.17 represent predictions for PKS 2155-304 in high-state and 3C 279 respectively (Atoyan and Dermer, 2001, Becker, 2008).

²⁶ $\log_{10}(Y) = \log_{10}(\text{Size}[\text{p.e.}] * \cos(\alpha) - \log_{10}(\text{Length}[\text{deg}]) * \sin(\alpha))$, where $\alpha = 63.435^\circ$

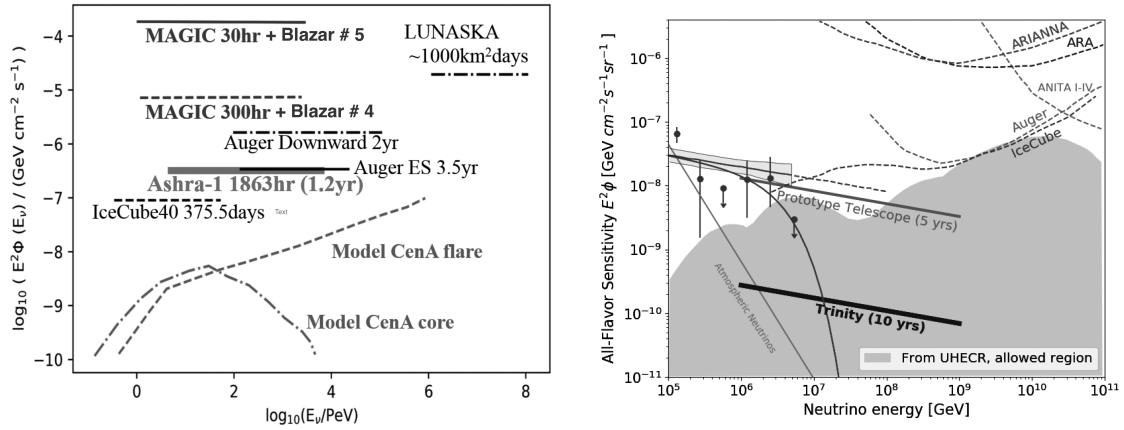


Figure 8.17: (Left) 90% C.L. upper limit on the point source tau neutrino flux obtained with the MAGIC telescopes with 30 hrs of observation (solid upper horizontal line) assuming a specific flux level from flaring blazars, as well as extrapolated to 300 h (dashed upper horizontal line) (Fig 3 of Ahnen et al., 2018b). (Right) Comparison of sensitivity for VHE and UHE neutrino experiments (Fig 5 of Brown et al., 2021).

The point-source sensitivity corresponding to 30 h of observation (Blazar #4 model are poorly constraining, of the order of $2 \times 10^{-4} \text{ GeV cm}^{-2} \text{ s}^{-1}$). Only if 300 h are considered, and a more optimistic flux model is adopted (Blazar #5), the sensitivity becomes of the order of the one obtained with downward (all-flavor) neutrinos by Auger (Aab et al., 2015). This is still far away from the sensitivity obtained with IceCube (Aartsen et al., 2016a). Yet, the sensitive region is different, being MAGIC indeed sensitive at somewhat higher energies than IceCube but at smaller energies than PAO, thus allowing for searches for a wider class of astrophysical emitters.

Similar results were obtained with the ASHRA-1 Cherenkov telescopes at Mauna Loa (Ogawa, 2020). This telescope, composed of electrostatic lenses with an optical system to generate convergent beams, observes ν_τ skimming through the Mauna Kea mountain. It performed a campaign of 1863 h over 1.2 years that led to limits on the diffuse flux more constraining than those obtained with MAGIC (see Fig. 8.17), further demonstrating the validity of the technique.

Outlook. Albeit these results may not look impressive, they demonstrate that IACTs do have a potential for ν_τ searches, and that the data reconstruction is well known. ASHRA-1 will continue gathering hundreds of observational hours each year. Improving on this result is possible with MAGIC considering that approximately 100 h per year are affected by the presence of cirrus clouds, and the telescope can be pointed at the Ocean. However, it is currently a non-standard operation and it will require time to integrate more than 300 h. In the future, CTA could be a better suited instrument. CTA has a wider F.O.V., especially at high energies where the SSTs operate, thus allowing for an increase in the acceptance which can be roughly estimated at a factor of 4. This will be accompanied with increased sensitivity. The larger number of telescopes may also allow to investigate less stringent selection cuts too. For the Northern Hemisphere, CTA will be located where MAGIC telescopes are. In this sense, CTA telescopes could adopt the same "Ocean window" used by MAGIC. If this was combined with clever scheduling (e.g. automatic pointing to the Ocean

whenever clouds are present, as well as an automatic scheduling of flaring objects that pass behind the Ocean window at a certain time of the night), this could improve the performance by at least one order of magnitude or more with respect to MAGIC, in case bright transients events to happen. In the Southern Hemisphere's CTA site, the orography does not allow such kind of observations.

Recently, an ad-hoc IACT array was proposed to overcome the limits to this technique present for MAGIC and CTA: the rather small F.O.V. and a non-dedicated observation program. The name of this project is Trinity (Otte, 2019). Trinity is composed by 18 units organized in three arrays of six units each. A single telescope covers a 5×60 deg F.O.V., so that a single array covers the whole circumference. Each array is placed on mountain tops to cover the whole horizon. Due to this much wider F.O.V. and dedicated observation mode, up to 1,200 hours/year would be available to this technique. With such performance, sensitivities of the order of 10^{-10} GeV cm⁻² s⁻¹ sr⁻¹ (see Fig. 8.17, right panel) could be reached, with tens to hundreds of diffuse neutrinos detectable in 10 years of operation. If approved, such instrument would provide very important results in a gap region between IceCube and radio-neutrino instruments such as GRAND or POEMMA.

Verification

- Q1. Why IACTs are sensitive to Earth-skimming ν_τ s and not to other neutrino families?
- Q2. Why the expected background in IACT observation of Earth-skimming tau neutrinos is expected to be small?
- Q3. Why the sensitivity of IACT observation of Earth-skimming tau neutrinos is concentrated in the region of PeV to EeV?
- Q4. What are the main limiting factors for the observation of Earth-skimming tau neutrinos for MAGIC and CTA?

8.5 Magnetic Monopoles

In the classical Maxwellian formulation of electromagnetism, if a magnetic charge g and a magnetic current ρ_m are introduced, the Maxwell equations would become symmetric if one swaps electric and magnetic fields, and the electric and magnetic constants:

$$\vec{\nabla} \cdot \epsilon \vec{E} = \rho_e \quad \vec{\nabla} \times \vec{E} = -\vec{j}_m - \frac{\partial \vec{B}}{\partial t} \quad (8.28)$$

$$\vec{\nabla} \cdot \vec{B} = \rho_m \quad \vec{\nabla} \times \vec{B}/\mu = \vec{j}_e + \frac{\partial \epsilon \vec{E}}{\partial t} \quad (8.29)$$

This symmetry, albeit tantalizing, is valid only in the trivial case in which neither an electric charge nor an electric current are present. In any other case, it is incompatible with the concept of vector potential \vec{A} , either because the divergence theorem states that the monopole field would be null, or because any magnetic field line is closed.

An elegant solution to this conundrum was found almost a century ago when Dirac (1931) introduced the concept of the (now-called) *Dirac string*, a hypothetical dimensionless entity that can be visualized as a solenoid, that shifts the magnetic field phase by multiples of 2π . This kind of a

phase-shift is similar to the observed Aharonov–Bohm solenoid effect (Aharonov and Bohm, 1959), a quantum-mechanical effect in which the electromagnetic field of a charged particle undergoes a phase-shift even in regions of null electric and magnetic fields such as within a long solenoid. The Dirac string theory embodies the *classical* magnetic monopole (MM) and it is still suggestive because it naturally predicts the quantization of the electric charge (so-called *Dirac quantization rule*). This rule affirms that the product of magnetic g and electric e charge is quantized as an integer multiple of 2π , as a consequence of the 2π phase shift induced by the Dirac string:

$$e g = 2\pi\hbar n \tag{8.30}$$

with $g = g_D$ defined as the Dirac elementary magnetic charge, or the unit *Dirac charge*. It naturally motivates the hitherto unexplained quantization of the electric charge. By assuming a Dirac string size such as that of the electron, it is possible to estimate that the Dirac string would have a mass of 2.4 GeV. The signatures of the Dirac string would have been seen at accelerators and the missing detection provides strong motivation for rejecting this elegant solution (Patrizii and Spurio, 2015). Dirac himself said of MM “*One would be surprised if Nature had made no use of it.*”

A change of paradigm happened few decades later, when ‘t Hooft (1974) and Polyakov (1974) realised that MMs were not only a feature arising from the asymmetry in the Maxwell equations, but also naturally predicted in Grand Unification Theories (GUTs). Unlike the Dirac MM, GUTs MMs would be extremely heavy, because directly related to the mass of the mediator of the unified interaction, in the range $10^{16} \div 10^{17}$ GeV (Preskill, 1984), or even above, in GUTs including gravity (Giacomelli and Patrizii, 2001). Considering they arise from a complete particle physics theory, GUTs MMs have the advantage of allowing a more complete theoretical mapping, with predictable properties such as internal structure and interactions with other fields. They are not structure-less as the Dirac MM, but on the contrary a huge conglomerate of particle fields arranged in layers, formed by a core of gauge bosons of the unified interaction, surrounded by shells of electroweak bosons and confined by a fermion-antifermion condensate region (Patrizii and Spurio, 2015).

At distances larger than few fm, such a MM would behave like a pointlike magnetic charge generating a radial magnetic field. These objects are also called a *topological soliton* and they could even show excited states in which they acquire a net electrical charge, going under the more general name of dyon (Schwinger, 1969). These MM would be stable relics of events happened in the early Universe, such as the *freeze-out* of some conditions or a symmetry breaking. Their decay would be thereafter forbidden due to the conservation of the magnetic charge. A further scenario is that of intermediate mass MM, generated at later cosmic times, during other phase transitions (Polyakov, 1974), allowing for masses of the order of $10^7 \div 10^{13}$ GeV (Patrizii and Spurio, 2015). Depending on their mass and number density, MMs could actually constitute all or a fraction of the total DM of the Universe (Khoze and Ro, 2014). For further readings see, e.g., Shmir (2005).

The Universe expansion must have slowed down the initial velocity of MMs down to the non-relativistic speed. However, dynamo effects in magnetic fields of galaxy clusters, active galactic nuclei or even possible magnetars could have re-accelerated a fraction of MMs: such acceleration process could be in fact highly efficient. A MM traversing a magnetic field B with coherence length L gains $K = g B L$ in kinetic energy (Wick et al., 2003). For values of $B = 3 \mu\text{G}$ and $L = 1 \text{ kpc}$, like those typical of galaxy clusters, the gain corresponds to 1.8×10^{11} GeV. This mechanism could even allow the thesis that MMs could be associated to ultra-high-energy (EeV) cosmic rays (Kephart

and Weiler, 1996). The acceleration of MM happens at the expense of local magnetic fields. Out of this, Parker (1970) obtained a conservative limit on the MM density requiring that this 'draw' of magnetic energy was sufficiently slow not to disrupt galactic magnetic fields completely. This is the so-called Parker bound. Galactic objects such as the Sun could accumulate MMs in their core. The enhanced overdensity could ignite MM catalyzed nucleon decay. Because of the presence of GUTs gauge bosons in their core, interactions such as $p + \text{MM} \rightarrow e^+ + \text{MM} + \pi_0$, may have ample cross sections if the interaction is independent from the grand unification gauge boson mass (Callan-Rubakov process; Callan, 1982, Rubakov, 1982), generating huge pion fluxes and providing strong photons or neutrino bursts after the pion decays (Tanabashi and others., 2018). Not long ago, Super Kamiokande provided very strong constraints on MMs (Ueno et al., 2012). The Callan-Rubakov process is efficient only for GUTs MMs of moderate speed $\beta < 0.3$.

In the passage through matter, a MM with $\beta > 0.1$ would behave like an equivalent huge electric charge, with strong exciting and ionizing power. Dyons, being electrically charged, would also directly generate Cherenkov light. The number of photons N per unit length x and wavelength λ for charged particles is computed by Tamm and Frank (1937) in air:

$$\frac{d^2 N}{dx d\lambda}(\text{MM}) \simeq \frac{n^2}{4\alpha^2} \frac{d^2 N}{dx d\lambda}(e, \mu), \quad (8.31)$$

and computed for MM using Eq. 8.30. In Eq. 8.31, n is the air refraction index and α is the electromagnetic fine structure constant. In air, $n^2/(4\alpha^2) \simeq 4,700$ and therefore the number of photons produced by a MM is significantly larger than that by an electron or a muon, and it corresponds to an energy loss of about $8 \text{ GeV g}^{-1} \text{ cm}^{-2}$ compared to $2 \text{ MeV g}^{-1} \text{ cm}^{-2}$ for the muons (Cecchini et al., 2016, Tompkins, 1965). Such a strong interaction with matter opens up interesting possibilities for the detection of MMs, for example by generating local damages on high-Z material slabs when traversed by MMs that are inspected off-line. For masses above 10^3 GeV , the MACRO (Ambrosio et al., 2002) and MoEDAL (Patrizii and Spurio, 2015) instruments are successful examples of highly sensitive nuclear track detectors.

MMs could be also identified by their passage through the Earth's atmosphere. In this occurrence, they will strongly radiate Cherenkov light, either directly, if electrically charged, or through the secondary charged particle generated through ionization, as well as through luminescence (Oberlacke Pollmann, 2017). Even a globally neutral MM, due to its charged outer layer, would excite atmospheric nuclei throughout the full length of the atmosphere. Such an effect does not happen for cosmic rays, that are absorbed in the high atmosphere. The search for such a signature was investigated with the PAO. Aab et al. (2016) reported strong constraints searching for fluorescence light induced by MMs. The IceCube Collaboration (Aartsen et al., 2014a, 2016a, Abbasi et al., 2013), improving on the results obtained with AMANDA (Achterberg et al., 2010), performed extensive searches for non-relativistic and relativistic MMs. GUTs MMs could catalyze proto decays in the surrounding Antarctic ice via the Callan-Rubakov effect. This would generate relativistic charged particles emitting Cherenkov light with a characteristic hit pattern in the detector. No such pattern was observed, allowing to limit the flux of non-relativistic GUT MMs to three orders of magnitude below the Parker bound. A collection of the limits discussed above on the MM flux is shown in Fig.8.19.

Magnetic Monopoles searches with IACTs. The search for MM signatures was so far only investigated with a simplified approach by Spengler (2009) and Spengler and Schwanke (2011).

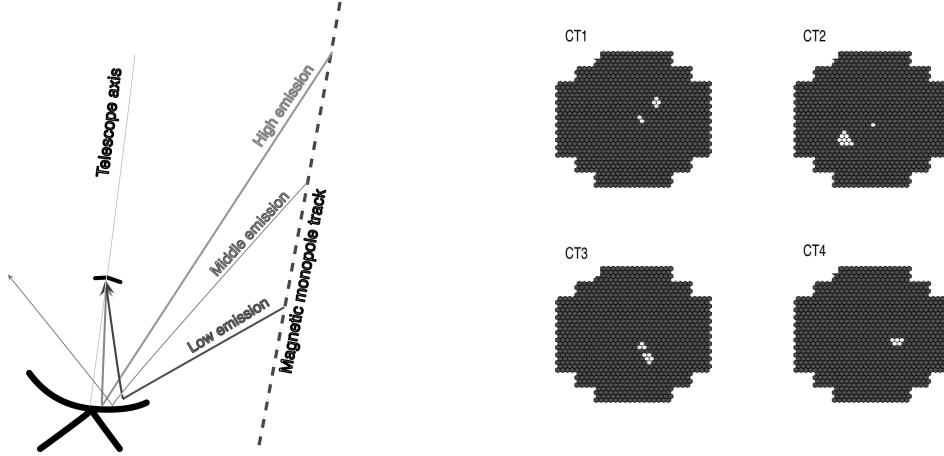


Figure 8.18: Left: Emission scheme from an ultrarelativistic MM emitting Cherenkov radiation throughout the full length of the atmosphere. Right: A simulated MM event on H.E.S.S. cameras. Courtesy of (Spengler, 2009).

Spengler (2009) provided preliminary discussion of the sensitivity to MMs by studying dedicated MC simulations, optimization of the selection cuts, and real data selection.

A MM entering the Earth’s atmosphere will start generating Cherenkov light in the high atmosphere, at 80 km altitude or above. This emission will start within a narrow Cherenkov cone angle of 0.1 deg, increasing to angles of 1.2 deg when the MM will hit the ground. Differently than cosmic rays, the Cherenkov emission will last throughout the full length of the MM track. The Cherenkov emission depends on the MM Lorentz factor γ , which is related to the air local refraction index n by the relation:

$$\gamma > \frac{1}{\sqrt{2(n-1)}} \quad (8.32)$$

For the atmosphere close to the ground $n - 1 = 10^{-4}$ and therefore a minimum boost of $\gamma > 70$ is required to have Cherenkov emission throughout the full length of the track. This condition in turn allows for a significant effectiveness in the separation from the background. This is illustrated in Fig. 8.18: the MM would be observed as a double-spot system in the IACT cameras: a first due to the very high altitude emission, and a second due to the low-altitude emission, while the emission from the central part of the track would not be geometrically focused. A second simplification was applied in order to guarantee minimal energy loss of the MM during the track. Spengler (2009) computed a total energy loss of 22.5 TeV throughout the atmosphere. This required therefore that $\gamma > 22.5 \text{ TeV}/m_{\text{MM}}c^2 \sim 10^5$ or, in other words, the analysis is limited to ultra-relativistic MM. We will discuss the effect of these limitations further below.

The images formed by MMs in the IACTs cameras will be mostly composed of small clusters of very illuminated pixels, for the high-altitude signal, or very bright fraction or rings, similarly to the muon case, for low-altitude originating emission. An example of a simulated event is shown in the right panel of Fig. 8.18. Considering the large Cherenkov photon yield, thousands of times larger than that of a muon, all illuminated pixels will show extremely high signals, often saturating the reach of the camera photomultiplier tube (PMT)s. This further characteristic was used by Spengler (2009) as main selection cut: an event was to show a large fraction of saturated pixels in at least two out of four telescopes. Further cuts, also optimised through MC, were applied to

exclude all the remaining background. For example, less than 200 pixels were to trigger in each camera, in order to remove high energy hadronic showers surviving previous cuts. The selection cuts were optimized on a sample of about 10^6 MC events from 0 to 60 deg zenith angle, and applied to 5 years of (selected) H.E.S.S. data, for a total of 2400 h. No MM candidate event was found, and from this, limits of $< 4.5 \times 10^{-14} \text{ cm}^{-2}\text{s}^{-1}\text{sr}^{-1}$ were computed and shown in Fig. 8.19. These values are extremely poorly constraining, less than the conservative Parker bound, and orders of magnitude less constraining than Auger or IceCube limits. This is due to the larger aperture and duty cycle of these instruments. In any case, these limits should be taken as conservative limits in a very simplified scenario, and further exploration is required.

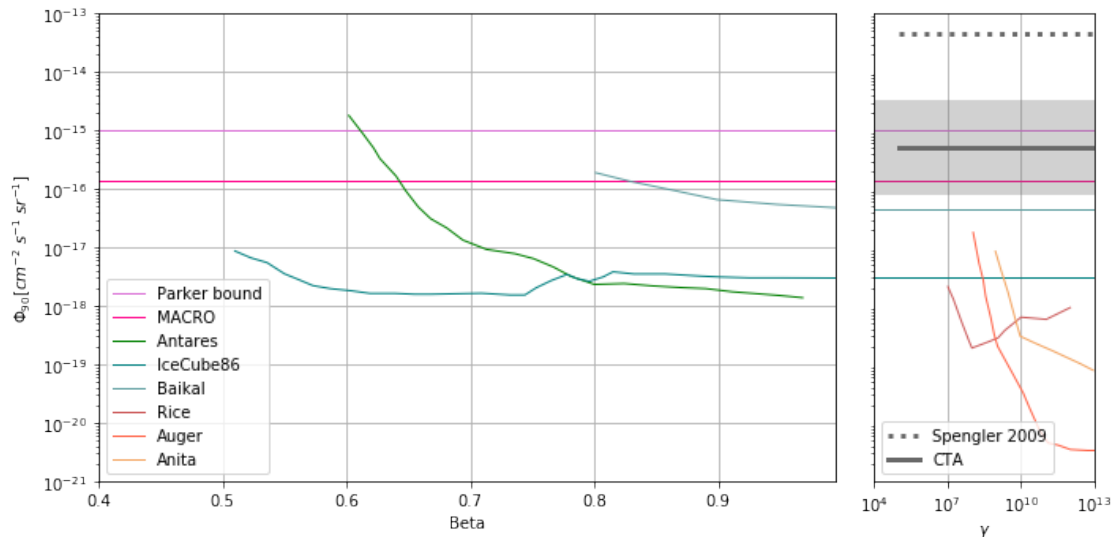


Figure 8.19: Current limits on the flux of MM as a function of the speed of MM at the detector. Upper limits obtained with the H.E.S.S. instrument are shown as a grey dashed line in the inset to the right (Spengler, 2009). Preliminary predictions for CTA are also shown as a thick grey line (Doro, 2017).

Outlook. Improving on this work would require to reassess the MC simulations, by allowing lower speed connected effect such as more significant energy loss during the MM tracking, appearance of secondary hadronic sub-showers which would alter the signatures in the IACTs camera and therefore the simplified picture of background/signal separation. Furthermore, Spengler (2009) did not use the time of arrival of photons to separate candidate events from background, which requires an isochronous paraboloid such as that of the CTA Large Size Telescopes (LSTs). CTA also features a wider F.O.V. that allows to increase the acceptance to MM events, allowing those with farther impact parameters. Finally, one should mention that by pointing the telescope to very high zenith angles (low altitude above the horizon) one could in principle modify the geometry of the event and increase largely the effective area. MMs investigation with CTA would also profit by the 10-fold increase in effective area, and the improvement in energy resolution, angular resolution and off-axis performance. A back of the envelope estimation for CTA performance was discussed in Doro et al. (2013), however, a full quantification of the performance is yet to be done. CTA also features a more flexible software inter-trigger system, which could allow dedicated search campaigns. Still,

MM events could survive trigger criteria and be hidden in current IACT data archive. In MAGIC, the number of background events stored on disk is roughly 1.2×10^9 events/year for two telescopes (Doro, 2017),²⁷ thus providing a rich search sample. Nonetheless, specific on-line or off-line fast selection criteria need to be envisaged to avoid rejecting possible triggers from MMs and thus increasing the chances of detection or the constraining power of any consequent limit. If detected, MMs would provide possibly clear signature in an IACT. Despite the smaller strengths of IACTs compared to other techniques, it is important to notice that this search would be achievable at no cost of dedicated telescope pointings nor specifically allocated observation time, but making use of archival data and tailored analyses.

Verification

- Q1. Why does a MM leave a different imprint in the cameras of IACTs with respect to a primary γ shower?
- Q2. What is the time imprint of a shower initiated by a MM?
- Q3. What is the main reason why IACTs are mostly sensitive to ultra-relativistic MMs?
- Q4. If you were to optimize your search analysis on MMs, on what would you base your classification algorithm?

8.6 Summary and Conclusions

Fundamental physics is probably a slippery wording, because every piece of evidence found in scientific pursues is fundamental in the increase of knowledge. Yet, there is no single word that can properly encompass the searches for massive particle DM, axion-like particles, primordial black holes, tau neutrinos, and magnetic monopoles that have been summarized in this chapter. In most cases, we do not possess a full theoretical mapping. Therefore we often cannot sharpen our instruments to aim for detection, but merely to set yet-another constraints. Nevertheless, we believe that placing many independent and complementary constraints to exotic phenomena - and, in some cases, IACTs provide the strongest ones - is how we build trust in successful theories, and how we rule out alternative explanations or extended models. It is a crucial part of physical observation to continuously challenge the current worldview and to test predictions of novel phenomena. This is the reason for us to have devoted thousands of hours of IACT observations and invested tenfold hours of data analysis and investigation in the search for the *unknown*. All in all, astrophysical gamma rays are wonderful probes: they do not only trace back to the emitting source, but reveal to us nuclear and sub-nuclear interactions that have taken place billions of billions of kilometers away, that is, tens or hundreds of millions of years back in time, and at energy scales hardly accessible in the laboratory. For DM, if the mass of its constituent, elusive particle is above several hundreds GeV, gamma rays may represent one of the few probes - perhaps the only one - to unveil its true nature beyond gravitational pull. We may be hunting far from the right spot, yet constraints set by IACTs on the nature of DM are the strongest in the TeV regime as of today, and they will likely stay so for many years to come. Current limits from the Galactic centre halo by H.E.S.S. have reached the thermal cross section value of $3 \times 10^{-26} \text{ cm}^3\text{s}^{-1}$, a reference value for WIMP

²⁷for CTA this number could be a factor of 50 larger in principle

DM models. However, these limits could suffer from significant uncertainties regarding the precise amount and distribution of DM in the Galactic centre region. This kind of uncertainty is less severe in the case of using Milky Way dwarf satellite galaxies. Therefore, not in vain H.E.S.S., MAGIC and VERITAS have also extensively searched for DM in the best candidates among them, although as well without detecting a signal so far.

While on searches for WIMP DM IACTs are bannermen, their role in the search for axion-like particles, primordial black holes, and magnetic monopoles is more that of pawns compared to other instruments. Nevertheless, the potential of these searches is large, and it is important to recall that these are made on archival data. There is no need of new specific observations but rather of careful and complex analyses. A similar situation occurs for tau neutrinos. Even if the sensitivity of IACTs is not competitive to instruments entirely designed for the detection of astrophysical neutrinos, it has been shown that IACT may play a significant role, specially if specific conditions are met at the site.

The upcoming CTA will provide a performance boost in all of these fields. We might finally unequivocally exclude – or confirm – the hypothesis of massive particle DM, and also search for axion-like particles, primordial black holes, magnetic monopoles, and tau neutrinos with in all cases a several factors higher sensitivity. Yet, in order to adequately profit of this boost, some prerequisites have to be guaranteed: first, that the theoretical and analysis experience gained from the pioneering studies here presented should not be lost, and we hope to have contributed to that. Second, and more importantly: the IACT community should be aware of the relevance of these pursues for fundamental physics, and take as an obligation to devote time and resources to them, a fact that often clashes with the need of longer observations for other astrophysical endeavours. Last, but by no means least: we should guarantee that CTA – or any future IACT experiment – and its corresponding data processing pipelines are put in a position to potentially catch fundamental physics events. As examples, along these pages we have shown how peculiar magnetic monopoles signatures are expected to be, or how serendipitous primordial black hole events may show up, lasting just a few seconds anywhere in the field of view. We should therefore make an extra effort to guarantee that at no place we simplify our systems so to drop information to catch fundamental physics events. For example, by selecting only the brightest pixels in the camera and throwing away all others from the data acquisition and analysis, we may lose all means to identify a rare event occurring in the camera (Doro, 2017). It is important to revive in the community the discussion on the best strategy to search for fundamental physics with CTA; one that will also be in a good balance with the rest of physics cases. Let nature provide the rest in our hope to ever catch signatures of new physics with IACT data.

Acknowledgements. The authors would like to warmly thank for useful discussions to E. Bernardini, A. De Angelis, M. Gaug, D. Gora, D. Krennrich, M. Meyer, N. Otte, L. Patrizii, A. Raccanelli, J. Rico, U. Schwanke, and G. Spengler.

Bibliography

- A. Aab et al. Improved limit to the diffuse flux of ultrahigh energy neutrinos from the Pierre Auger Observatory. *Phys. Rev.*, D91(9):092008, 2015. doi: 10.1103/PhysRevD.91.092008.
- A. Aab et al. Search for ultrarelativistic magnetic monopoles with the Pierre Auger Observatory. *Phys. Rev.*, D94(8):082002, 2016. doi: 10.1103/PhysRevD.94.082002.
- M. G. Aartsen et al. Search for non-relativistic Magnetic Monopoles with IceCube. *Eur. Phys. J.*, C74(7):2938, 2014a. doi: 10.1140/epjc/s10052-014-2938-8.
- M. G. Aartsen et al. Observation of High-Energy Astrophysical Neutrinos in Three Years of IceCube Data. *Phys. Rev. Lett.*, 113:101101, 2014b. doi: 10.1103/PhysRevLett.113.101101.
- M. G. Aartsen et al. Searches for Relativistic Magnetic Monopoles in IceCube. *Eur. Phys. J.*, C76(3):133, 2016a. doi: 10.1140/epjc/s10052-016-3953-8.
- M. G. Aartsen et al. Search for Astrophysical Tau Neutrinos in Three Years of IceCube Data. *Phys. Rev. D*, 93(2):022001, 2016b. doi: 10.1103/PhysRevD.93.022001.
- M. G. Aartsen et al. Multimessenger observations of a flaring blazar coincident with high-energy neutrino IceCube-170922A. *Science*, 361(6398):eaat1378, 2018. doi: 10.1126/science.aat1378.
- R. Abbasi et al. Search for Relativistic Magnetic Monopoles with IceCube. *Phys. Rev.*, D87(2):022001, 2013. doi: 10.1103/PhysRevD.87.022001.
- B. P. Abbott et al. Observation of Gravitational Waves from a Binary Black Hole Merger. *Phys. Rev. Lett.*, 116(6):061102, 2016a. doi: 10.1103/PhysRevLett.116.061102.
- B. P. Abbott et al. Observation of Gravitational Waves from a Binary Black Hole Merger. *Phys. Rev. Lett.*, 116(6):061102, 2016b. doi: 10.1103/PhysRevLett.116.061102.
- B. P. Abbott et al. GW151226: Observation of Gravitational Waves from a 22-Solar-Mass Binary Black Hole Coalescence. *Phys. Rev. Lett.*, 116(24):241103, 2016c. doi: 10.1103/PhysRevLett.116.241103.
- B. P. Abbott et al. Binary Black Hole Mergers in the first Advanced LIGO Observing Run. *Phys. Rev.*, X6(4):041015, 2016d. doi: 10.1103/PhysRevX.6.041015.
- T. M. C. Abbott et al. The Dark Energy Survey Data Release 1. *Astrophys. J. Suppl.*, 239(2):18, 2018. doi: 10.3847/1538-4365/aae9f0.

- H. Abdalla et al. H.E.S.S. Limits on Linelike Dark Matter Signatures in the 100 GeV to 2 TeV Energy Range Close to the Galactic Center. *Phys. Rev. Lett.*, 117(15):151302, 2016. doi: 10.1103/PhysRevLett.117.151302.
- H. Abdalla et al. Searches for gamma-ray lines and 'pure WIMP' spectra from Dark Matter annihilations in dwarf galaxies with H.E.S.S. *JCAP*, 11:037, 2018a. doi: 10.1088/1475-7516/2018/11/037.
- H. Abdalla et al. Search for γ -Ray Line Signals from Dark Matter Annihilations in the Inner Galactic Halo from 10 Years of Observations with H.E.S.S. *Phys. Rev. Letter*, 120(20):201101, 2018b. doi: 10.1103/PhysRevLett.120.201101.
- H. Abdalla et al. Search for dark matter signals towards a selection of recently detected DES dwarf galaxy satellites of the Milky Way with H.E.S.S. *Phys. Rev. D*, 102(6):062001, 2020. doi: 10.1103/PhysRevD.102.062001.
- H. Abdalla et al. Sensitivity of the Cherenkov Telescope Array for probing cosmology and fundamental physics with gamma-ray propagation. *JCAP*, 02:048, 2021. doi: 10.1088/1475-7516/2021/02/048.
- H. Abdallah et al. Search for dark matter annihilations towards the inner Galactic halo from 10 years of observations with H.E.S.S. *Phys. Rev. Letter*, 117(11):111301, 2016. doi: 10.1103/PhysRevLett.117.111301.
- H. Abdallah et al. Search for dark matter annihilation signals from unidentified Fermi-LAT objects with H.E.S.S. 6 2021a.
- H. Abdallah et al. Search for dark matter annihilation in the dwarf irregular galaxy WLM with H.E.S.S. 5 2021b.
- A. Abdo et al. Milagro limits and HAWC sensitivity for the rate-density of evaporating Primordial Black Holes. *Astrop. Phys.*, 64:4–12, apr 2015. doi: 10.1016/j.astropartphys.2014.10.007.
- A. A. Abdo, M. Ackermann, M. Ajello, A. Allafort, E. Antolini, W. B. Atwood, M. Axelsson, L. Baldini, J. Ballet, G. Barbiellini, and et al. Fermi Large Area Telescope First Source Catalog. *ApJS*, 188:405–436, June 2010. doi: 10.1088/0067-0049/188/2/405.
- S. Abdollahi et al. *Fermi* Large Area Telescope Fourth Source Catalog. *Astrophys. J. Suppl.*, 247(1):33, 2020. doi: 10.3847/1538-4365/ab6bcb.
- A. U. Abeysekara, A. Albert, R. Alfaro, C. Alvarez, J. D. Álvarez, R. Arceo, J. C. Arteaga-Velázquez, H. A. Ayala Solares, A. S. Barber, N. Bautista-Elivar, A. Becerril, E. Belmont-Moreno, S. Y. BenZvi, D. Berley, J. Braun, C. Brisbois, K. S. Caballero-Mora, T. Capistrán, A. Carramiñana, S. Casanova, M. Castillo, U. Cotti, J. Cotzomi, S. Coutiño de León, E. de la Fuente, C. De León, T. DeYoung, B. L. Dingus, M. A. DuVernois, J. C. Díaz-Vélez, R. W. Ellsworth, D. W. Fiorino, N. Fraija, J. A. García-González, M. Gerhardt, A. González Muñoz, M. M. González, J. A. Goodman, Z. Hampel-Arias, J. P. Harding, S. Hernandez, A. Hernandez-Almada, J. Hinton, C. M. Hui, P. Hütemeyer, A. Iriarte, A. Jardin-Blicq, V. Joshi, S. Kaufmann, D. Kieda, A. Lara, R. J. Lauer, W. H. Lee, D. Lennarz, H. León Vargas, J. T. Linemann, A. L. Longinotti, G. L. Raya, R. Luna-García, R. López-Coto, K. Malone, S. S.

- Marinelli, O. Martinez, I. Martinez-Castellanos, J. Martínez-Castro, H. Martínez-Huerta, J. A. Matthews, P. Mirand a-Romagnoli, E. Moreno, M. Mostafá, L. Nellen, M. Newbold, M. U. Nisa, R. Noriega-Papaqui, R. Pelayo, J. Pretz, E. G. Pérez-Pérez, Z. Ren, C. D. Rho, C. Rivière, D. Rosa-González, M. Rosenberg, E. Ruiz-Velasco, H. Salazar, F. Salesa Greus, A. Sand oval, M. Schneider, H. Schoorlemmer, G. Sinnis, A. J. Smith, R. W. Springer, P. Surajbali, I. Taboada, O. Tibolla, K. Tollefson, I. Torres, T. N. Ukwatta, L. Villaseñor, T. Weisgarber, S. Westerhoff, I. G. Wisher, J. Wood, T. Yapici, G. B. Yodh, P. W. Younk, A. Zepeda, and H. Zhou. Observation of the Crab Nebula with the HAWC Gamma-Ray Observatory. *ApJ*, 843:39, Jul 2017. doi: 10.3847/1538-4357/aa7555.
- A. U. Abeysekara, A. Albert, R. Alfaro, C. Alvarez, R. Arceo, J. C. Arteaga-Velázquez, D. Avila Rojas, H. A. Ayala Solares, E. Belmont-Moreno, S. Y. BenZvi, C. Brisbois, K. S. Caballero-Mora, A. Carramiñana, S. Casanova, J. Cotzomi, S. Coutiño de León, C. De León, E. De la Fuente, S. Dichiara, B. L. Dingus, M. A. DuVernois, J. C. Díaz-Vélez, K. Engel, C. Espinoza, H. Fleischhack, N. Fraija, A. Galván-Gámez, J. A. García-González, M. M. González, J. A. Goodman, J. P. Harding, B. Hona, F. Hueyotl-Zahuantitla, P. Hüntemeyer, A. Iriarte, A. Lara, W. H. Lee, H. León Vargas, J. T. Linnemann, A. L. Longinotti, G. Luis-Raya, J. Lundeen, K. Malone, S. S. Marinelli, O. Martinez, I. Martinez-Castellanos, J. Martínez-Castro, J. A. Matthews, P. Miranda-Romagnoli, E. Moreno, M. Mostafá, A. Nayerhoda, L. Nellen, M. Newbold, M. U. Nisa, R. Noriega-Papaqui, E. G. Pérez-Pérez, Z. Ren, C. D. Rho, C. Rivière, D. Rosa-González, M. Rosenberg, H. Salazar, F. Salesa Greus, A. Sandoval, M. Schneider, G. Sinnis, A. J. Smith, R. W. Springer, K. Tollefson, I. Torres, G. Vianello, T. Weisgarber, J. Wood, T. Yapici, A. Zepeda, H. Zhou, and J. D. Álvarez. Searching for Dark Matter Sub-structure with HAWC. *arXiv e-prints*, Nov. 2018.
- A. Abramowski, F. Acero, F. Aharonian, F. Ait Benkhali, A. G. Akhperjanian, E. Angüner, G. Anton, S. Balenderan, A. Balzer, A. Barnacka, and et al. Constraints on axionlike particles with H.E.S.S. from the irregularity of the PKS 2155-304 energy spectrum. *Physical Review D*, 88(10): 102003, Nov. 2013a. doi: 10.1103/PhysRevD.88.102003.
- A. Abramowski et al. H.E.S.S. constraints on Dark Matter annihilations towards the Sculptor and Carina Dwarf Galaxies. *Astrop. Phys.* , 34:608–616, 2011. doi: 10.1016/j.astropartphys.2010.12.006.
- A. Abramowski et al. Search for a Dark Matter Annihilation Signal from the Galactic Center Halo with H.E.S.S. *Phys. Rev. Letter*, 106(16):161301–+, Apr. 2011. doi: 10.1103/PhysRevLett.106.161301.
- A. Abramowski et al. HESS observations of the globular clusters NGC 6388 and M 15 and search for a Dark Matter signal. *ApJ*, 735:12, 2011. doi: 10.1088/0004-637X/735/1/12.
- A. Abramowski et al. Search for Dark Matter Annihilation Signals from the Fornax Galaxy Cluster with H.E.S.S. *ApJ*, 750:123, 2012. doi: 10.1088/0004-637X/750/2/123.
- A. Abramowski et al. Measurement of the extragalactic background light imprint on the spectra of the brightest blazars observed with H.E.S.S. *A&A*, 550:A4, Feb. 2013b. doi: 10.1051/0004-6361/201220355.

- A. Abramowski et al. Search for photon line-like signatures from Dark Matter annihilations with HESS. *Phys. Rev. Letter*, 110:041301, 2013c. doi: 10.1103/PhysRevLett.110.041301.
- A. Abramowski et al. Search for dark matter annihilation signatures in H.E.S.S. observations of Dwarf Spheroidal Galaxies. *Phys. Rev. D*, D90:112012, 2014. doi: 10.1103/PhysRevD.90.112012.
- A. Abramowski et al. Constraints on an Annihilation Signal from a Core of Constant Dark Matter Density around the Milky Way Center with H.E.S.S. *Phys. Rev. Lett.*, 114(8):081301, 2015. doi: 10.1103/PhysRevLett.114.081301.
- V. A. Acciari, S. Ansoldi, L. A. Antonelli, A. Arbet Engels, C. Arcaro, D. Baack, A. Babić, B. Banerjee, P. Bangale, U. Barres de Almeida, J. A. Barrio, J. Becerra González, W. Bednarek, E. Bernardini, A. Berti, J. Besenrieder, W. Bhattacharyya, C. Bigongiari, A. Biland, O. Blanch, G. Bonnoli, R. Carosi, G. Ceribella, S. Cikota, S. M. Colak, P. Colin, E. Colombo, J. L. Contreras, J. Cortina, S. Covino, V. D’Elia, P. da Vela, F. Dazzi, A. de Angelis, B. de Lotto, M. Delfino, J. Delgado, F. di Pierro, E. Do Souto Espiñera, A. Domínguez, D. Dominis Prester, D. Dorner, M. Doro, S. Einecke, D. Elsaesser, V. Fallah Ramazani, A. Fattorini, A. Fernández-Barral, G. Ferrara, D. Fidalgo, L. Foffano, M. V. Fonseca, L. Font, C. Fruck, D. Galindo, S. Gallozzi, R. J. García López, M. Garczarczyk, M. Gaug, P. Giammaria, N. Godinović, D. Guberman, D. Hadasch, A. Hahn, T. Hassan, J. Herrera, J. Hoang, D. Hrupec, S. Inoue, K. Ishio, Y. Iwamura, H. Kubo, J. Kushida, D. Kuveždić, A. Lamastra, D. Lelas, F. Leone, E. Lindfors, S. Lombardi, F. Longo, M. López, A. López-Oramas, C. Maggio, P. Majumdar, M. Makariev, G. Maneva, M. Manganaro, K. Mannheim, L. Maraschi, M. Mariotti, M. Martínez, S. Masuda, D. Mazin, M. Mineev, J. M. Miranda, R. Mirzoyan, E. Molina, A. Moralejo, V. Moreno, E. Moretti, P. Munar-Adrover, V. Neustroev, A. Niedzwiecki, M. Nieves Rosillo, C. Nigro, K. Nilsson, D. Ninci, K. Nishijima, K. Noda, L. Nogués, S. Paiano, J. Palacio, D. Paneque, R. Paoletti, J. M. Paredes, G. Pedalletti, P. Peñil, M. Peresano, M. Persic, P. G. Prada Moroni, E. Prandini, I. Puljak, J. R. Garcia, W. Rhode, M. Ribó, J. Rico, C. Righi, A. Rugliancich, L. Saha, T. Saito, K. Satalecka, T. Schweizer, J. Sitarek, I. Šnidarić, D. Sobczynska, A. Somero, A. Stamerra, M. Strzys, T. Surić, F. Tavecchio, P. Temnikov, T. Terzić, M. Teshima, N. Torres-Albà, S. Tsujimoto, G. Vanzo, M. Vazquez Acosta, I. Vovk, J. E. Ward, M. Will, D. Zarić, and MAGIC Collaboration. Constraining dark matter lifetime with a deep gamma-ray survey of the Perseus galaxy cluster with MAGIC. *Physics of the Dark Universe*, 22:38–47, Dec. 2018. doi: 10.1016/j.dark.2018.08.002.
- V. A. Acciari et al. VERITAS Search for VHE Gamma-ray Emission from Dwarf Spheroidal Galaxies. *ApJ*, 720:1174–1180, 2010. doi: 10.1088/0004-637X/720/2/1174.
- V. A. Acciari et al. Constraining Dark Matter lifetime with a deep gamma-ray survey of the Perseus Galaxy Cluster with MAGIC. *Submitted to: Phys. Dark Univ.*, 2018.
- V. A. Acciari et al. Deep observations of the globular cluster M15 with the MAGIC telescopes. *Mon. Not. Roy. Astron. Soc.*, 484(2):2876–2885, 2019. doi: 10.1093/mnras/stz179.
- V. A. Acciari et al. A search for dark matter in Triangulum II with the MAGIC telescopes. *Phys. Dark Univ.*, 28:100529, 2020. doi: 10.1016/j.dark.2020.100529.
- F. Acero et al. Fermi Large Area Telescope Third Source Catalog. *Astrophys. J. Suppl.*, 218(2):23, 2015. doi: 10.1088/0067-0049/218/2/23.

- B. S. Acharya et al. Introducing the CTA concept. *Astropart. Phys.*, 43:3–18, 2013. doi: 10.1016/j.astropartphys.2013.01.007.
- B. S. Acharya et al. Science with the Cherenkov Telescope Array. 2017.
- A. Acharyya et al. Sensitivity of the Cherenkov Telescope Array to a dark matter signal from the Galactic centre. *JCAP*, 01:057, 2021. doi: 10.1088/1475-7516/2021/01/057.
- A. Achterberg et al. Search for relativistic magnetic monopoles with the amanda-ii neutrino telescope. *The European Physical Journal C - Particles and Fields*, 69:361–378, 2010. ISSN 1434-6044.
- M. Ackermann, A. Albert, L. Baldini, J. Ballet, G. Barbiellini, D. Bastieri, K. Bechtol, R. Bellazzini, R. D. Blandford, E. D. Bloom, E. Bonamente, A. W. Borgland, E. Bottacini, T. J. Brandt, J. Bregeon, M. Brigida, P. Bruel, R. Buehler, T. H. Burnett, G. A. Caliandro, R. A. Cameron, P. A. Caraveo, J. M. Casandjian, C. Cecchi, E. Charles, J. Chiang, S. Ciprini, R. Claus, J. Cohen-Tanugi, J. Conrad, S. Cutini, F. de Palma, C. D. Dermer, S. W. Digel, E. d. C. e. Silva, P. S. Drell, A. Drlica-Wagner, R. Essig, L. Falletti, C. Favuzzi, S. J. Fegan, W. B. Focke, Y. Fukazawa, S. Funk, P. Fusco, F. Gargano, S. Germani, N. Giglietto, F. Giordano, M. Giroletti, T. Glanzman, G. Godfrey, I. A. Grenier, S. Guiriec, M. Gustafsson, D. Hadasch, M. Hayashida, X. Hou, R. E. Hughes, R. P. Johnson, A. S. Johnson, T. Kamae, H. Katagiri, J. Kataoka, J. Knödseder, M. Kuss, J. Lande, L. Latronico, S.-H. Lee, A. M. Lionetto, M. Llena Garde, F. Longo, F. Loparco, M. N. Lovellette, P. Lubrano, M. N. Mazziotta, J. E. McEnery, P. F. Michelson, W. Mitthumsiri, T. Mizuno, A. A. Moiseev, C. Monte, M. E. Monzani, A. Morselli, I. V. Moskalenko, S. Murgia, M. Naumann-Godo, J. P. Norris, E. Nuss, T. Ohsugi, A. Okumura, E. Orlando, J. F. Ormes, M. Ozaki, D. Paneque, V. Pelassa, M. Pierbattista, F. Piron, G. Pivato, T. A. Porter, S. Rainò, R. Rando, M. Razzano, A. Reimer, O. Reimer, S. Ritz, H. F.-W. Sadrozinski, N. Sehgal, C. Sgrò, E. J. Siskind, P. Spinelli, L. Strigari, D. J. Suson, H. Tajima, H. Takahashi, T. Tanaka, J. G. Thayer, J. B. Thayer, L. Tibaldo, M. Tinivella, D. F. Torres, E. Troja, Y. Uchiyama, T. L. Usher, J. Vandenbroucke, V. Vasileiou, G. Vianello, V. Vitale, A. P. Waite, P. Wang, B. L. Winer, K. S. Wood, Z. Yang, S. Zalewski, and S. Zimmer. Search for Dark Matter Satellites Using Fermi-LAT. *ApJ*, 747:121, Mar. 2012a. doi: 10.1088/0004-637X/747/2/121.
- M. Ackermann et al. Measurement of Separate Cosmic-Ray Electron and Positron Spectra with the Fermi Large Area Telescope. *Phys. Rev. Letter*, 108:011103, Jan. 2012b. doi: 10.1103/PhysRevLett.108.011103.
- M. Ackermann et al. The Imprint of the Extragalactic Background Light in the Gamma-Ray Spectra of Blazars. *Science*, 338:1190, Nov. 2012c. doi: 10.1126/science.1227160.
- M. Ackermann et al. CONSTRAINTS ON THE GALACTIC HALO DARK MATTER FROM FERMI-LAT DIFFUSE MEASUREMENTS. *The Astrophysical Journal*, 761(2):91, nov 2012d. doi: 10.1088/0004-637x/761/2/91. URL <https://doi.org/10.1088/0004-637x/761/2/91>.
- M. Ackermann et al. 2FHL: The Second Catalog of Hard Fermi-LAT Sources. *Astrophys. J. Suppl.*, 222(1):5, 2016. doi: 10.3847/0067-0049/222/1/5.
- M. Ackermann et al. The Fermi Galactic Center GeV Excess and Implications for Dark Matter. *ApJ*, 840(1):43, 2017. doi: 10.3847/1538-4357/aa6cab.

M. Ackermann et al. Fundamental Physics with High-Energy Cosmic Neutrinos. *Bull. Am. Astron. Soc.*, 51:215, 2019.

S. Adrián-Martínez, M. Ageron, F. Aharonian, S. Aiello, A. Albert, F. Ameli, E. Anassontzis, M. Andre, G. Androulakis, M. Anghinolfi, G. Anton, M. Ardid, T. Avgitas, G. Barbarino, E. Barbarito, B. Baret, J. Barrios-Martí, B. Belhorma, A. Belias, E. Berbee, A. van den Berg, V. Bertin, S. Beurthey, V. van Beveren, N. Beverini, S. Biagi, A. Biagioni, M. Billault, M. Bondì, R. Bor-muth, B. Bouhadeh, G. Bourlis, S. Bourret, C. Boutonnet, M. Bouwhuis, C. Bozza, R. Bruijn, J. Brunner, E. Buis, J. Busto, G. Cacopardo, L. Caillat, M. Calamai, D. Calvo, A. Capone, L. Caramete, S. Cecchini, S. Celli, C. Champion, R. C. E. Moursli, S. Cherubini, T. Chiarusi, M. Circella, L. Classen, R. Cocimano, J. A. B. Coelho, A. Coleiro, S. Colonges, R. Coniglione, M. Cordelli, A. Cosquer, P. Coyle, A. Creusot, G. Cuttone, A. D’Amico, G. D. Bonis, G. D. Rosa, C. D. Sio, F. D. Capua, I. D. Palma, A. F. D. García, C. Distefano, C. Donzaud, D. Dornic, Q. Dorosti-Hasankiadeh, E. Drakopoulou, D. Drouhin, L. Drury, M. Durocher, T. Eberl, S. Eichie, D. van Eijk, I. E. Bojaddaini, N. E. Khayati, D. Elsaesser, A. Enzenhöfer, F. Fassi, P. Favali, P. Fermani, G. Ferrara, C. Filippidis, G. Frascadore, L. A. Fusco, T. Gal, S. Galatà, F. Garufi, P. Gay, M. Gebyehu, V. Giordano, N. Gizani, R. Gracia, K. Graf, T. Grégoire, G. Grella, R. Habel, S. Hallmann, H. van Haren, S. Harissopulos, T. Heid, A. Heijboer, E. Heine, S. Henry, J. J. Hernández-Rey, M. Hevinga, J. Hofestädt, C. M. F. Hugon, G. Illuminati, C. W. James, P. Jansweijer, M. Jongen, M. de Jong, M. Kadler, O. Kalekin, A. Kappes, U. F. Katz, P. Keller, G. Kieft, D. Kießling, E. N. Koffeman, P. Kooijman, A. Kouchner, V. Kulikovskiy, R. Lahmann, P. Lamare, A. Leisos, E. Leonora, M. L. Clark, A. Liolios, C. D. L. Alvarez, D. L. Presti, H. Löhner, A. Lonardo, M. Lotze, S. Loucatos, E. Maccioni, K. Mannheim, A. Margiotta, A. Marinelli, O. Mariş, C. Markou, J. A. Martínez-Mora, A. Martini, R. Mele, K. W. Melis, T. Michael, P. Migliozi, E. Migneco, P. Mijakowski, A. Miraglia, C. M. Mollo, M. Mongelli, M. Morganti, A. Moussa, P. Musico, M. Musumeci, S. Navas, C. A. Nicolau, I. Olcina, C. Olivetto, A. Orlando, A. Papaikonomou, R. Papaleo, G. E. Pāvālaš, H. Peek, C. Pellegrino, C. Perrina, M. Pfitzner, P. Piattelli, K. Pikounis, G. E. Poma, V. Popa, T. Pradier, F. Prato-longo, G. Pühlhofer, S. Pulvirenti, L. Quinn, C. Racca, F. Raffaelli, N. Randazzo, P. Rapidis, P. Razis, D. Real, L. Resvanis, J. Reubelt, G. Riccobene, C. Rossi, A. Rovelli, M. Saldaña, I. Salvadori, D. F. E. Samtleben, A. S. García, A. S. Losa, M. Sanguineti, A. Santangelo, D. Santonocito, P. Sapienza, F. Schimmel, J. Schmelling, V. Sciacca, M. Sedita, T. Seitz, I. Sgura, F. Simeone, I. Siotis, V. Sipala, B. Spisso, M. Spurio, G. Stavropoulos, J. Steijger, S. M. Stellacci, D. Stransky, M. Taiuti, Y. Tayalati, D. Tézier, S. Theraube, L. Thompson, P. Timmer, C. Tönnis, L. Trasatti, A. Trovato, A. Tsirigotis, S. Tzamarias, E. Tzamariudaki, B. Vallage, V. V. Elewycck, J. Vermeulen, P. Vicini, S. Viola, D. Vivolo, M. Volkert, G. Voulgaris, L. Wiggers, J. Wilms, E. de Wolf, K. Zachariadou, J. D. Zornoza, and J. Zúñiga. Letter of intent for KM3net 2.0. *Journal of Physics G: Nuclear and Particle Physics*, 43(8):084001, jun 2016. doi: 10.1088/0954-3899/43/8/084001. URL <https://doi.org/10.1088/0954-3899/43/8/084001>.

S. Adrian-Martinez et al. First Search for Point Sources of High Energy Cosmic Neutrinos with the ANTARES Neutrino Telescope. *ApJL*, 743, 2011.

O. Adriani et al. An anomalous positron abundance in cosmic rays with energies 1.5-100 GeV. *Nature*, 458:607–609, 2009. doi: 10.1038/nature07942.

O. Adriani et al. Extended Measurement of the Cosmic-Ray Electron and Positron Spectrum from

- 11 GeV to 4.8 TeV with the Calorimetric Electron Telescope on the International Space Station. *Phys. Rev. Lett.*, 120(26):261102, 2018. doi: 10.1103/PhysRevLett.120.261102.
- N. Aghanim et al. Planck 2018 results. VI. Cosmological parameters. *Astron. Astrophys.*, 641:A6, 2020. doi: 10.1051/0004-6361/201833910.
- M. Aguilar et al. First result from the alpha magnetic spectrometer on the international space station: Precision measurement of the positron fraction in primary cosmic rays of 0.5–350 gev. *Phys. Rev. Lett.*, 110:141102, Apr 2013. doi: 10.1103/PhysRevLett.110.141102. URL <https://link.aps.org/doi/10.1103/PhysRevLett.110.141102>.
- F. Aharonian, A. G. Akhperjanian, A. R. Bazer-Bachi, M. Beilicke, W. Benbow, D. Berge, K. Bernlöhr, C. Boisson, O. Bolz, V. Borrel, I. Braun, F. Breitling, A. M. Brown, P. M. Chadwick, L.-M. Chounet, R. Cornils, L. Costamante, B. Degrange, H. J. Dickinson, A. Djannati-Ataï, L. O. Drury, G. Dubus, D. Emmanoulopoulos, P. Espigat, F. Feinstein, G. Fontaine, Y. Fuchs, S. Funk, Y. A. Gallant, B. Giebels, S. Gillessen, J. F. Glicenstein, P. Goret, C. Hadjichristidis, D. Hauser, M. Hauser, G. Heinzlmann, G. Henri, G. Hermann, J. A. Hinton, W. Hofmann, M. Holleran, D. Horns, A. Jacholkowska, O. C. de Jager, B. Khélifi, S. Klages, N. Komin, A. Konopelko, I. J. Latham, R. Le Gallou, A. Lemièrre, M. Lemoine-Goumard, N. Leroy, T. Lohse, J. M. Martin, O. Martineau-Huynh, A. Marcowith, C. Masterson, T. J. L. McComb, M. de Naurois, S. J. Nolan, A. Noutsos, K. J. Orford, J. L. Osborne, M. Ouchrif, M. Panter, G. Pelletier, S. Pita, G. Pühlhofer, M. Punch, B. C. Raubenheimer, M. Raue, J. Raux, S. M. Rayner, A. Reimer, O. Reimer, J. Ripken, L. Rob, L. Rolland, G. Rowell, V. Sahakian, L. Saugé, S. Schlenker, R. Schlickeiser, C. Schuster, U. Schwanke, M. Siewert, H. Sol, D. Spangler, R. Steenkamp, C. Stegmann, J.-P. Tavernet, R. Terrier, C. G. Théoret, M. Tluczykont, C. van Eldik, G. Vasileiadis, C. Venter, P. Vincent, H. J. Völk, and S. J. Wagner. A low level of extragalactic background light as revealed by gamma-rays from blazars. *Nature*, 440:1018–1021, Apr. 2006. doi: 10.1038/nature04680.
- F. Aharonian, W. Essey, A. Kusenko, and A. Prosekin. TeV gamma rays from blazars beyond $z=1$? *Phys. Rev. D*, 87(6):063002, Mar. 2013. doi: 10.1103/PhysRevD.87.063002.
- F. Aharonian et al. HESS observations of the Galactic Center region and their possible dark matter interpretation. *Phys. Rev. Letter*, 97:221102, 2006. doi: 10.1103/PhysRevLett.97.221102.
- F. Aharonian et al. Observations of the Sagittarius Dwarf galaxy by the H.E.S.S. experiment and search for a Dark Matter signal. *Astrop. Phys.*, 29:55–62, 2008. doi: 10.1016/j.astropartphys.2007.11.007.
- F. Aharonian et al. Search for Gamma-rays from Dark Matter annihilations around Intermediate Mass Black Holes with the H.E.S.S. experiment. *Phys. Rev. D*, D78:072008, 2008a. doi: 10.1103/PhysRevD.78.072008.
- F. Aharonian et al. The energy spectrum of cosmic-ray electrons at TeV energies. *Phys. Rev. Letter*, 101:261104, 2008b. doi: 10.1103/PhysRevLett.101.261104.
- F. Aharonian et al. A Search for a Dark Matter Annihilation Signal Toward the Canis Major Overdensity with H.E.S.S. *ApJ*, 691:175–181, Jan. 2009a. doi: 10.1088/0004-637X/691/1/175.

- F. Aharonian et al. Probing the ATIC peak in the cosmic-ray electron spectrum with H.E.S.S. *á*, 508:561, 2009b.
- F. A. Aharonian, D. Khangulyan, and L. Costamante. Formation of hard very high energy gamma-ray spectra of blazars due to internal photon-photon absorption. *MNRAS*, 387:1206–1214, July 2008. doi: 10.1111/j.1365-2966.2008.13315.x.
- Y. Aharonov and D. Bohm. Significance of Electromagnetic Potentials in the Quantum Theory. *Physical Review*, 115:485–491, Aug. 1959. doi: 10.1103/PhysRev.115.485.
- M. L. Ahnen, S. Ansoldi, L. A. Antonelli, P. Antoranz, A. Babic, B. Banerjee, P. Bangale, U. Barres de Almeida, J. A. Barrio, J. Becerra González, W. Bednarek, E. Bernardini, B. Biasuzzi, A. Biland, O. Blanch, S. Bonnefoy, G. Bonnoli, F. Borracci, T. Bretz, S. Buson, E. Carmona, A. Carosi, A. Chatterjee, R. Clavero, P. Colin, E. Colombo, J. L. Contreras, J. Cortina, S. Covino, P. Da Vela, F. Dazzi, A. De Angelis, B. De Lotto, E. de Oña Wilhelmi, C. Delgado Mendez, F. Di Pierro, A. Domínguez, D. Dominis Prester, D. Dorner, M. Doro, S. Einecke, D. Eisenacher Glawion, D. Elsaesser, A. Fernández-Barral, D. Fidalgo, M. V. Fonseca, L. Font, K. Frantzen, C. Fruck, D. Galindo, R. J. García López, M. Garczarczyk, D. Garrido Terrats, M. Gaug, P. Giannaria, N. Godinović, A. González Muñoz, D. Gora, D. Guberman, D. Hadasch, A. Hahn, Y. Hanabata, M. Hayashida, J. Herrera, J. Hose, D. Hrupec, G. Hughes, W. Idec, K. Kodani, Y. Konno, H. Kubo, J. Kushida, A. La Barbera, D. Lelas, E. Lindfors, S. Lombardi, F. Longo, M. López, R. López-Coto, E. Lorenz, P. Majumdar, M. Makariev, K. Mallot, G. Maneva, M. Manganaro, K. Mannheim, L. Maraschi, B. Marcote, M. Mariotti, M. Martínez, D. Mazin, U. Menzel, J. M. Miranda, R. Mirzoyan, A. Moralejo, E. Moretti, D. Nakajima, V. Neustroev, A. Niedzwiecki, M. Nieves Rosillo, K. Nilsson, K. Nishijima, K. Noda, R. Orito, A. Overkemping, S. Paiano, J. Palacio, M. Palatiello, D. Paneque, R. Paoletti, J. M. Paredes, X. Paredes-Fortuny, G. Pedalletti, M. Persic, J. Poutanen, P. G. Prada Moroni, E. Prandini, I. Puljak, W. Rhode, M. Ribó, J. Rico, J. Rodriguez Garcia, T. Saito, K. Satalecka, C. Schultz, T. Schweizer, A. Siljanpää, J. Sitarek, I. Snidaric, D. Sobczynska, A. Stamerra, T. Steinbring, M. Strzys, L. Takalo, H. Takami, F. Tavecchio, P. Temnikov, T. Terzić, D. Tescaro, M. Teshima, J. Thaele, D. F. Torres, T. Toyama, A. Treves, M. Vazquez Acosta, V. Verguilov, I. Vovk, J. E. Ward, M. Will, M. H. Wu, R. Zanin, C. Pfrommer, A. Pinzke, and F. Zandanel. Deep observation of the NGC 1275 region with MAGIC: search of diffuse *gamma*-ray emission from cosmic rays in the Perseus cluster. *Astronomy & Astrophysics*, 589:A33, May 2016a. doi: 10.1051/0004-6361/201527846.
- M. L. Ahnen et al. Limits to dark matter annihilation cross-section from a combined analysis of MAGIC and Fermi-LAT observations of dwarf satellite galaxies. *J. Cosmology Astropart. Phys.*, 1602(02):039, 2016b. doi: 10.1088/1475-7516/2016/02/039.
- M. L. Ahnen et al. Indirect dark matter searches in the dwarf satellite galaxy Ursa Major II with the MAGIC Telescopes. *JCAP*, 1803(03):009, 2018a. doi: 10.1088/1475-7516/2018/03/009.
- M. L. Ahnen et al. Limits on the flux of tau neutrinos from 1 PeV to 3 EeV with the MAGIC telescopes. *Astropart. Phys.*, 102:77–88, 2018b. doi: 10.1016/j.astropartphys.2018.05.002.
- M. Ajello et al. 3FHL: The Third Catalog of Hard Fermi-LAT Sources. *Astrophys. J. Suppl.*, 232(2):18, 2017. doi: 10.3847/1538-4365/aa8221.

- M. o. Ajello. Search for Spectral Irregularities due to Photon-Axion-like-Particle Oscillations with the Fermi Large Area Telescope. *Phys. Rev. Letter*, 116(16):161101, Apr. 2016. doi: 10.1103/PhysRevLett.116.161101.
- A. Albert et al. Dark Matter Limits From Dwarf Spheroidal Galaxies with The HAWC Gamma-Ray Observatory. *Astrophys. J.*, 853(2):154, 2018. doi: 10.3847/1538-4357/aaa6d8.
- J. Albert et al. Observation of gamma-rays from the Galactic Center with the MAGIC telescope. *ApJ*, 638:L101–L104, 2006. doi: 10.1086/501164.
- J. Albert et al. Very-High-Energy gamma rays from a Distant Quasar: How Transparent Is the Universe? *Science*, 320:1752, June 2008a. doi: 10.1126/science.1157087.
- J. Albert et al. Upper limit for gamma-ray emission above 140-GeV from the dwarf spheroidal galaxy Draco. *ApJ*, 679:428–431, 2008b. doi: 10.1086/529135.
- J. Aleksic, J. Rico, and M. Martinez. Optimized analysis method for indirect dark matter searches with Imaging Air Cherenkov Telescopes. *J. Cosmology Astropart. Phys.*, 1210:032, 2012. doi: 10.1088/1475-7516/2012/10/032.
- J. Aleksic et al. MAGIC Gamma-Ray Telescope Observation of the Perseus Cluster of Galaxies: Implications for Cosmic Rays, Dark Matter and NGC 1275. *ApJ*, 710:634–647, 2010. doi: 10.1088/0004-637X/710/1/634.
- J. Aleksic et al. Searches for Dark Matter annihilation signatures in the Segue 1 satellite galaxy with the MAGIC-I telescope. *J. Cosmology Astropart. Phys.*, 1106:035, 2011. doi: 10.1088/1475-7516/2011/06/035.
- J. Aleksic et al. Optimized dark matter searches in deep observations of Segue 1 with MAGIC. *J. Cosmology Astropart. Phys.*, 1402:008, 2014. doi: 10.1088/1475-7516/2014/02/008.
- E. Aliu et al. MAGIC upper limits on the VHE gamma-ray emission from the satellite galaxy Willman 1. *ApJ*, 697:1299–1304, 2009. doi: 10.1088/0004-637X/697/2/1299.
- E. Aliu et al. VERITAS Deep Observations of the Dwarf Spheroidal Galaxy Segue 1. *Phys. Rev. D*, D85:062001, 2012. doi: 10.1103/PhysRevD.85.062001.
- J. Alvarez-Muñiz, W. R. Carvalho, A. L. Cummings, K. Payet, A. Romero-Wolf, H. Schoorlemmer, and E. Zas. Comprehensive approach to tau-lepton production by high-energy tau neutrinos propagating through the Earth. *Phys. Rev. D*, 97(2):023021, 2018. doi: 10.1103/PhysRevD.97.023021. [Erratum: Phys.Rev.D 99, 069902 (2019)].
- J. Alvarez-Muñiz et al. The Giant Radio Array for Neutrino Detection (GRAND): Science and Design. 2018.
- G. Ambrosi et al. Direct detection of a break in the teraelectronvolt cosmic-ray spectrum of electrons and positrons. *Nature*, 552:63–66, 2017. doi: 10.1038/nature24475.
- M. Ambrosio et al. Final results of magnetic monopole searches with the MACRO experiment. *Eur. Phys. J.*, C25:511–522, 2002. doi: 10.1140/epjc/s2002-01046-9.

- V. Anastassopoulos, S. Aune, K. Barth, A. Belov, H. Bräuninger, G. Cantatore, J. M. Carmona, J. F. Castel, S. A. Cetin, F. Christensen, J. I. Collar, T. Dafni, M. Davenport, T. A. Decker, A. Dermenev, K. Desch, C. Eleftheriadis, G. Fanourakis, E. Ferrer-Ribas, H. Fischer, J. A. García, A. Gardikiotis, J. G. Garza, E. N. Gazis, T. Gerialis, I. Giomataris, S. Gninenko, C. J. Hailey, M. D. Hasinoff, D. H. H. Hoffmann, F. J. Iguaz, I. G. Irastorza, A. Jakobsen, J. Jacoby, K. Jakovčić, J. Kaminski, M. Karuza, N. Kralj, M. Krčmar, S. Kostoglou, C. Krieger, B. Lakić, J. M. Laurent, A. Liolios, A. Ljubičić, G. Luzón, M. Maroudas, L. Miceli, S. Neff, I. Ortega, T. Papaevangelou, K. Paraschou, M. J. Pivovarov, G. Raffelt, M. Rosu, J. Ruz, E. R. Chóliz, I. Savvidis, S. Schmidt, Y. K. Semertzidis, S. K. Solanki, L. Stewart, T. Vafeiadis, J. K. Vogel, S. C. Yildiz, and K. Zioutas. New CAST limit on the axion-photon interaction. *Nature Physics*, 13:584–590, June 2017. doi: 10.1038/nphys4109.
- S. Ando, A. Geringer-Sameth, N. Hiroshima, S. Hoof, R. Trotta, and M. G. Walker. Structure formation models weaken limits on WIMP dark matter from dwarf spheroidal galaxies. *Phys. Rev. D*, 102(6):061302, 2020. doi: 10.1103/PhysRevD.102.061302.
- S. Andriamonje et al. An improved limit on the axion photon coupling from the CAST experiment. *J. Cosmology Astropart. Phys.*, 4:010, Apr. 2007. doi: 10.1088/1475-7516/2007/04/010.
- S. Archambault et al. Dark Matter Constraints from a Joint Analysis of Dwarf Spheroidal Galaxy Observations with VERITAS. *Phys. Rev. D*, 95(8):082001, 2017. doi: 10.1103/PhysRevD.95.082001.
- A. Archer et al. Measurement of Cosmic-ray Electrons at TeV Energies by VERITAS. *Phys. Rev.*, D98(6):062004, 2018. doi: 10.1103/PhysRevD.98.062004.
- M. Archidiacono, T. Basse, J. Hamann, S. Hannestad, G. Raffelt, and Y. Y. Y. Wong. Future cosmological sensitivity for hot dark matter axions. *J. Cosmology Astropart. Phys.*, 5:050, May 2015. doi: 10.1088/1475-7516/2015/05/050.
- E. Ardi and H. Baumgardt. Depletion of dark matter within globular clusters. *J. Phys. Conf. Ser.*, 1503(1):012023, 2020. doi: 10.1088/1742-6596/1503/1/012023.
- P. Arias, D. Cadamuro, M. Goodsell, J. Jaeckel, J. Redondo, and A. Ringwald. WISPy cold dark matter. *J. Cosmology Astropart. Phys.*, 2012(06):013–013, 2012. ISSN 1475-7516. doi: 10.1088/1475-7516/2012/06/013.
- C. Arina, T. Hambye, A. Ibarra, and C. Weniger. Intense Gamma-Ray Lines from Hidden Vector Dark Matter Decay. *JCAP*, 03:024, 2010. doi: 10.1088/1475-7516/2010/03/024.
- T. A. Arlen et al. Constraints on Cosmic Rays, Magnetic Fields, and Dark Matter from Gamma-Ray Observations of the Coma Cluster of Galaxies with VERITAS and Fermi. *ApJ*, 757:123, 2012. doi: 10.1088/0004-637X/757/2/123.
- C. Armand et al. Combined dark matter searches towards dwarf spheroidal galaxies with Fermi-LAT, HAWC, H.E.S.S., MAGIC, and VERITAS. In *37th International Cosmic Ray Conference*, 8 2021.
- A. Arvanitaki, S. Dimopoulos, S. Dubovsky, N. Kaloper, and J. March-Russell. String axiverse. *Phys. Rev. D*, 81(12):123530, June 2010. doi: 10.1103/PhysRevD.81.123530.

- Y. Asaoka and M. Sasaki. Cherenkov tau shower earth-skimming method for pev-eev tau neutrino observation with ashra. *Astroparticle Physics*, 41:7 – 16, 2013. ISSN 0927-6505. doi: <http://dx.doi.org/10.1016/j.astropartphys.2012.10.001>. URL <http://www.sciencedirect.com/science/article/pii/S0927650512001855>.
- A. Atoyan and C. D. Dermer. High-energy neutrinos from photomeson processes in blazars. *Phys. Rev. Lett.*, 87:221102, Nov 2001. doi: 10.1103/PhysRevLett.87.221102. URL <https://link.aps.org/doi/10.1103/PhysRevLett.87.221102>.
- H. W. Babcock. The rotation of the Andromeda Nebula. *Lick Observatory Bulletin*, 498:41–51, Jan. 1939. doi: 10.5479/ADS/bib/1939LicOB.19.41B.
- R. Bähre et al. Any light particle search II —Technical Design Report. *JINST*, 8:T09001, 2013. doi: 10.1088/1748-0221/8/09/T09001.
- X. Bai et al. The Large High Altitude Air Shower Observatory (LHAASO) Science White Paper. 5 2019.
- M. Bailes, B. K. Berger, P. R. Brady, M. Branchesi, K. Danzmann, M. Evans, K. Holley-Bockelmann, B. R. Iyer, T. Kajita, S. Katsanevas, M. Kramer, A. Lazzarini, L. Lehner, G. Lorusso, H. Lück, D. E. McClelland, M. A. McLaughlin, M. Punturo, S. Ransom, S. Raychaudhury, D. H. Reitze, F. Ricci, S. Rowan, Y. Saito, G. H. Sanders, B. S. Sathyaprakash, B. F. Schutz, A. Sesana, H. Shinkai, X. Siemens, D. H. Shoemaker, J. Thorpe, J. F. J. van den Brand, and S. Vitale. Gravitational-wave physics and astronomy in the 2020s and 2030s. *Nature Reviews Physics*, 3(5):344–366, 2021. ISSN 2522-5820. doi: 10.1038/s42254-021-00303-8. URL <https://doi.org/10.1038/s42254-021-00303-8>.
- L. Barack et al. Black holes, gravitational waves and fundamental physics: a roadmap. 2018.
- B. Baret and V. Van Elewyck. High-energy neutrino astronomy: Detection methods and first achievements. *Rept. Prog. Phys.*, 74:046902, 2011. doi: 10.1088/0034-4885/74/4/046902.
- U. Barres de Almeida. The Southern Wide-Field Gamma-ray Observatory. *Astron. Nachr.*, 342 (1-2):431–437, 2021. doi: 10.1002/asna.202113946.
- R. Bartels and T. Edwards. Comment on ”Understanding the γ -ray emission from the globular cluster 47 Tuc: evidence for dark matter?”. 2018.
- I. Batković, A. De Angelis, M. Doro, and M. Manganaro. Axion-Like Particle Searches with IACTs. *Universe*, 7:185, 2021. doi: 10.3390/universe7060185.
- H. Baumgardt. N -body modelling of globular clusters: masses, mass-to-light ratios and intermediate-mass black holes. *MNRAS*, 464(2):2174–2202, Jan. 2017. doi: 10.1093/mnras/stw2488.
- J. K. Becker. High-energy neutrinos in the context of multimessenger physics. *Phys. Rept.*, 458: 173–246, 2008. doi: 10.1016/j.physrep.2007.10.006.
- M. Beilicke. The Galactic Center Region Imaged by VERITAS from 2010-2012. *AIP Conf.Proc.*, 1505:462–465, 2012. doi: 10.1063/1.4772297.

- A. V. Belikov, L. Goodenough, and D. Hooper. No indications of axionlike particles from Fermi. *Phys. Rev. D*, 83(6):063005, Mar. 2011. doi: 10.1103/PhysRevD.83.063005.
- A. V. Belikov, M. R. Buckley, and D. Hooper. Searching for dark matter subhalos in the Fermi-LAT second source catalog. *Phys. Rev. D*, 86(4):043504, Aug. 2012. doi: 10.1103/PhysRevD.86.043504.
- M. Beneke, A. Broggio, C. Hasner, and M. Vollmann. Energetic γ -rays from TeV scale dark matter annihilation resummed. *Phys. Lett. B*, 786:347–354, 2018. doi: 10.1016/j.physletb.2018.10.008. [Erratum: Phys.Lett.B 810, 135831 (2020)].
- M. Benito, A. Cuoco, and F. Iocco. Handling the Uncertainties in the Galactic Dark Matter Distribution for Particle Dark Matter Searches. *JCAP*, 03:033, 2019. doi: 10.1088/1475-7516/2019/03/033.
- M. Benito, F. Iocco, and A. Cuoco. Uncertainties in the Galactic dark matter distribution: an update. *Phys. Dark Univ.*, 32:100826, 2021. doi: 10.1016/j.dark.2021.100826.
- V. S. Berezinsky and G. T. Zatsepin. Cosmic rays at ultrahigh-energies (neutrino?). *Phys. Lett.*, 28B:423–424, 1969. doi: 10.1016/0370-2693(69)90341-4.
- M. Berg, J. P. Conlon, F. Day, N. Jennings, S. Krippendorf, A. J. Powell, and M. Rummel. Constraints on Axion-like Particles from X-Ray Observations of NGC1275. *ApJ*, 847:101, Oct. 2017. doi: 10.3847/1538-4357/aa8b16.
- L. Bergstrom and D. Hooper. Dark matter and gamma-rays from Draco: MAGIC, GLAST and CACTUS. *Phys. Rev. D*, D73:063510, 2006. doi: 10.1103/PhysRevD.73.063510.
- L. Bergstrom and J. Kaplan. Gamma-ray lines from TeV dark matter. *Astropart. Phys.*, 2:261–268, 1994. doi: 10.1016/0927-6505(94)90005-1.
- L. Bergstrom and P. Ullio. Full one loop calculation of neutralino annihilation into two photons. *Nucl. Phys. B*, 504:27–44, 1997. doi: 10.1016/S0550-3213(97)00530-0.
- L. Bergstrom, P. Ullio, and J. H. Buckley. Observability of gamma-rays from dark matter neutralino annihilations in the Milky Way halo. *Astrop. Phys.*, 9:137–162, 1998. doi: 10.1016/S0927-6505(98)00015-2.
- A. Berlin and D. Hooper. Stringent constraints on the dark matter annihilation cross section from subhalo searches with the Fermi Gamma-Ray Space Telescope. *Phys. Rev. D*, 89(1):016014, Jan. 2014. doi: 10.1103/PhysRevD.89.016014.
- G. Bertone and D. Hooper. A History of Dark Matter. *Submitted to: Rev. Mod. Phys.*, 2016.
- G. Bertone, M. Fornasa, M. Taoso, and A. R. Zentner. Dark Matter Annihilation around Intermediate Mass Black Holes: an update. *New J. Phys.*, 11:105016, 2009. doi: 10.1088/1367-2630/11/10/105016.
- G. Bertone et al. Particle dark matter: Evidence, candidates and constraints. *Phys.Rept.*, 405:279–390, 2005a. doi: 10.1016/j.physrep.2004.08.031.

- G. Bertone et al. A new signature of dark matter annihilations: Gamma-rays from intermediate-mass black holes. *Phys. Rev. D*, D72:103517, 2005b. doi: 10.1103/PhysRevD.72.103517.
- B. Bertoni, D. Hooper, and T. Linden. Examining The Fermi-LAT Third Source Catalog in search of dark matter subhalos. *J. Cosmology Astropart. Phys.*, 12:035, Dec. 2015. doi: 10.1088/1475-7516/2015/12/035.
- B. Bertoni, D. Hooper, and T. Linden. Is the gamma-ray source 3FGL J2212.5+0703 a dark matter subhalo? *J. Cosmology Astropart. Phys.*, 5:049, May 2016. doi: 10.1088/1475-7516/2016/05/049.
- R. Bird. Observing the Cosmic Ray Moon Shadow with VERITAS. *PoS*, ICRC2015:852, 2016. doi: 10.22323/1.236.0852.
- S. Bird, I. Cholis, J. B. Muñoz, Y. Ali-Haïmoud, M. Kamionkowski, E. D. Kovetz, A. Raccanelli, and A. G. Riess. Did LIGO detect dark matter? *Phys. Rev. Lett.*, 116(20):201301, 2016. doi: 10.1103/PhysRevLett.116.201301.
- J. Biteau and D. A. Williams. The Extragalactic Background Light, the Hubble Constant, and Anomalies: Conclusions from 20 Years of TeV Gamma-ray Observations. *The Astrophysical Journal*, 812:60, Oct. 2015. doi: 10.1088/0004-637X/812/1/60.
- P. Blasi and S. Colafrancesco. Cosmic rays, radio halos and non-thermal x-ray emission in clusters of galaxies. *Astropart. Phys.*, 12:169–183, 1999. doi: 10.1016/S0927-6505(99)00079-1,10.1016/S0927-6505(99)00079-1.
- V. Bonnivard, C. Combet, D. Maurin, and M. G. Walker. Spherical Jeans analysis for dark matter indirect detection in dwarf spheroidal galaxies - Impact of physical parameters and triaxiality. *Mon. Not. Roy. Astron. Soc.*, 446:3002–3021, 2015a. doi: 10.1093/mnras/stu2296.
- V. Bonnivard, D. Maurin, and M. G. Walker. Contamination of stellar-kinematic samples and uncertainty about dark matter annihilation profiles in ultrafaint dwarf galaxies: the example of Segue I. *Mon. Not. Roy. Astron. Soc.*, 462(1):223–234, 2016. doi: 10.1093/mnras/stw1691.
- V. Bonnivard et al. Dark matter annihilation and decay in dwarf spheroidal galaxies: The classical and ultrafaint dSphs. *Mon. Not. Roy. Astron. Soc.*, 453(1):849–867, 2015b. doi: 10.1093/mnras/stv1601.
- D. Borla Tridon, P. Colin, L. Cossio, M. Doro, and V. Scalzotto. Measurement of the cosmic electron spectrum with the MAGIC telescopes. In *32nd International Cosmic Ray Conference*, 10 2011. doi: 10.7529/ICRC2011/V06/0680.
- A. Bosma. *The distribution and kinematics of neutral hydrogen in spiral galaxies of various morphological types*. 1978.
- M. Boylan-Kolchin et al. Too big to fail? The puzzling darkness of massive Milky Way subhaloes. *Mon. Not. Roy. Astron. Soc.*, 415:L40, 2011.
- J. D. Bradford, M. Geha, R. Muñoz, F. A. Santana, J. D. Simon, P. Côté, P. B. Stetson, E. Kirby, and S. G. Djorgovski. Structure and Dynamics of the Globular Cluster Palomar 13. *Astrophys. J.*, 743:167, 2011. doi: 10.1088/0004-637X/743/2/167. [Erratum: *Astrophys. J.* 778, 85 (2013)].

- T. Bringmann and F. Calore. Significant Enhancement of Neutralino Dark Matter Annihilation from Electroweak Bremsstrahlung. *Phys. Rev. Lett.*, 112:071301, 2014. doi: 10.1103/PhysRevLett.112.071301.
- T. Bringmann, L. Bergstrom, and J. Edsjo. New Gamma-Ray Contributions to Supersymmetric Dark Matter Annihilation. *JHEP*, 01:049, 2008. doi: 10.1088/1126-6708/2008/01/049.
- T. Bringmann, M. Doro, and M. Fornasa. Dark Matter signals from Draco and Willman 1: Prospects for MAGIC II and CTA. *JCAP*, 0901:016, 2009. doi: 10.1088/1475-7516/2009/01/016.
- J. W. Brockway, E. D. Carlson, and G. G. Raffelt. SN 1987A gamma-ray limits on the conversion of pseudoscalars. *Physics Letters B*, 383:439–443, Feb. 1996. doi: 10.1016/0370-2693(96)00778-2.
- A. M. Brooks and A. Zolotov. Why Baryons Matter: The Kinematics of Dwarf Spheroidal Satellites. *ApJ*, 786:87, May 2014. doi: 10.1088/0004-637X/786/2/87.
- A. M. Brown, T. Lacroix, S. Lloyd, C. Boehm, and P. Chadwick. Understanding the gamma-ray emission from the globular cluster 47 Tuc: evidence for dark matter? 2018.
- A. M. Brown, M. Bagheri, M. Doro, E. Gazda, D. Kieda, C. Lin, Y. Onel, N. Otte, I. Taboada, and A. Wang. Trinity: An Imaging Air Cherenkov Telescope to Search for Ultra-High-Energy Neutrinos. In *37th International Cosmic Ray Conference*, 9 2021.
- P. Brun, E. Moulin, J. Diemand, and J.-F. Glicenstein. Searches for dark matter subhaloes with wide-field Cherenkov telescope surveys. *Phys. Rev. D*, 83(1):015003, Jan. 2011. doi: 10.1103/PhysRevD.83.015003.
- W. Buchmuller, L. Covi, K. Hamaguchi, A. Ibarra, and T. Yanagida. Gravitino Dark Matter in R-Parity Breaking Vacua. *JHEP*, 03:037, 2007. doi: 10.1088/1126-6708/2007/03/037.
- M. R. Buckley and D. Hooper. Dark matter subhalos in the Fermi first source catalog. *Phys. Rev. D*, 82(6):063501, Sept. 2010. doi: 10.1103/PhysRevD.82.063501.
- J. S. Bullock and M. Boylan-Kolchin. Small-Scale Challenges to the Λ CDM Paradigm. *Ann. Rev. Astron. Astrophys.*, 55:343–387, 2017. doi: 10.1146/annurev-astro-091916-055313.
- E. M. Burbidge, G. R. Burbidge, W. A. Fowler, and F. Hoyle. Synthesis of the elements in stars. *Rev. Mod. Phys.*, 29:547–650, Oct 1957. doi: 10.1103/RevModPhys.29.547. URL <https://link.aps.org/doi/10.1103/RevModPhys.29.547>.
- A. Burkert. The Structure of dark matter halos in dwarf galaxies. *IAU Symp.*, 171:175, 1996. doi: 10.1086/309560. [Astrophys. J.447,L25(1995)].
- M. Cahill-Rowley, R. Cotta, A. Drlica-Wagner, S. Funk, J. Hewett, A. Ismail, T. Rizzo, and M. Wood. Complementarity of dark matter searches in the phenomenological MSSM. *Phys. Rev.*, D91(5):055011, 2015. doi: 10.1103/PhysRevD.91.055011.
- C. G. Callan. Disappearing dyons. *Phys. Rev. D*, 25:2141–2146, Apr 1982. doi: 10.1103/PhysRevD.25.2141. URL <https://link.aps.org/doi/10.1103/PhysRevD.25.2141>.

- F. Calore, V. De Romeri, M. Di Mauro, F. Donato, and F. Marinacci. Realistic estimation for the detectability of dark matter subhalos using Fermi-LAT catalogs. *Phys. Rev. D*, 96(6):063009, Sept. 2017. doi: 10.1103/PhysRevD.96.063009.
- F. Calore, M. Hütten, and M. Stref. Gamma-ray sensitivity to dark matter subhalo modelling at high latitudes. *Galaxies*, 7(4):90, 2019. doi: 10.3390/galaxies7040090.
- R. Caputo, M. Meyer, M. Sánchez-Conde, and AMEGO. Exploring the particle nature of dark matter with the All-sky Medium Energy Gamma-ray Observatory (AMEGO). volume 231 of *American Astronomical Society Meeting Abstracts*, Jan. 2018.
- B. Carr, F. Kuhnel, and M. Sandstad. Primordial Black Holes as Dark Matter. *Phys. Rev. D*, 94(8):083504, 2016. doi: 10.1103/PhysRevD.94.083504.
- B. J. Carr. Primordial black holes: Do they exist and are they useful? In *59th Yamada Conference on Inflating Horizon of Particle Astrophysics and Cosmology Tokyo, Japan, June 20-24, 2005*, 2005.
- B. J. Carr et al. New cosmological constraints on primordial black holes. *Phys. Rev.*, D81:104019, 2010. doi: 10.1103/PhysRevD.81.104019.
- M. Cassanyes. *MAGIC sensitivity to Primordial Black Hole bursts and modelization of BH chromospheres and gamma-ray emission spectra*. PhD thesis, 2015.
- S. Cecchini, L. Patrizii, Z. Sahnoun, G. Sirri, and V. Togo. Energy Losses of Magnetic Monopoles in Aluminum, Iron and Copper. 2016.
- J. Chang et al. An excess of cosmic ray electrons at energies of 300-800 GeV. *Nature*, 456:362–365, 2008. doi: 10.1038/nature07477.
- A. Chiappo, J. Cohen-Tanugi, J. Conrad, L. E. Strigari, B. Anderson, and M. A. Sanchez-Conde. Dwarf spheroidal J-factors without priors: A likelihood-based analysis for indirect dark matter searches. *Mon. Not. Roy. Astron. Soc.*, 466(1):669–676, 2017. doi: 10.1093/mnras/stw3079.
- Y. Chikashige, Y. Fujii, and K. Mima. Lorentz Invariant String Regularized Dimensionally by Means of Hyperfunctions. II. *Progress of Theoretical Physics*, 59:274–288, Jan. 1978. doi: 10.1143/PTP.59.274.
- M. Cicoli, M. D. Goodsell, and A. Ringwald. The type IIB string axiverse and its low-energy phenomenology. *Journal of High Energy Physics*, 10:146, Oct. 2012. doi: 10.1007/JHEP10(2012)146.
- M. Cirelli, G. Corcella, A. Hektor, G. Hutsi, M. Kadastik, P. Panci, M. Raidal, F. Sala, and A. Strumia. PPC 4 DM ID: A Poor Particle Physicist Cookbook for Dark Matter Indirect Detection. *JCAP*, 1103:051, 2011. doi: 10.1088/1475-7516/2012/10/E01,10.1088/1475-7516/2011/03/051. [Erratum: JCAP1210,E01(2012)].
- S. Colafrancesco, S. Profumo, and P. Ullio. Multi-frequency analysis of neutralino dark matter annihilations in the Coma cluster. *Astron. Astrophys.*, 455:21, 2006. doi: 10.1051/0004-6361:20053887.

- S. Colafrancesco, R. Lieu, P. Marchegiani, M. Pato, and L. Pieri. On the DM interpretation of the origin of non-thermal phenomena in galaxy clusters. *Astron.Astrophys.*, 527:A80, 2011.
- P. Colin, D. Borla Tridon, A. Diago Ortega, M. Doert, M. Doro, J. Pochon, N. Strah, T. Surić, and M. Teshima. Probing the CR positron/electron ratio at few hundreds GeV through Moon shadow observation with the MAGIC telescopes. In *PoS, 32nd International Cosmic Ray Conference (ICRC 2011): Beijing, China, August 11-18, 2011*, volume 6, pages 194–197, 2011. doi: 10.7529/ICRC2011/V06/1114.
- J. P. Conlon. The QCD axion and moduli stabilisation. *Journal of High Energy Physics*, 5:078, May 2006. doi: 10.1088/1126-6708/2006/05/078.
- V. Connaughton, C. Akerlof, S. Biller, P. Boyle, J. Buckley, D. Carter-Lewis, M. Catanese, M. Cawley, D. Fegan, J. Finley, J. Gaidos, A. Hillas, R. Lamb, R. Lessard, J. McEnery, G. Mohanty, N. Porter, J. Quinn, H. Rose, M. Schubnell, G. Sembroski, R. Srinivasan, T. Weekes, C. Wilson, and J. Zweerink. A search for tev gamma-ray bursts on a 1-second time-scale. *Astroparticle Physics*, 8(3):179 – 191, 1998. ISSN 0927-6505. doi: [https://doi.org/10.1016/S0927-6505\(97\)00055-8](https://doi.org/10.1016/S0927-6505(97)00055-8). URL <http://www.sciencedirect.com/science/article/pii/S0927650597000558>.
- J. Coronado-Blázquez and M. A. Sánchez-Conde. Constraints to Dark Matter Annihilation from High-Latitude HAWC Unidentified Sources. *Galaxies*, 8(1):5, Jan. 2020. doi: 10.3390/galaxies8010005.
- J. Coronado-Blázquez, M. A. Sánchez-Conde, M. Di Mauro, A. Aguirre-Santaella, I. Ciucă, A. Domínguez, D. Kawata, and N. Mirabal. Spectral and spatial analysis of the dark matter subhalo candidates among *Fermi* Large Area Telescope unidentified sources. *JCAP*, 11:045, 2019a. doi: 10.1088/1475-7516/2019/11/045.
- J. Coronado-Blázquez, M. A. Sanchez-Conde, A. Dominguez, A. Aguirre-Santaella, M. Di Mauro, N. Mirabal, D. Nieto, and E. Charles. Unidentified Gamma-ray Sources as Targets for Indirect Dark Matter Detection with the Fermi-Large Area Telescope. *JCAP*, 07:020, 2019b. doi: 10.1088/1475-7516/2019/07/020.
- J. Coronado-Blázquez, M. Doro, M. A. Sánchez-Conde, and A. Aguirre-Santaella. Sensitivity of the Cherenkov Telescope Array to dark subhalos. *Phys. Dark Univ.*, 32:100845, 2021. doi: 10.1016/j.dark.2021.100845.
- P. Creasey, L. V. Sales, E. W. Peng, and O. Sameie. Globular clusters formed within dark haloes I: present-day abundance, distribution, and kinematics. *Mon. Not. Roy. Astron. Soc.*, 482(1): 219–230, 2019. doi: 10.1093/mnras/sty2701.
- C. Csáki, N. Kaloper, and J. Terning. Dimming Supernovae without Cosmic Acceleration. *Phys. Rev. Letter*, 88(16):161302, Apr. 2002. doi: 10.1103/PhysRevLett.88.161302.
- C. Csáki, N. Kaloper, M. Peloso, and J. Terning. Super-GZK photons from photon-axion mixing. *J. Cosmology Astropart. Phys.*, 5:005, May 2003. doi: 10.1088/1475-7516/2003/05/005.
- CTA Consortium. *Science with the Cherenkov Telescope Array*. 2019. doi: 10.1142/10986.

- A. de Angelis, M. Roncadelli, and O. Mansutti. Evidence for a new light spin-zero boson from cosmological gamma-ray propagation? *Phys. Rev. D*, 76(12):121301, Dec. 2007. doi: 10.1103/PhysRevD.76.121301.
- A. de Angelis, O. Mansutti, and M. Roncadelli. Axion-like particles, cosmic magnetic fields and gamma-ray astrophysics. *Physics Letters B*, 659:847–855, Feb. 2008. doi: 10.1016/j.physletb.2007.12.012.
- A. de Angelis, O. Mansutti, M. Persic, and M. Roncadelli. Photon propagation and the very high energy gamma-ray spectra of blazars: how transparent is the Universe? *MNRAS*, 394:L21–L25, Mar. 2009. doi: 10.1111/j.1745-3933.2008.00602.x.
- A. de Angelis, G. Galanti, and M. Roncadelli. Relevance of axionlike particles for very-high-energy astrophysics. *Phys. Rev. D*, 84(10):105030, Nov. 2011. doi: 10.1103/PhysRevD.84.105030.
- A. De Angelis, V. Tatischeff, I. A. Grenier, J. McEnery, M. Mallamaci, M. Tavani, U. Oberlack, L. Hanlon, R. Walter, A. Argan, and et al. Science with e-ASTROGAM (A space mission for MeV-GeV gamma-ray astrophysics). *ArXiv e-prints*, Nov. 2017.
- M. den Brok, G. van de Ven, R. van den Bosch, and L. Watkins. The central mass and mass-to-light profile of the Galactic globular cluster M15. *MNRAS*, 438(1):487–493, Feb. 2014. doi: 10.1093/mnras/stt2221.
- DESI Collaboration, A. Aghamousa, J. Aguilar, S. Ahlen, S. Alam, L. E. Allen, C. Allende Prieto, J. Annis, S. Bailey, C. Balland, O. Ballester, C. Baltay, L. Beaufore, C. Bebek, T. C. Beers, E. F. Bell, J. L. Bernal, R. Besuner, F. Beutler, C. Blake, H. Bleuler, M. Blomqvist, R. Blum, A. S. Bolton, C. Briceno, D. Brooks, J. R. Brownstein, E. Buckley-Geer, A. Burden, E. Burtin, N. G. Busca, R. N. Cahn, Y.-C. Cai, L. Cardiel-Sas, R. G. Carlberg, P.-H. Carton, R. Casas, F. J. Castander, J. L. Cervantes-Cota, T. M. Claybaugh, M. Close, C. T. Coker, S. Cole, J. Comparat, A. P. Cooper, M. C. Cousinou, M. Crocce, J.-G. Cuby, D. P. Cunningham, T. M. Davis, K. S. Dawson, A. de la Macorra, J. De Vicente, T. Delubac, M. Derwent, A. Dey, G. Dhungana, Z. Ding, P. Doel, Y. T. Duan, A. Ealet, J. Edelman, S. Eftekharzadeh, D. J. Eisenstein, A. Elliott, S. Escoffier, M. Evatt, P. Fagrelus, X. Fan, K. Fanning, A. Farahi, J. Farihi, G. Favole, Y. Feng, E. Fernandez, J. R. Findlay, D. P. Finkbeiner, M. J. Fitzpatrick, B. Flaugher, S. Flender, A. Font-Ribera, J. E. Forero-Romero, P. Fosalba, C. S. Frenk, M. Fumagalli, B. T. Gaensicke, G. Gallo, J. Garcia-Bellido, E. Gaztanaga, N. Pietro Gentile Fusillo, T. Gerard, I. Gershkovich, T. Gianantonio, D. Gillet, G. Gonzalez-de-Rivera, V. Gonzalez-Perez, S. Gott, O. Graur, G. Gutierrez, J. Guy, S. Habib, H. Heetderks, I. Heetderks, K. Heitmann, W. A. Hellwing, D. A. Herrera, S. Ho, S. Holland, K. Honscheid, E. Huff, T. A. Hutchinson, D. Huterer, H. S. Hwang, J. M. Illa Laguna, Y. Ishikawa, D. Jacobs, N. Jeffrey, P. Jelinsky, E. Jennings, L. Jiang, J. Jimenez, J. Johnson, R. Joyce, E. Jullo, S. Juneau, S. Kama, A. Karcher, S. Karkar, R. Kehoe, N. Kennamer, S. Kent, M. Kilbinger, A. G. Kim, D. Kirkby, T. Kisner, E. Kitanidis, J.-P. Kneib, S. Kopolov, E. Kovacs, K. Koyama, A. Kremin, R. Kron, L. Kronig, A. Kueter-Young, C. G. Lacey, R. Lafever, O. Lahav, A. Lambert, M. Lampton, M. Landriau, D. Lang, T. R. Lauer, J.-M. Le Goff, L. Le Guillou, A. Le Van Suu, J. H. Lee, S.-J. Lee, D. Leitner, M. Lesser, M. E. Levi, B. L’Huillier, B. Li, M. Liang, H. Lin, E. Linder, S. R. Loebman, Z. Lukić, J. Ma, N. MacCrann, C. Magneville, L. Makarem, M. Manera, C. J. Manser, R. Marshall, P. Martini, R. Massey, T. Matheson, J. McCauley, P. McDonald, I. D. McGreer, A. Meisner, N. Metcalfe, T. N. Miller, R. Miquel,

- J. Moustakas, A. Myers, M. Naik, J. A. Newman, R. C. Nichol, A. Nicola, L. Nicolati da Costa, J. Nie, G. Niz, P. Norberg, B. Nord, D. Norman, P. Nugent, T. O'Brien, M. Oh, K. A. G. Olsen, C. Padilla, H. Padmanabhan, N. Padmanabhan, N. Palanque-Delabrouille, A. Palmese, D. Pappalardo, I. Pâris, C. Park, A. Patej, J. A. Peacock, H. V. Peiris, X. Peng, W. J. Percival, S. Perruchot, M. M. Pieri, R. Pogge, J. E. Pollack, C. Poppett, F. Prada, A. Prakash, R. G. Probst, D. Rabinowitz, A. Raichoor, C. H. Ree, A. Refregier, X. Regal, B. Reid, K. Reil, M. Rezaie, C. M. Rockosi, N. Roe, S. Ronayette, A. Roodman, A. J. Ross, N. P. Ross, G. Rossi, E. Rozo, V. Ruhlmann-Kleider, E. S. Rykoff, C. Sabiu, L. Samushia, E. Sanchez, J. Sanchez, D. J. Schlegel, M. Schneider, M. Schubnell, A. Secroun, U. Seljak, H.-J. Seo, S. Serrano, A. Shafieloo, H. Shan, R. Sharples, M. J. Sholl, W. V. Shourt, J. H. Silber, D. R. Silva, M. M. Sirk, A. Slosar, A. Smith, G. F. Smoot, D. Som, Y.-S. Song, D. Sprayberry, R. Staten, A. Stefanik, G. Tarle, S. Sien Tie, J. L. Tinker, R. Tojeiro, F. Valdes, O. Valenzuela, M. Valluri, M. Vargas-Magana, L. Verde, A. R. Walker, J. Wang, Y. Wang, B. A. Weaver, C. Weaverdyck, R. H. Wechsler, D. H. Weinberg, M. White, Q. Yang, C. Yeche, T. Zhang, G.-B. Zhao, Y. Zheng, X. Zhou, Z. Zhou, Y. Zhu, H. Zou, and Y. Zu. The DESI Experiment Part I: Science, Targeting, and Survey Design. *arXiv e-prints*, art. arXiv:1611.00036, Oct. 2016.
- A. Di Cintio et al. The dependence of dark matter profiles on the stellar to halo mass ratio: a prediction for cusps vs cores. *arXiv e-Print*:1306.0898, 2013.
- M. Di Mauro and M. W. Winkler. Multimessenger constraints on the dark matter interpretation of the Fermi-LAT Galactic center excess. *Phys. Rev. D*, 103(12):123005, 2021. doi: 10.1103/PhysRevD.103.123005.
- D. A. Dicus, E. W. Kolb, V. L. Teplitz, and R. V. Wagoner. Astrophysical bounds on the masses of axions and Higgs particles. *Phys. Rev. D*, 18:1829–1834, Sept. 1978. doi: 10.1103/PhysRevD.18.1829.
- J. Diemand et al. Clumps and streams in the local dark matter distribution. *Nature*, 454:735–738, Aug. 2008. doi: 10.1038/nature07153.
- P. A. M. Dirac. Quantised Singularities in the Electromagnetic Field. *Proceedings of the Royal Society of London Series A*, 133:60–72, Sept. 1931. doi: 10.1098/rspa.1931.0130.
- S. Dodelson. *Modern Cosmology*. Academic Press, Amsterdam, 2003. ISBN 9780122191411. URL <http://www.slac.stanford.edu/spires/find/books/www?cl=QB981:D62:2003>.
- A. Domínguez and M. Ajello. Spectral Analysis of Fermi-LAT Blazars above 50 GeV. *ApJL*, 813:L34, Nov. 2015. doi: 10.1088/2041-8205/813/2/L34.
- A. Domínguez, M. A. Sánchez-Conde, and F. Prada. Axion-like particle imprint in cosmological very-high-energy sources. *Journal of Cosmology and Astroparticle Physics*, 11:020, Nov. 2011. doi: 10.1088/1475-7516/2011/11/020.
- F. Donato, N. Fornengo, D. Maurin, and P. Salati. Antiprotons in cosmic rays from neutralino annihilation. *Phys. Rev.*, D69:063501, 2004. doi: 10.1103/PhysRevD.69.063501.
- M. Doro. A decade of dark matter searches with ground-based Cherenkov telescopes. *Nucl. Instrum. and Meth. in Phys. Research A*, A742:99–106, 2014. doi: 10.1016/j.nima.2013.12.010.

- M. Doro. Rare Events searches with Cherenkov Telescopes. 2017. doi: 10.1051/epjconf/201713601003. [EPJ Web Conf.136,01003(2017)].
- M. Doro, J. Conrad, D. Emmanoulopoulos, M. A. Sánchez-Conde, J. A. Barrio, E. Birsin, J. Bolmont, P. Brun, S. Colafrancesco, S. H. Connell, J. L. Contreras, M. K. Daniel, M. Fornasa, M. Gaug, J. F. Glicenstein, A. González-Muñoz, T. Hassan, D. Horns, A. Jacholkowska, C. Jahn, R. Mazini, N. Mirabal, A. Moralejo, E. Moulin, D. Nieto, J. Ripken, H. Sandaker, U. Schwanke, G. Spengler, A. Stamerra, A. Viana, H.-S. Zechlin, S. Zimmer, and CTA Consortium. Dark matter and fundamental physics with the Cherenkov Telescope Array. *Astroparticle Physics*, 43: 189–214, Mar. 2013. doi: 10.1016/j.astropartphys.2012.08.002.
- M. Doro et al. Indirect Dark Matter Search at Intermediate Mass Black Holes with the MAGIC Telescope. In *Proc. of the 30th ICRC*, Mérida, Mexico, 2007.
- M. Doro et al. Dark Matter and Fundamental Physics with the Cherenkov Telescope Array. *Astrop. Phys.*, 43:189–214, 2013. doi: 10.1016/j.astropartphys.2012.08.002.
- A. Drlica-Wagner et al. Eight Ultra-faint Galaxy Candidates Discovered in Year Two of the Dark Energy Survey. *Astrophys. J.*, 813(2):109, 2015. doi: 10.1088/0004-637X/813/2/109.
- A. Drlica-Wagner et al. Dark Energy Survey Year 1 Results: Photometric Data Set for Cosmology. *Astrophys. J. Suppl.*, 235(2):33, 2018. doi: 10.3847/1538-4365/aab4f5.
- A. Drlica-Wagner et al. Probing the Fundamental Nature of Dark Matter with the Large Synoptic Survey Telescope. 2 2019.
- G. Dubus, J. L. Contreras, S. Funk, Y. Gallant, T. Hassan, J. Hinton, Y. Inoue, J. Knödseder, P. Martin, N. Mirabal, M. de Naurois, M. Renaud, and CTA Consortium. Surveys with the Cherenkov Telescope Array. *Astroparticle Physics*, 43:317–330, Mar 2013. doi: 10.1016/j.astropartphys.2012.05.020.
- L. D. Duffy, P. Sikivie, D. B. Tanner, S. J. Asztalos, C. Hagmann, D. Kinion, L. J. Rosenberg, K. van Bibber, D. B. Yu, and R. F. Bradley. High resolution search for dark-matter axions. *Phys. Rev. D*, 74(1):012006, July 2006. doi: 10.1103/PhysRevD.74.012006.
- J. Einasto, A. Kaasik, and E. N. N. Saar. Dynamic evidence on massive coronas of galaxies. *Nature*, 250:309, jul 1974. URL <http://dx.doi.org/10.1038/250309a0><http://10.0.4.14/250309a0>.
- W. Essey and A. Kusenko. A new interpretation of the gamma-ray observations of distant active galactic nuclei. *Astroparticle Physics*, 33:81–85, Mar. 2010. doi: 10.1016/j.astropartphys.2009.11.007.
- W. Essey and A. Kusenko. On Weak Redshift Dependence of Gamma-Ray Spectra of Distant Blazars. *ApJL*, 751:L11, May 2012. doi: 10.1088/2041-8205/751/1/L11.
- W. Essey, O. Kalashev, A. Kusenko, and J. F. Beacom. Role of Line-of-sight Cosmic-ray Interactions in Forming the Spectra of Distant Blazars in TeV Gamma Rays and High-energy Neutrinos. *The Astrophysical Journal*, 731:51, Apr. 2011. doi: 10.1088/0004-637X/731/1/51.

- D. Fargion. Horizontal Tau air showers from mountains in deep vally: Traces of Ultrahigh neutrino tau. In *International Cosmic Ray Conference*, volume 2 of *International Cosmic Ray Conference*, pages 396–+, Aug. 1999.
- D. Fargion. Discovering Ultra High Energy Neutrinos by Horizontal and Upward tau Air-Showers: Evidences in Terrestrial Gamma Flashes? *Astrophys. J.*, 570:909–925, 2002. doi: 10.1086/339772.
- D. Fargion, P. G. De Sanctis Lucentini, and M. De Santis. Tau air showers from earth. *Astrophys. J.*, 613:1285–1301, 2004. doi: 10.1086/423124.
- M. Farina, D. Pappadopulo, F. Rompineve, and A. Tesi. The photo-philic QCD axion. *Journal of High Energy Physics*, 2017:95, Jan 2017. doi: 10.1007/JHEP01(2017)095.
- J. L. Feng. Naturalness and the Status of Supersymmetry. UCI-TR-2013-01, 2013.
- J. L. Feng and J. Kumar. The WIMPless Miracle: Dark-Matter Particles without Weak-Scale Masses or Weak Interactions. *Phys. Rev. Lett.*, 101:231301, 2008. doi: 10.1103/PhysRevLett.101.231301.
- J. A. Frieman, C. T. Hill, A. Stebbins, and I. Waga. Cosmology with Ultralight Pseudo Nambu-Goldstone Bosons. *Phys. Rev. Letter*, 75:2077–2080, Sept. 1995. doi: 10.1103/PhysRevLett.75.2077.
- G. Galanti and M. Roncadelli. Extragalactic photon-axion-like particle oscillations up to 1000 TeV. *Journal of High Energy Astrophysics*, 20:1–17, Nov. 2018. doi: 10.1016/j.jheap.2018.07.002.
- G. Galanti, M. Roncadelli, A. De Angelis, and G. F. Bignami. Hint at an axion-like particle from the redshift dependence of blazar spectra. *Mon. Not. Roy. Astron. Soc.*, 493(2):1553–1564, 2020. doi: 10.1093/mnras/stz3410.
- L. Gao et al. Where will supersymmetric dark matter first be seen? *MNRAS*, 419:1721, 2012. doi: 10.1111/j.1365-2966.2011.19836.x.
- S. Garrison-Kimmel, P. F. Hopkins, A. Wetzel, J. S. Bullock, M. Boylan-Kolchin, D. Keres, C.-A. Faucher-Giguere, K. El-Badry, A. Lamberts, E. Quataert, and R. Sanderson. The Local Group on FIRE: Dwarf galaxy populations across a suite of hydrodynamic simulations. *arXiv e-prints*, June 2018.
- M. Gaug et al. Tau neutrino search with the MAGIC telescope. *Procs of the 30th International Cosmic Ray Conference*, 3:1273–1278, 2007.
- A. Gazizov and M. P. Kowalski. ANIS: High energy neutrino generator for neutrino telescopes. *Comput. Phys. Commun.*, 172:203–213, 2005. doi: 10.1016/j.cpc.2005.03.113.
- A. Geringer-Sameth, S. M. Koushiappas, and M. Walker. Dwarf galaxy annihilation and decay emission profiles for dark matter experiments. *Astrophys. J.*, 801(2):74, 2015. doi: 10.1088/0004-637X/801/2/74.
- A. f. Geringer-Sameth. The VERITAS Dark Matter Program. *arXiv e-prints*, Mar. 2013.

- G. Giacomelli and L. Patrizzii. Magnetic monopoles. In *NATO Advanced Research Workshop on Cosmic Radiation: From Astronomy to Particle Physics Oujda, Morocco, March 21-23, 2001*, 2001.
- D. Gora and E. Bernardini. Detection of tau neutrinos by Imaging Air Cherenkov Telescopes. *Astropart. Phys.*, 82:77–85, 2016. doi: 10.1016/j.astropartphys.2016.06.002.
- D. Gora, M. Roth, and A. Tamburro. A MC approach to simulate up- and down-going neutrino showers including local topographic conditions. *Astroparticle Physics*, 26:402–413, Jan. 2007. doi: 10.1016/j.astropartphys.2006.08.008.
- D. Gora, E. Bernardini, K. Satalecka, K. Noda, M. Manganaro, and M. López. MAGIC gamma-ray telescopes hunting for neutrinos and their sources. *J. Phys. Conf. Ser.*, 888(1):012147, 2017a. doi: 10.1088/1742-6596/888/1/012147.
- D. Gora, M. Manganaro, E. Bernardini, M. Doro, M. Will, S. Lombardi, J. Rico, D. Sobczynska, and J. Palacio. Sensitivity for tau neutrinos at PeV energies and beyond with the MAGIC telescopes. *PoS, ICRC2017:992*, 2017b.
- A. M. Green and B. J. Kavanagh. Primordial Black Holes as a dark matter candidate. *J. Phys. G*, 48(4):043001, 2021. doi: 10.1088/1361-6471/abc534.
- K. Griest and M. Kamionkowski. Unitarity Limits on the Mass and Radius of Dark Matter Particles. *Phys. Rev. Lett.*, 64:615, 1990. doi: 10.1103/PhysRevLett.64.615.
- J. A. Grifols, E. Massó, and R. Toldrà. Gamma Rays from SN 1987A due to Pseudoscalar Conversion. *Physical Review Letters*, 77:2372–2375, Sept. 1996. doi: 10.1103/PhysRevLett.77.2372.
- J. Guo, H.-J. Li, X.-J. Bi, S.-J. Lin, and P.-F. Yin. Implications of axion-like particles from the Fermi-LAT and H.E.S.S. observations of PG 1553+113 and PKS 2155–304. *Chin. Phys. C*, 45(2):025105, 2021. doi: 10.1088/1674-1137/abcd2e.
- R. Hagedorn. Hadronic matter near the boiling point. *Nuovo Cim.*, A56:1027–1057, 1968. doi: 10.1007/BF02751614.
- F. Halzen, E. Zas, J. H. MacGibbon, and T. C. Weekes. Gamma-rays and energetic particles from primordial black holes. *Nature*, 353:807–815, 1991. doi: 10.1038/353807a0.
- J. R. Hargis, B. Willman, and A. H. G. Peter. Too Many, Too Few, or Just Right? The Predicted Number and Distribution of Milky Way Dwarf Galaxies. *Astrophys. J.*, 795(1):L13, 2014. doi: 10.1088/2041-8205/795/1/L13.
- D. Hartmann and AMEGO. Advancing the MeV Frontier with AMEGO. volume 231, Jan. 2018.
- S. Hawking. Gravitationally collapsed objects of very low mass. *Mon. Not. Roy. Astron. Soc.*, 152:75, 1971.
- S. W. Hawking. Black hole explosions. *Nature*, 248:30–31, 1974. doi: 10.1038/248030a0.
- K. Hayashi, M. Chiba, and T. Ishiyama. Diversity of Dark Matter Density Profiles in the Galactic Dwarf Spheroidal Satellites. *Astrophys. J.*, 904(1):45, 2020. doi: 10.3847/1538-4357/abbe0a.

- D.-Z. He, X.-J. Bi, S.-J. Lin, P.-F. Yin, and X. Zhang. Prospect for dark matter annihilation signatures from gamma-ray observation of dwarf galaxies by LHAASO. *Phys. Rev. D*, 100(8): 083003, 2019. doi: 10.1103/PhysRevD.100.083003.
- D. Heck, G. Schatz, T. Thouw, J. Knapp, and J. N. Capdevielle. CORSIKA: A Monte Carlo code to simulate extensive air showers. 1998.
- A. Heger, C. L. Fryer, S. E. Woosley, N. Langer, and D. H. Hartmann. How massive single stars end their life. *Astrophys. J.*, 591:288–300, 2003. doi: 10.1086/375341.
- K. Helgason and A. Kashlinsky. Reconstructing the gamma-Ray Photon Optical Depth of the Universe to $z \sim 4$ from Multiwavelength Galaxy Survey Data. *ApJL*, 758:L13, Oct. 2012. doi: 10.1088/2041-8205/758/1/L13.
- A. Helmi, M. A. Breddels, C. A. Vera-Ciro, and E. Starckenburg. Not too big, not too small: the dark haloes of the dwarf spheroidals in the Milky Way. *Monthly Notices of the Royal Astronomical Society*, 428(2):1696–1703, 10 2012.
- A. Helmi et al. Gaia Data Release 2: Kinematics of globular clusters and dwarf galaxies around the Milky Way. *Astron. Astrophys.*, 616:A12, 2018. doi: 10.1051/0004-6361/201832698. [Erratum: *Astron. Astrophys.* 637, C3 (2020), Erratum: *Astron. Astrophys.* 642, C1 (2020)].
- L. Hernquist. An Analytical Model for Spherical Galaxies and Bulges. *Astrophys. J.*, 356:359, 1990. doi: 10.1086/168845.
- N. Hiroshima, S. Ando, and T. Ishiyama. Modeling evolution of dark matter substructure and annihilation boost. *Phys. Rev.*, D97(12):123002, 2018. doi: 10.1103/PhysRevD.97.123002.
- K. A. Hochmuth and G. Sigl. Effects of axion-photon mixing on gamma-ray spectra from magnetized astrophysical sources. *Phys. Rev. D*, 76(12):123011, Dec. 2007. doi: 10.1103/PhysRevD.76.123011.
- D. Hooper. *Dark cosmos : in search of our universe's missing mass and energy*. 2006.
- D. Hooper. TASI Lectures on Indirect Detection of Dark Matter. 2017. URL <http://arxiv.org/abs/1710.05137>.
- D. Hooper and P. D. Serpico. Detecting Axion-Like Particles With Gamma Ray Telescopes. pages 8–11, 2007. doi: 10.1103/PhysRevLett.99.231102.
- D. Hooper and S. J. Witte. Gamma rays from dark matter subhalos revisited: refining the predictions and constraints. *J. Cosmology Astropart. Phys.*, 4:018, Apr. 2017. doi: 10.1088/1475-7516/2017/04/018.
- D. Horns and M. Meyer. Indications for a pair-production anomaly from the propagation of VHE gamma-rays. *J. Cosmology Astropart. Phys.*, 2:033, Feb. 2012. doi: 10.1088/1475-7516/2012/02/033.
- D. Horns, L. Maccione, M. Meyer, A. Mirizzi, D. Montanino, and M. Roncadelli. Hardening of TeV gamma spectrum of active galactic nuclei in galaxy clusters by conversions of photons into axionlike particles. *Phys. Rev. D*, 86(7):075024, Oct. 2012. doi: 10.1103/PhysRevD.86.075024.

- E. Hubble and M. L. Humason. The Velocity-Distance Relation among Extra-Galactic Nebulae. *ApJ*, 74:43, July 1931. doi: 10.1086/143323.
- M. Hütten, C. Combet, G. Maier, and D. Maurin. Dark matter substructure modelling and sensitivity of the Cherenkov Telescope Array to Galactic dark halos. *J. Cosmology Astropart. Phys.*, 9:047, Sept. 2016. doi: 10.1088/1475-7516/2016/09/047.
- A. Ibarra, S. Lopez Gehler, and M. Pato. Dark matter constraints from box-shaped gamma-ray features. *JCAP*, 1207:043, 2012. doi: 10.1088/1475-7516/2012/07/043.
- R. Ibata, C. Nipoti, A. Sollima, M. Bellazzini, S. Chapman, and E. Dalessandro. Do globular clusters possess Dark Matter halos? A case study in NGC 2419. *Mon. Not. Roy. Astron. Soc.*, 428:3648, 2013. doi: 10.1093/mnras/sts302.
- K. Ichikawa, M. N. Ishigaki, S. Matsumoto, M. Ibe, H. Sugai, K. Hayashi, and S.-i. Horigome. Foreground effect on the J -factor estimation of classical dwarf spheroidal galaxies. *Mon. Not. Roy. Astron. Soc.*, 468(3):2884–2896, 2017. doi: 10.1093/mnras/stx682.
- K. Ichikawa, S.-i. Horigome, M. N. Ishigaki, S. Matsumoto, M. Ibe, H. Sugai, and K. Hayashi. Foreground effect on the J -factor estimation of ultrafaint dwarf spheroidal galaxies. *Mon. Not. Roy. Astron. Soc.*, 479(1):64–74, 2018. doi: 10.1093/mnras/sty1387.
- T. Inada, D. Kerszberg, M. Hütten, M. Teshima, J. Rico, and D. Ninci. Upper limits on the WIMP annihilation cross section from a joint analysis of dwarf spheroidal satellite galaxy observations with the MAGIC telescopes. *PoS, ICRC2021:520*, 2021. doi: 10.22323/1.395.0512.
- I. G. Irastorza and J. Redondo. New experimental approaches in the search for axion-like particles. *Progress in Particle and Nuclear Physics*, 102:89–159, Sept. 2018. doi: 10.1016/j.pnpnp.2018.05.003.
- I. G. Irastorza, F. T. Avignone, G. Cantatore, J. M. Carmona, S. Caspi, S. A. Cetin, F. E. Christensen, A. Dael, T. Dafni, M. Davenport, A. V. Derbin, K. Desch, A. Diago, B. Döbrich, A. Dudarev, C. Eleftheriadis, G. Fanourakis, E. Ferrer-Ribas, J. Galán, J. A. García, J. G. Garza, T. Gerialis, B. Gimeno, I. Giomataris, S. Gninenko, H. Gómez, E. Guendelman, C. J. Hailey, T. Hiramatsu, D. H. H. Hoffmann, D. Horns, F. J. Iguaz, J. Isern, A. C. Jakobsen, J. Jaeckel, K. Jakovčić, J. Kaminski, M. Kawasaki, M. Krčmar, C. Krieger, B. Lakić, A. Lindner, A. Liolios, G. Luzón, I. Ortega, T. Papaevangelou, M. J. Pivovarov, G. Raffelt, J. Redondo, A. Ringwald, S. Russenschuck, J. Ruz, K. Saikawa, I. Savvidis, T. Sekiguchi, I. Shilon, P. Sikivie, H. Silva, H. ten Kate, A. Tomas, S. Troitsky, T. Vafeiadis, K. van Bibber, P. Vedrine, J. A. Villar, J. K. Vogel, L. Walckiers, W. Wester, S. C. Yildiz, and K. Zioutas. Future axion searches with the International Axion Observatory (IAXO). In *Journal of Physics Conference Series*, volume 460 of *Journal of Physics Conference Series*, page 012002, Oct. 2013. doi: 10.1088/1742-6596/460/1/012002.
- T. E. Jeltema, J. Kehayias, and S. Profumo. Gamma Rays from Clusters and Groups of Galaxies: Cosmic Rays versus Dark Matter. *Phys.Rev.*, D80:023005, 2009. doi: 10.1103/PhysRevD.80.023005.
- G. Jungman and M. Kamionkowski. Gamma-rays from neutralino annihilation. *Phys. Rev. D*, 51:3121–3124, 1995. doi: 10.1103/PhysRevD.51.3121.

- F. Kahlhoefer, M. Kaplinghat, T. R. Slatyer, and C.-L. Wu. Diversity in density profiles of self-interacting dark matter satellite halos. *JCAP*, 12:010, 2019. doi: 10.1088/1475-7516/2019/12/010.
- A. Kartavtsev, G. Raffelt, and H. Vogel. Extragalactic photon-ALP conversion at CTA energies. *J. Cosmology Astropart. Phys.*, 1:024, Jan. 2017. doi: 10.1088/1475-7516/2017/01/024.
- N. Kelley-Hoskins. The veritas dark matter and astroparticle physics program, 2018.
- T. W. Kephart and T. J. Weiler. Magnetic monopoles as the highest energy cosmic ray primaries. *Astropart. Phys.*, 4:271–279, 1996. doi: 10.1016/0927-6505(95)00043-7.
- M. Yu. Khlopov. Primordial Black Holes. *Res. Astron. Astrophys.*, 10:495–528, 2010. doi: 10.1088/1674-4527/10/6/001.
- V. V. Khoze and G. Ro. Dark matter monopoles, vectors and photons. *JHEP*, 10:061, 2014. doi: 10.1007/JHEP10(2014)061.
- N. Klop, F. Zandanel, K. Hayashi, and S. Ando. Impact of axisymmetric mass models for dwarf spheroidal galaxies on indirect dark matter searches. *Phys. Rev. D*, 95(12):123012, 2017. doi: 10.1103/PhysRevD.95.123012.
- A. A. Klypin, A. V. Kravtsov, O. Valenzuela, and F. Prada. Where are the missing galactic satellites? *ApJ*, 522:82–92, 1999. doi: 10.1086/307643.
- S. M. Koushiappas, J. S. Bullock, and A. Dekel. Massive black hole seeds from low angular momentum material. *Mon. Not. Roy. Astron. Soc.*, 354:292, 2004. doi: 10.1111/j.1365-2966.2004.08190.x.
- F. Krennrich, S. L. Bohec, and T. C. Weekes. Detection techniques of microsecond gamma-ray bursts using ground-based telescopes. *The Astrophysical Journal*, 529(1):506, 2000. URL <http://stacks.iop.org/0004-637X/529/i=1/a=506>.
- M. Kuhlen, M. Vogelsberger, and R. Angulo. Numerical Simulations of the Dark Universe: State of the Art and the Next Decade. *Phys. Dark Univ.*, 1:50–93, 2012. doi: 10.1016/j.dark.2012.10.002.
- R. Laha, J. B. Muñoz, and T. R. Slatyer. Integral constraints on primordial black holes and particle dark matter. *Physical Review D*, 101(12), Jun 2020. ISSN 2470-0029. doi: 10.1103/physrevd.101.123514. URL <http://dx.doi.org/10.1103/PhysRevD.101.123514>.
- R. R. Lane, L. L. Kiss, G. F. Lewis, R. A. Ibata, A. Siebert, T. R. Bedding, P. Szekely, Z. Balog, and G. M. Szabo. Halo globular clusters observed with AAOmega: dark matter content, metallicity and tidal heating. *Mon. Not. Roy. Astron. Soc.*, 406:2732–2742, 2010. doi: 10.1111/j.1365-2966.2010.16874.x.
- P. Langacker, R. D. Peccei, and T. Yanagida. Invisible Axions and Light Neutrinos. Are they Connected? *Modern Physics Letters A*, 1:541–552, 1986. doi: 10.1142/S0217732386000683.
- A. Lazar et al. A dark matter profile to model diverse feedback-induced core sizes of Λ CDM haloes. *Mon. Not. Roy. Astron. Soc.*, 497(2):2393–2417, 2020. doi: 10.1093/mnras/staa2101.

- S. LeBohec, F. Krennrich, and G. Slegee. SGARFACE: A Novel detector for microsecond gamma ray bursts. *Astropart. Phys.*, 23:235–248, 2005. doi: 10.1016/j.astropartphys.2005.01.003.
- J. LeyVa et al. Exploring MeV gamma rays from dark matter annihilation and evaporating primordial black holes in the GRAMS experiment. Number Icrc, page 552, 2021. doi: 10.22323/1.395.0552.
- Y.-F. Liang, C. Zhang, Z.-Q. Xia, L. Feng, Q. Yuan, and Y.-Z. Fan. Constraints on axion-like particle properties with TeV gamma-ray observations of Galactic sources. *JCAP*, 06:042, 2019. doi: 10.1088/1475-7516/2019/06/042.
- E. T. Linton et al. A new search for primordial black hole evaporations using the Whipple gamma-ray telescope. *JCAP*, 0601:013, 2006. doi: 10.1088/1475-7516/2006/01/013.
- M. Lisanti. Lectures on Dark Matter Physics. In *New Front. Fields Strings*, pages 399–446. WORLD SCIENTIFIC, jan 2017. ISBN 978-981-314-943-4. doi: 10.1142/9789813149441_0007. URL <http://arxiv.org/abs/1603.03797>http://dx.doi.org/10.1142/9789813149441_{_}0007https://www.worldscientific.com/doi/abs/10.1142/9789813149441_{_}0007.
- G. Long, S. Chen, S. Xu, and H.-H. Zhang. Probing μeV ALPs with future LHAASO observation of AGN γ -ray spectra. 1 2021.
- R. López-Coto, M. Doro, A. de Angelis, M. Mariotti, and J. P. Harding. Prospects for the Observation of Primordial Black Hole evaporation with the Southern Wide Field of View Gamma-ray Observatory. 3 2021. doi: 10.1088/1475-7516/2021/08/040.
- J. H. MacGibbon, T. N. Ukwatta, J. T. Linnemann, S. S. Marinelli, D. Stump, and K. Tollefson. Primordial Black Holes. In *5th International Fermi Symposium Nagoya, Japan, October 20-24, 2014*, 2015. URL <https://inspirehep.net/record/1347228/files/arXiv:1503.01166.pdf>.
- P. Madau and M. J. Rees. Massive black holes as Population III remnants. *Astrophys. J. Lett.*, 551:L27–L30, 2001. doi: 10.1086/319848.
- C. Maggio, D. Kerszberg, D. Ninci, and V. Vitale. Upper limits on the WIMP annihilation cross section from a joint analysis of dwarf spheroidal satellite galaxy observations with the MAGIC telescopes. *PoS, ICRC2021*:512, 2021. doi: 10.22323/1.395.0512.
- J. Majumdar, F. Calore, and D. Horns. Search for gamma-ray spectral modulations in Galactic pulsars. *J. Cosmology Astropart. Phys.*, 4:048, Apr. 2018. doi: 10.1088/1475-7516/2018/04/048.
- D. Malyshev, A. Neronov, D. Semikoz, A. Santangelo, and J. Jochum. Improved limit on axion-like particles from gamma-ray data on Perseus cluster. *ArXiv e-prints*, May 2018.
- S. Mashchenko and A. Sills. Globular clusters with dark matter halos. 1. Initial relaxation. *Astrophys. J.*, 619:243, 2005a. doi: 10.1086/426132.
- S. Mashchenko and A. Sills. Globular clusters with dark matter halos. 2. Evolution in tidal field. *Astrophys. J.*, 619:258, 2005b. doi: 10.1086/426133.

- J. F. Meekins, G. Fritz, T. A. Chubb, H. Friedman, and R. C. Henry. Physical Sciences: X-rays from the Coma Cluster of Galaxies. *Nature*, 231:107, may 1971.
- O. Mena and S. Razzaque. Hints of an axion-like particle mixing in the GeV gamma-ray blazar data? *Journal of Cosmology and Astroparticle Physics*, 11:023, Nov. 2013. doi: 10.1088/1475-7516/2013/11/023.
- M. Meyer and J. Conrad. Sensitivity of the Cherenkov Telescope Array to the detection of axion-like particles at high gamma-ray opacities. *J. Cosmology Astropart. Phys.*, 12:016, Dec. 2014. doi: 10.1088/1475-7516/2014/12/016.
- M. Meyer, D. Horns, and M. Raue. First lower limits on the photon-axion-like particle coupling from very high energy gamma-ray observations. *Phys. Rev. D*, 87(3):035027, Feb. 2013. doi: 10.1103/PhysRevD.87.035027.
- M. Milgrom. A modification of the Newtonian dynamics as a possible alternative to the hidden mass hypothesis. *ApJ*, 270:365–370, July 1983. doi: 10.1086/161130.
- N. Mirabal, V. Frías-Martínez, T. Hassan, and E. Frías-Martínez. Fermi’s SIBYL: mining the gamma-ray sky for dark matter subhaloes. *MNRAS*, 424:L64–L68, July 2012. doi: 10.1111/j.1745-3933.2012.01287.x.
- N. Mirabal, E. Charles, E. C. Ferrara, P. L. Gonthier, A. K. Harding, M. A. Sánchez-Conde, and D. J. Thompson. 3FGL Demographics Outside the Galactic Plane using Supervised Machine Learning: Pulsar and Dark Matter Subhalo Interpretations. *ApJ*, 825:69, July 2016. doi: 10.3847/0004-637X/825/1/69.
- A. Mirizzi and D. Montanino. Stochastic conversions of TeV photons into axion-like particles in extragalactic magnetic fields. *J. Cosmology Astropart. Phys.*, 12:004, Dec. 2009. doi: 10.1088/1475-7516/2009/12/004.
- A. Mirizzi, G. G. Raffelt, and P. D. Serpico. Photon-axion conversion as a mechanism for supernova dimming: Limits from CMB spectral distortion. *Phys. Rev. D*, 72(2):023501, July 2005. doi: 10.1103/PhysRevD.72.023501.
- A. Mirizzi, G. G. Raffelt¹, and P. D. Serpico. Photon-Axion Conversion in Intergalactic Magnetic Fields and Cosmological Consequences. In M. Kuster, G. Raffelt, and B. Beltrán, editors, *Axions*, volume 741 of *Lecture Notes in Physics*, Berlin Springer Verlag, page 115, 2008.
- A. Moliné, M. A. Sánchez-Conde, S. Palomares-Ruiz, and F. Prada. Characterization of subhalo structural properties and implications for dark matter annihilation signals. *Mon. Not. Roy. Astron. Soc.*, 466(4):4974–4990, 2017. doi: 10.1093/mnras/stx026.
- A. Montanari, E. Moulin, and D. Malyshev. Search for dark matter annihilation signals from the Galactic Center with the H.E.S.S. Inner Galaxy Survey. *PoS, ICRC2021*:511, 2021.
- B. Moore, S. Ghigna, F. Governato, G. Lake, T. R. Quinn, J. Stadel, and P. Tozzi. Dark matter substructure within galactic halos. *Astrophys. J.*, 524:L19–L22, 1999. doi: 10.1086/312287.
- M. Nagayama, J. Sato, Y. Takanishi, and K. Tsunemi. Sensitivity of indirect detection of Neutralino dark matter by Sommerfeld enhancement mechanism. 2 2021.

- J. F. Navarro, C. S. Frenk, and S. D. M. White. The Structure of cold dark matter halos. *Astrophys. J.*, 462:563–575, 1996. doi: 10.1086/177173.
- J. F. Navarro, E. Hayashi, C. Power, A. R. Jenkins, C. S. Frenk, S. D. M. White, V. Springel, J. Stadel, and T. R. Quinn. The inner structure of Λ CDM haloes - III. Universality and asymptotic slopes. *MNRAS*, 349(3):1039–1051, Apr. 2004. doi: 10.1111/j.1365-2966.2004.07586.x.
- D. Nieto, J. Aleksić, J. A. Barrio, J. L. Contreras, M. Doro, S. Lombardi, N. Mirabal, A. Moralejo, S. Pardo, J. Rico, F. Zandanel, and for the MAGIC Collaboration. The search for galactic dark matter clump candidates with Fermi and MAGIC. *arXiv e-prints*, art. arXiv:1109.5935, Sep 2011a.
- D. Nieto, V. Martínez, N. Mirabal, J. A. Barrio, K. Satalecka, S. Pardo, and I. Lozano. A search for possible dark matter subhalos as IACT targets in the First Fermi-LAT Source Catalog. *arXiv e-prints*, art. arXiv:1110.4744, Oct 2011b.
- D. f. Nieto. Hunting for dark matter subhalos among the Fermi-LAT sources with VERITAS. *arXiv e-prints*, Aug. 2015.
- D. Ninci, T. Inada, J. Rico, D. Kerszberg, M. Doro, M. Vazquez Acosta, S. Lombardi, C. Maggio, and M. Hüthen. Searching for Dark Matter decay signals in the Galactic Halo with the MAGIC telescopes. *PoS, ICRC2019:538*, 2019. doi: 10.22323/1.358.0538.
- P. L. Nolan, A. A. Abdo, M. Ackermann, M. Ajello, A. Allafort, E. Antolini, W. B. Atwood, M. Axelsson, L. Baldini, J. Ballet, and et al. Fermi Large Area Telescope Second Source Catalog. *ApJS*, 199:31, Apr. 2012. doi: 10.1088/0067-0049/199/2/31.
- A. Obertacke Pollmann. Luminescence of water or ice as a new detection method for magnetic monopoles. *EPJ Web Conf.*, 164:07019, 2017. doi: 10.1051/epjconf/201716407019.
- S. Ogawa. Observation of Optical Transients and Search for PeV-EeV Tau Neutrinos with Ashra-1. *PoS, ICRC2019:970*, 2020. doi: 10.22323/1.358.0970.
- A. V. Olinto et al. The POEMMA (Probe of Extreme Multi-Messenger Astrophysics) Observatory. 12 2020.
- A. N. Otte. Studies of an air-shower imaging system for the detection of ultrahigh-energy neutrinos. *Phys. Rev. D*, 99(8):083012, 2019. doi: 10.1103/PhysRevD.99.083012.
- H. Pagels and J. R. Primack. Supersymmetry, Cosmology and New TeV Physics. *Phys. Rev. Lett.*, 48:223, 1982. doi: 10.1103/PhysRevLett.48.223.
- E. N. Parker. The Origin of Magnetic Fields. *ApJ*, 160:383, May 1970. doi: 10.1086/150442.
- L. Patrizii and M. Spurio. Status of Searches for Magnetic Monopoles. *Ann. Rev. Nucl. Part. Sci.*, 65:279–302, 2015. doi: 10.1146/annurev-nucl-102014-022137.
- R. D. Peccei and H. R. R. D. Quinn. CP conservation in the presence of pseudoparticles. *Phys. Rev. Letter*, 38:1440–1443, June 1977. doi: 10.1103/PhysRevLett.38.1440.
- J. S. Perkins et al. TeV gamma-ray observations of the perseus and abell 2029 galaxy clusters. *ApJ*, 644:148–154, 2006. doi: 10.1086/503321.

- K. Pfrang. Deep Learning Transient Detection with VERITAS. *PoS, ICRC2021*:822, 2021. doi: 10.22323/1.395.0822.
- K. Pfrang, T. Hassan, and E. Pueschel. Optical Microlensing by Primordial Black Holes with IACTs. *PoS, ICRC2021*:495, 2021. doi: 10.22323/1.395.0495.
- A. Pinzke et al. Prospects of detecting gamma-ray emission from galaxy clusters: cosmic rays and dark matter annihilations. *Phys. Rev. D*, 84:123509, 2011.
- H. Poincare. *Astronomie*, 158, 1906.
- A. Polyakov. *JETP Lett.*, 20, 1974.
- N. A. Porter and T. C. Weekes. A search for high energy gamma-ray bursts from primordial black holes or other astronomical objects. *Monthly Notices of the Royal Astronomical Society*, 183(2): 205–210, 1978. doi: 10.1093/mnras/183.2.205. URL <http://dx.doi.org/10.1093/mnras/183.2.205>.
- T. Porter and N. A. Weekes. Upper limits for gamma-ray bursts from primordial black holes. 277: 199, 1979.
- J. Preskill. Magnetic monopoles. *Ann. Rev. Nucl. Part. Sci.*, 34:461, 1984.
- J. R. Primack and M. A. K. Gross. Hot dark matter in cosmology. 7 2000.
- S. Profumo. TASI 2012 Lectures on Astrophysical Probes of Dark Matter. In *Search. New Phys. Small Large Scales*, pages 143–189. WORLD SCIENTIFIC, nov 2013. ISBN 978-981-4525-21-3. doi: 10.1142/9789814525220.0004. URL <http://arxiv.org/abs/1301.0952>http://www.worldscientific.com/doi/abs/10.1142/9789814525220_{_}0004.
- S. Profumo. *An Introduction to Particle Dark Matter*. 2017. doi: 10.1142/Q0001.
- A. Raccanelli, F. Vidotto, and L. Verde. Effects of primordial black holes quantum gravity decay on galaxy clustering. 2017.
- A. Ray, R. Laha, J. B. Muñoz, and R. Caputo. Near future MeV telescopes can discover asteroid-mass primordial black hole dark matter. *Phys. Rev. D*, 104(2):023516, 2021. doi: 10.1103/PhysRevD.104.023516.
- J. I. Read, M. I. Wilkinson, N. W. Evans, G. Gilmore, and J. T. Kleyana. The importance of tides for the Local Group dwarf spheroidals. *MNRAS*, 367:387–399, Mar. 2006. doi: 10.1111/j.1365-2966.2005.09959.x.
- J. I. Read, M. G. Walker, and P. Steger. Dark matter heats up in dwarf galaxies. *Mon. Not. Roy. Astron. Soc.*, 484(1):1401–1420, 2019. doi: 10.1093/mnras/sty3404.
- M. Regis et al. The EMU view of the Large Magellanic Cloud: Troubles for sub-TeV WIMPs. 6 2021.
- J. Rico. Gamma-Ray Dark Matter Searches in Milky Way Satellites—A Comparative Review of Data Analysis Methods and Current Results. *Galaxies*, 8(1):25, 2020. doi: 10.3390/galaxies8010025.

- L. Rinchuso, N. L. Rodd, I. Moul, E. Moulin, M. Baumgart, T. Cohen, T. R. Slatyer, I. W. Stewart, and V. Vaidya. Hunting for Heavy Winos in the Galactic Center. *Phys. Rev. D*, 98(12): 123014, 2018. doi: 10.1103/PhysRevD.98.123014.
- M. Rocha, A. H. G. Peter, J. S. Bullock, M. Kaplinghat, S. Garrison-Kimmel, J. Onorbe, and L. A. Moustakas. Cosmological Simulations with Self-Interacting Dark Matter I: Constant Density Cores and Substructure. *Mon. Not. Roy. Astron. Soc.*, 430:81–104, 2013. doi: 10.1093/mnras/sts514.
- V. A. Rubakov. Adler-bell-jackiw anomaly and fermion-number breaking in the presence of a magnetic monopole. *Nuclear Physics B*, 203(2):311 – 348, 1982. ISSN 0550-3213. doi: [https://doi.org/10.1016/0550-3213\(82\)90034-7](https://doi.org/10.1016/0550-3213(82)90034-7).
- V. C. Rubin, W. K. Ford, Jr., and N. Thonnard. Extended rotation curves of high-luminosity spiral galaxies. IV - Systematic dynamical properties, SA through SC. *ApJL*, 225:L107–L111, Nov. 1978. doi: 10.1086/182804.
- V. C. Rubin, N. Thonnard, and W. K. Ford, Jr. Rotational properties of 21 SC galaxies with a large range of luminosities and radii, from NGC 4605 / $R = 4\text{kpc}$ / to UGC 2885 / $R = 122\text{kpc}$ /. *Astrophys. J.*, 238:471, 1980. doi: 10.1086/158003.
- G. I. Rubtsov and S. V. Troitsky. Breaks in gamma-ray spectra of distant blazars and transparency of the Universe. *Soviet Journal of Experimental and Theoretical Physics Letters*, 100:355–359, Nov. 2014. doi: 10.1134/S0021364014180088.
- G. S. and Z. Y. *JETP Lett*, 4:120, 1966.
- D. A. Sanchez, S. Fegan, and B. Giebels. Evidence for a cosmological effect in gamma-ray spectra of BL Lacertae. *A&A*, 554:A75, June 2013. doi: 10.1051/0004-6361/201220631.
- M. A. Sánchez-Conde and F. Prada. The flattening of the concentration–mass relation towards low halo masses and its implications for the annihilation signal boost. *Mon. Not. Roy. Astron. Soc.*, 442(3):2271–2277, 2014. doi: 10.1093/mnras/stu1014.
- M. A. Sánchez-Conde, D. Paneque, E. Bloom, F. Prada, and A. Domínguez. Hints of the existence of axionlike particles from the gamma-ray spectra of cosmological sources. *Phys. Rev. D*, 79(12): 123511, June 2009. doi: 10.1103/PhysRevD.79.123511.
- M. A. Sanchez-Conde, S. Funk, F. Krennrich, and A. Weinstein. The hunt for axionlike particles with the Cherenkov Telescope Array. *ArXiv e-prints*, May 2013.
- M.-A. Sanchez-Conde et al. Dark matter searches with Cherenkov telescopes: nearby dwarf galaxies or local galaxy clusters? *J. Cosmology Astropart. Phys.*, 1112:011, 2011. doi: 10.1088/1475-7516/2011/12/011.
- R. H. Sanders. *The Dark Matter Problem*. 2014.
- M. Sasaki, T. Suyama, T. Tanaka, and S. Yokoyama. Primordial black holes—perspectives in gravitational wave astronomy. *Class. Quant. Grav.*, 35(6):063001, 2018. doi: 10.1088/1361-6382/aaa7b4.

- T. Sawala, C. S. Frenk, A. Fattahi, J. F. Navarro, R. G. Bower, R. A. Crain, C. Dalla Vecchia, M. Furlong, A. Jenkins, I. G. McCarthy, Y. Qu, M. Schaller, J. Schaye, and T. Theuns. Bent by baryons: the low-mass galaxy-halo relation. *MNRAS*, 448(3):2941–2947, Apr. 2015. doi: 10.1093/mnras/stu2753.
- D. Schoonenberg, J. Gaskins, G. Bertone, and J. Diemand. Dark matter subhalos and unidentified sources in the Fermi 3FGL source catalog. *J. Cosmology Astropart. Phys.*, 5:028, May 2016. doi: 10.1088/1475-7516/2016/05/028.
- M. Schroedter et al. Search for Short Bursts of Gamma Rays Above 100 MeV from the Crab using VERITAS and SGARFACE. *ArXiv e-prints*, Aug. 2009.
- M. Schumann. Direct Detection of WIMP Dark Matter: Concepts and Status. *J. Phys. G*, 46(10): 103003, 2019. doi: 10.1088/1361-6471/ab2ea5.
- J. Schwinger. A Magnetic Model of Matter. *Science*, 165:757–761, Aug. 1969. doi: 10.1126/science.165.3895.757.
- Y. M. Shnir. *Magnetic Monopoles*. Text and Monographs in Physics. Springer, Berlin/Heidelberg, 2005. ISBN 9783540252771, 9783540290827. doi: 10.1007/3-540-29082-6.
- P. Sikivie. Experimental tests of the 'invisible' axion. *Phys. Rev. Letter*, 51:1415–1417, Oct. 1983. doi: 10.1103/PhysRevLett.51.1415.
- P. Sikivie. Axion Cosmology. In M. Kuster, G. Raffelt, and B. Beltrán, editors, *Axions*, volume 741 of *Lecture Notes in Physics*, Berlin Springer Verlag, page 19, 2008.
- M. Simet, D. Hooper, and P. D. Serpico. Milky Way as a kiloparsec-scale axionscope. *Physical Review D*, 77(6):063001, Mar. 2008. doi: 10.1103/PhysRevD.77.063001.
- T. Sjostrand, S. Mrenna, and P. Z. Skands. PYTHIA 6.4 Physics and Manual. *JHEP*, 05:026, 2006. doi: 10.1088/1126-6708/2006/05/026.
- G. Spengler. Signatures of ultrarelativistic magnetic monopoles in imaging cherenkov telescopes. Master's thesis, Humboldt-University of Berlin, 2009.
- G. Spengler and U. Schwanke. Signatures of ultrarelativistic magnetic monopoles in imaging atmospheric cherenkov telescopes. In *Proceedings to the 32nd ICRC*, Oct. 2011.
- V. Springel, J. Wang, M. Vogelsberger, A. Ludlow, A. Jenkins, A. Helmi, J. F. Navarro, C. S. Frenk, and S. D. M. White. The Aquarius Project: the subhalos of galactic halos. *Mon. Not. Roy. Astron. Soc.*, 391:1685–1711, 2008a. doi: 10.1111/j.1365-2966.2008.14066.x.
- V. Springel et al. The Aquarius Project: the subhaloes of galactic haloes. *MNRAS*, 391:1685–1711, 2008b. doi: 10.1111/j.1365-2966.2008.14066.x.
- J. Stadel, D. Potter, B. Moore, J. Diemand, P. Madau, M. Zemp, M. Kuhlen, and V. Quilis. Quantifying the heart of darkness with GHALO - a multibillion particle simulation of a galactic halo. *MNRAS*, 398:L21–L25, Sept. 2009. doi: 10.1111/j.1745-3933.2009.00699.x.

- F. W. Stecker and S. T. Scully. Is the Universe More Transparent to Gamma Rays Than Previously Thought? *The Astrophysical Journal Letters*, 691:L91–L94, Feb. 2009. doi: 10.1088/0004-637X/691/2/L91.
- F. W. Stecker, M. G. Baring, and E. J. Summerlin. Blazar gamma-Rays, Shock Acceleration, and the Extragalactic Background Light. *The Astrophysical Journal Letters*, 667:L29–L32, Sept. 2007. doi: 10.1086/522005.
- G. Steigman, B. Dasgupta, and J. F. Beacom. Precise Relic WIMP Abundance and its Impact on Searches for Dark Matter Annihilation. *Phys. Rev.*, D86:023506, 2012. doi: 10.1103/PhysRevD.86.023506.
- L. E. Strigari. Galactic Searches for Dark Matter. 2012. *Phys. Rev. D*.
- L. E. Strigari. Galactic searches for dark matter. *Physics Reports*, 531:1–88, Oct. 2013. doi: 10.1016/j.physrep.2013.05.004.
- L. E. Strigari. Dark matter in dwarf spheroidal galaxies and indirect detection: a review. *Rept. Prog. Phys.*, 81(5):056901, 2018. doi: 10.1088/1361-6633/aaae16.
- L. E. Strigari, S. M. Koushiappas, J. S. Bullock, and M. Kaplinghat. Precise constraints on the dark matter content of MilkyWay dwarf galaxies for gamma-ray experiments. *Phys.Rev.D*, 75(8):083526, Apr. 2007. doi: 10.1103/PhysRevD.75.083526.
- L. E. Strigari et al. A common mass scale for satellite galaxies of the Milky Way. *Nature*, 454:1096–1097, 2008.
- E. Tamm and M. Frank. *Dokl. Akad. Nauk SSSR (Akad. of Science of the USSR)*, 14:107, 1937.
- N. Tamura, N. Takato, A. Shimono, Y. Moritani, K. Yabe, Y. Ishizuka, Y. Kamata, A. Ueda, H. Aghazarian, S. Arnouts, R. H. Barkhouser, P. Balard, R. Barette, M. Belhadi, J. A. Burnham, N. Caplar, M. A. Carr, P.-Y. Chabaud, Y.-C. Chang, H.-Y. Chen, C.-Y. Chou, Y.-H. Chu, J. G. Cohen, R. P. de Almeida, A. C. de Oliveira, L. S. de Oliveira, R. G. Dekany, K. Dohlen, J. B. dos Santos, L. H. dos Santos, R. S. Ellis, M. Fabricius, D. Ferreira, H. Furusawa, J. Garcia-Carpio, M. Golebiowski, J. Gross, J. E. Gunn, R. Hammond, A. Harding, M. Hart, T. M. Heckman, P. T. P. Ho, S. C. Hope, D. J. Hover, S.-F. Hsu, Y.-S. Hu, P.-J. Huang, S. Jamal, M. Jaquet, E. Jeschke, Y. Jing, E. Kado-Fong, J. L. Karr, M. Kimura, M. E. King, M. Koike, E. Komatsu, V. Le Brun, O. Le Fèvre, A. Le Fur, D. Le Mignant, H.-H. Ling, C. P. Loomis, R. H. Lupton, F. Madec, P. H. Mao, D. Marchesini, L. S. Marrara, D. Medvedev, S. Mineo, Y. Minowa, H. Murayama, G. J. Murray, Y. Ohyama, M. Onodera, J. Orndorff, S. Pascal, J. Peebles, G. Perrot, R. Pourcelot, D. J. Reiley, M. Reinecke, M. Roberts, J. A. Rosa, J. Rousselle, A. Schmitt, M. A. Schwochert, M. D. Seiffert, H. Siddiqui, S. A. Smee, L. Sodré, A. J. Steinkraus, M. A. Strauss, C. Surace, P. J. Tait, M. Takada, T. Tamura, M. Tanaka, Y. Tanaka, A. R. Thakar, O. Verducci, D. Vibert, S.-Y. Wang, Z. Wang, C.-Y. Wen, S. Werner, Y. Yamada, C.-H. Yan, N. Yasuda, H. Yoshida, and M. Yoshida. Prime Focus Spectrograph (PFS) for the Subaru telescope: ongoing integration and future plans. In C. J. Evans, L. Simard, and H. Takami, editors, *Ground-based and Airborne Instrumentation for Astronomy VII*, volume 10702 of *Society of Photo-Optical Instrumentation Engineers (SPIE) Conference Series*, page 107021C, July 2018. doi: 10.1117/12.2311871.

- M. Tanabashi and others. Review of particle physics. *Phys. Rev. D*, 98:030001, Aug 2018. doi: 10.1103/PhysRevD.98.030001. URL <https://link.aps.org/doi/10.1103/PhysRevD.98.030001>.
- F. Tavecchio, M. Roncadelli, G. Galanti, and G. Bonnoli. Evidence for an axion-like particle from PKS 1222+216? *Phys. Rev. D*, 86:085036, Oct 2012. doi: 10.1103/PhysRevD.86.085036.
- T. Tavernier, J.-F. Glicenstein, and F. Brun. Search for Primordial Black Hole evaporations with H.E.S.S. *PoS, ICRC2019:804*, 2019. doi: 10.22323/1.358.0804.
- T. Tavernier, F. Brun, J.-F. Glicenstein, and V. Marandon. Limits on primordial black hole evaporation from H.E.S.S. observations. *PoS, ICRC2021:518*, 2021.
- M. Tluczykont, D. Hampf, D. Horns, D. Spitschan, L. Kuzmichev, V. Prosin, C. Spiering, and R. Wischnewski. The HiSCORE concept for gamma-ray and cosmic-ray astrophysics beyond 10 TeV. *Astroparticle Physics*, 56:42–53, Apr. 2014. doi: 10.1016/j.astropartphys.2014.03.004.
- E. J. Tollerud, J. S. Bullock, L. E. Strigari, and B. Willman. Hundreds of Milky Way Satellites? Luminosity Bias in the Satellite Luminosity Function. *Astrophys. J.*, 688:277–289, 2008. doi: 10.1086/592102.
- E. Tollet et al. NIHAO – IV: core creation and destruction in dark matter density profiles across cosmic time. *Mon. Not. Roy. Astron. Soc.*, 456(4):3542–3552, 2016. doi: 10.1093/mnras/stv2856. [Erratum: *Mon.Not.Roy.Astron.Soc.* 487, 1764 (2019)].
- M. Tomozeiu, L. Mayer, and T. Quinn. TIDAL STIRRING OF SATELLITES WITH SHALLOW DENSITY PROFILES PREVENTS THEM FROM BEING TOO BIG TO FAIL. *The Astrophysical Journal*, 827(1):L15, aug 2016. doi: 10.3847/2041-8205/827/1/L15. URL <https://doi.org/10.3847%2F2041-8205%2F827%2F1%2FL15>.
- D. R. Tompkins. Total energy loss and Čerenkov emission from monopoles. *Phys. Rev.*, 138: B248–B250, Apr 1965.
- S. Tulin and H.-B. Yu. Dark Matter Self-interactions and Small Scale Structure. *Phys. Rept.*, 730: 1–57, 2018. doi: 10.1016/j.physrep.2017.11.004.
- K. Ueno et al. Search for GUT monopoles at Super-Kamiokande. *Astropart. Phys.*, 36:131–136, 2012. doi: 10.1016/j.astropartphys.2012.05.008.
- L. Visinelli and P. Gondolo. Axion cold dark matter in nonstandard cosmologies. *Phys. Rev. D*, 81(6):063508, Mar. 2010. doi: 10.1103/PhysRevD.81.063508.
- G. Voit. Tracing cosmic evolution with clusters of galaxies. *Rev.Mod.Phys.*, 77:207–258, 2005. doi: 10.1103/RevModPhys.77.207.
- A. Wagner, G. Rybka, M. Hotz, L. J. Rosenberg, S. J. Asztalos, G. Carosi, C. Hagmann, D. Kinion, K. van Bibber, J. Hoskins, C. Martin, P. Sikivie, D. B. Tanner, R. Bradley, and J. Clarke. Search for Hidden Sector Photons with the ADMX Detector. *Phys. Rev. Letter*, 105(17):171801, Oct. 2010. doi: 10.1103/PhysRevLett.105.171801.
- J. Wang, S. Bose, C. S. Frenk, L. Gao, A. Jenkins, V. Springel, and S. D. M. White. Universal structure of dark matter haloes over a mass range of 20 orders of magnitude. *Nature*, 585(7823): 39–42, 2020. doi: 10.1038/s41586-020-2642-9.

- O. Wantz and E. P. S. Shellard. Axion cosmology revisited. *Physical Review D*, 82(12):123508, Dec. 2010. doi: 10.1103/PhysRevD.82.123508.
- S. Weinberg. A new light boson? *Phys. Rev. Letter*, 40:223–226, Jan. 1978. doi: 10.1103/PhysRevLett.40.223.
- S. D. M. White, C. S. Frenk, and M. Davis. Clustering in a Neutrino Dominated Universe. *Astrophys. J. Lett.*, 274:L1–L5, 1983. doi: 10.1086/161425.
- S. Wick, T. Kephart, T. Weiler, and B. P.L. *Astropart. Phys.*, 18:663, 2003.
- F. Wilczek. Problem of strong P and T invariance in the presence of instantons. *Phys. Rev. Letter*, 40:279–282, Jan. 1978. doi: 10.1103/PhysRevLett.40.279.
- F. Wilczek. Axions and family symmetry breaking. *Physical Review Letters*, 49:1549–1552, Nov. 1982. doi: 10.1103/PhysRevLett.49.1549.
- E. Witten. Some properties of O(32) superstrings. *Physics Letters B*, 149:351–356, Dec. 1984. doi: 10.1016/0370-2693(84)90422-2.
- M. Wood et al. A Search for Dark Matter Annihilation with the Whipple 10m Telescope. *ApJ*, 678:594, 2008.
- D. Wouters and P. Brun. Constraints on Axion-like Particles from X-Ray Observations of the Hydra Galaxy Cluster. *ApJ*, 772:44, July 2013. doi: 10.1088/0004-637X/772/1/44.
- Z.-Q. Xia, C. Zhang, Y.-F. Liang, L. Feng, Q. Yuan, Y.-Z. Fan, and J. Wu. Searching for spectral oscillations due to photon-axionlike particle conversion using the Fermi-LAT observations of bright supernova remnants. *Phys. Rev. D*, 97(6):063003, Mar. 2018. doi: 10.1103/PhysRevD.97.063003.
- Z.-Q. Xia, Y.-F. Liang, L. Feng, Q. Yuan, Y.-Z. Fan, and J. Wu. Searching for the possible signal of the photon-axionlike particle oscillation in the combined GeV and TeV spectra of supernova remnants. *Phys. Rev. D*, 100(12):123004, 2019. doi: 10.1103/PhysRevD.100.123004.
- D. G. York et al. The Sloan Digital Sky Survey: Technical Summary. *Astrophysical Journal*, 120:1579–1587, Sept. 2000. doi: 10.1086/301513.
- J. Zavala and N. Afshordi. Universal clustering of dark matter in phase space. *Mon. Not. Roy. Astron. Soc.*, 457(1):986–992, 2016. doi: 10.1093/mnras/stw048.
- E. Zavattini, G. Zavattini, G. Ruoso, E. Polacco, E. Milotti, M. Karuza, U. Gastaldi, G. di Domenico, F. Della Valle, R. Cimino, S. Carusotto, G. Cantatore, and M. Bregant. Experimental Observation of Optical Rotation Generated in Vacuum by a Magnetic Field. *Phys. Rev. Letter*, 96(11):110406, Mar. 2006. doi: 10.1103/PhysRevLett.96.110406.
- E. Zavattini, G. Zavattini, G. Ruoso, G. Raiteri, E. Polacco, E. Milotti, V. Lozza, M. Karuza, U. Gastaldi, G. di Domenico, F. Della Valle, R. Cimino, S. Carusotto, G. Cantatore, and M. Bregant. New PVLAS results and limits on magnetically induced optical rotation and ellipticity in vacuum. *Phys. Rev. D*, 77(3):032006, Feb. 2008. doi: 10.1103/PhysRevD.77.032006.

- H.-S. Zechlin and D. Horns. Unidentified sources in the Fermi-LAT second source catalog: the case for DM subhalos. *J. Cosmology Astropart. Phys.*, 11:050, Nov. 2012. doi: 10.1088/1475-7516/2012/11/050.
- H.-S. Zechlin, M. V. Fernandes, D. Elsässer, and D. Horns. Dark matter subhaloes as gamma-ray sources and candidates in the first Fermi-LAT catalogue. *A&A*, 538:A93, Feb. 2012. doi: 10.1051/0004-6361/201117655.
- Y. B. Zel'dovich and I. Novikov. *Sov. Astron.*, 10:602, 1967.
- C. Zhang, Y.-F. Liang, S. Li, N.-H. Liao, L. Feng, Q. Yuan, Y.-Z. Fan, and Z.-Z. Ren. New bounds on axionlike particles from the Fermi Large Area Telescope observation of PKS 2155-304. *Phys. Rev. D*, 97(6):063009, Mar. 2018. doi: 10.1103/PhysRevD.97.063009.
- H. Zhao. Analytical models for galactic nuclei. *Mon. Not. Roy. Astron. Soc.*, 278:488–496, 1996. doi: 10.1093/mnras/278.2.488.
- K. Zioutas, S. Andriamonje, V. Arsov, S. Aune, D. Autiero, F. T. Avignone, K. Barth, A. Belov, B. Beltrán, H. Bräuninger, J. M. Carmona, S. Cebrián, E. Chesi, J. I. Collar, R. Creswick, T. Dafni, M. Davenport, L. di Lella, C. Eleftheriadis, J. Englhauser, G. Fanourakis, H. Farach, E. Ferrer, H. Fischer, J. Franz, P. Friedrich, T. Gerasis, I. Giomataris, S. Gninenko, N. Golubev, M. D. Hasinoff, F. H. Heinsius, D. H. Hoffmann, I. G. Irastorza, J. Jacoby, D. Kang, K. Königsmann, R. Kotthaus, M. Krčmar, K. Kousouris, M. Kuster, B. Lakić, C. Lasseur, A. Liolios, A. Ljubičić, G. Lutz, G. Luzón, D. W. Miller, A. Morales, J. Morales, M. Mutterer, A. Nikolaidis, A. Ortiz, T. Papaevangelou, A. Placci, G. Raffelt, J. Ruz, H. Riege, M. L. Sarsa, I. Savvidis, W. Serber, P. Serpico, Y. Semertzidis, L. Stewart, J. D. Vieira, J. Villar, L. Walckiers, and K. Zachariadou. First Results from the CERN Axion Solar Telescope. *Phys. Rev. Letter*, 94(12):121301, Apr. 2005. doi: 10.1103/PhysRevLett.94.121301.
- F. Zwicky. *Helvetica Physica Acta*, 6:110, 1933.
- G. 't Hooft. *Nucl. Phys. B*, 79, 1974.